UNIVERSITÄT ZU LÜBECK

From the Department of Dermatology, Allergology and Venereology

of University of Lübeck

Director: Prof. Dr. med. Detlef Zillikens

The contribution of interleukin-1 and retinoid acid receptor-related orphan receptor alpha to the pathogenesis of epidermolysis bullosa acquisita

Dissertation

for Fulfillment of Requirements

for the Doctoral Degree

of the University of Lübeck

-From the Department of Natural Sciences-

Submitted by

Hengameh Sadeghi M.Sc.

From, Shahrekord, Iran

Lübeck 2014

First referee: Prof. Dr. Ralf J. Ludwig

Second referee: Prof. Dr. Karsten Seeger

Chairman: Prof. Dr. Ulrich Schaible

Date of oral examination: 18.03.2015

Approved for printing: 23.03.2015 Lübeck

I dedicate this thesis to my mother
for her constant support and unconditional love.

Table of Contents

1. Introduction

1.1. Skin structure

Human skin is comprised of two layers: dermis and epidermis, which are separated by the basement membrane zone *also called dermal-epidermal junction (DEJ)* (Figure 1) [1].

1.1.1. Epidermis

Epidermis, the outer, non-vascular layer of the skin, is a stratified epithelium made up predominantly of layers of specialized epithelial cells known as keratinocytes (95%), and, to a lesser amount, by melanocytes, Langerhans' cells and Merkel cells [2].

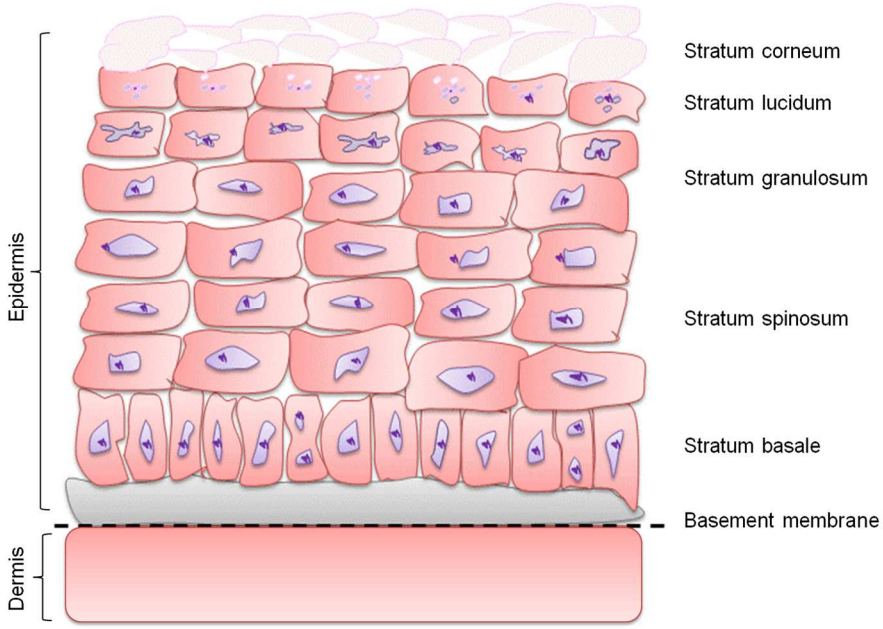

Figure 1: Structure of mammalian skin.

Skin consists of the epidermis and dermis, separated by a basement membrane. The epidermis is composed of the proliferative basal layer (single layer) and the three differentiated layers: spinous layer, granular layer and outermost stratum. Black line indicates DEJ (Adopted and changed from [2]).

On the basis of the morphological features of maturating keratinocytes, four to five layers of epidermis are distinguished, which from outward within are the horny (stratum corneum), the clear (stratum lucidum), the granular (stratum granulosum) the prickle cell (stratum spinosum) and the basal layer (stratum basale). The dermis, the fibro-elastic connective tissue located beneath epidermis, contains abundant vasculature, lymphatics, cutaneous nerves, and numerous sensory receptors.

1.1.2. Dermis

The dermis is composed largely of vascular connective tissue and the basement membrane is made up of extracellular matrix (ECM) proteins and proteoglycans and is rich in growth factors and dermal fibroblasts. Dermal fibroblasts produce supportive matrix while other cell types in the dermis are Lymphocytes, macrophages, mast cells and skin appendages cells. The upper layer of the dermis is the papillary, which contains a thin arrangement of collagen fibers, while the lower is the reticular layer, which is thicker and made of thick collagen fibers that are arranged parallel to the surface of the skin [3].

1.1.3. Dermal-epidermal junction

Between epidermis and dermis, an acellular basement membrane zone (BMZ) is located, known as the DEJ (Figure 2). It functions as a barrier protecting the organism from dehydration, mechanical trauma, and microbial insults. Ultrastructurally, the DEJ is divided into four areas: a) the cell membranes of the basal keratinocyte which contains the hemidesmosomes, b) the lamina lucida, an electron-lucent region where anchoring filaments traverse, c) the lamina densa, an electron-dense area and d) the sub-basal lamina, which contains anchoring fibrils, dermal microfibril bundles and collagen fibers. Ubiquitous basement membrane components are found in those zones, including laminin and nidogen in the upper regions, type IV collagen (COL4) and heparan sulphate proteoglycan in the lamina densa, and type VII collagen (COL7) in the sub-basal lamina densa [4].

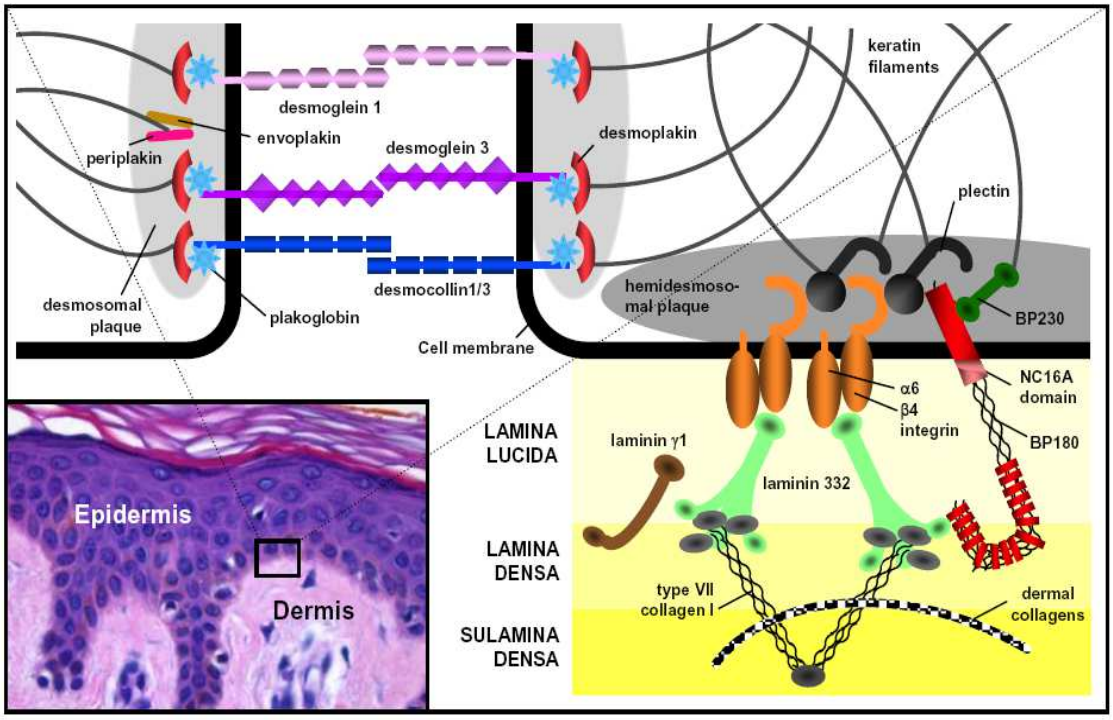

Figure 2: schematic view of the components of the DEJ and target antigens in autoimmune blistering diseases.

In the histological section of normal skin (bottom left), one sees the epidermis, the dermis, and the DEJ, which connects the epidermis to the dermis. Two neighboring basal keratinocytes are shown schematically (upper pannel). On the upper right, hemidesmosomal proteins anchor the epidermis to the dermis and are the target antigens in subepidermal autoimmune blistering skin diseases, in which cleavage occurs between the dermis and the epidermis (right side of the diagram). In epidermolysis bullosa acquisita (*EBA), COL7, which establishes a connection to dermal collagens is target antigens of autoantibodies (adopted from [5]).*

1.2. Autoimmune bullous dermatoses (AIBD)

AIBD are characterized by autoantibodies against (muco)-cutaneous structural proteins. Due to the improvement in AIBD diagnosis and the ageing population the incidence of AIBD has dramatically increased over the last decades [6]. The patients suffer from considerable morbidity and increased mortality. I.e. despite improved therapeutic options, mortality of patients with pemphigus and pemphigoid is still significantly increased [6], which can be partially attributed to the extent of immunosuppressive therapy [7]. In other autoimmune and chronic inflammatory diseases, cytokine-modulating therapies have greatly improved the therapeutic armamentarium; e.g. TNF-α inhibition in rheumatoid arthritis and psoriasis [7, 8].

1.2.1. Clinical presentation

Autoimmune blistering skin diseases are a group of organ specific, chronic and potentially life-threatening diseases clinically commonly characterized by blisters of the skin and/or surface-close mucous membranes.

1.2.2. Pathogenesis

In pemphigus disease antibodies are directed to the desmosomal proteins leading to blistering formation within the epidermis. In pemphigoid disease, a subepidermal AIBD type, the hemidismosomal proteins are the affected by antibodies leading to subepidermal cleavage [9].

1.2.3. Diagnosis

The current diagnostic for AIBD diagnosis is the detection of tissue-bound autoantibodies in skin or mucous membranes by direct immunofluorescence (IF) microscopy of a perilesional biopsy. More specifically, direct IF differentiates AIBD as intraepidermal (pemphigus) and subepidermal (pemphigoid) blistering diseases [10].

Regarding pemphigoid diseases, three distinct 'linear' fluorescence patterns at the BMZ can be recognized in direct IF microscopy, namely true linear, n-serrated or u-serrated. The true linear pattern, often seen in conjunction with either the n- or the u-serrated pattern, and can be found in any subepidermal immunobullous disease with nongranular depositions. In bullous pemphigoid (BP), mucous membrane pemphigoid, antiepiligrin cicatricial pemphigoid, 200 kDa protein (p200) pemphigoid, and linear immunoglobulin A (IgA) disease the n-serrated pattern is observed and corresponds with depositions located in hemidesmosomes, lamina lucida or lamina densa. Finally, the u-serrated staining pattern is characteristic for EBA and bullous systemic lupus erythematosus corresponding with the ultralocalization of COL7 in the sublamina densa zone. Notably, this pattern recognition by direct IF microscopy can correctly diagnose several cases of EBA which would otherwise have been erroneously diagnosed as a form of pemphigoid or linear IgA disease [11].

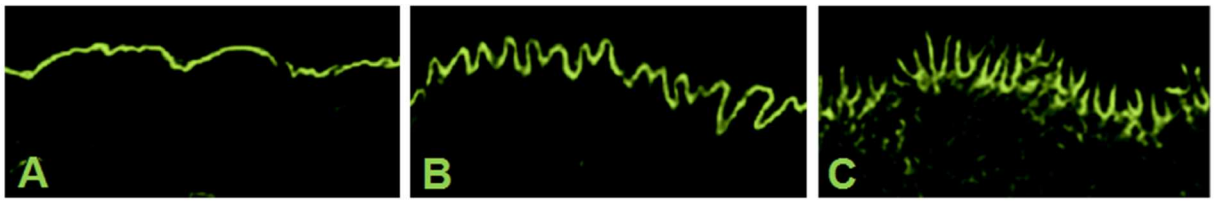

Figure 3: Direct IF staining patterns of in vivo bound IgG basement BMZ in perilesional skin from patients with BP (A, B), mechanobullous IgG-mediated EBA (C).

The linear (A) and n-serrated (B) patterns correspond with serum anti-BMZ autoantibodies locating at the epidermal side of NaCl-split skin, while the u-serrated (C) patterns correspond with serum anti-BMZ autoantibodies locating at the dermal side. Note that the u-serrated pattern specific for EBA. (Picture adopted from [11]).

Screening for presence of pemphigoid diseased is done by indirect IF microscopy on 1 M NaCl-split human skin. This method distinguishes between antigens localized on the epidermal side of the split such as BP180, BP230, and α6β4 integrin and those that localize at the dermal side of the artificial split including laminin 332, p200 antigen, and COL7 [12].

To further distinguish the individual pemphigus and pemphigoid diseases (table 1) serological analyses is used to determine the targeted autoantigen (and thus identify the respective AIBD). A number of sensitive and specific assays for the detection of circulating autoantibodies, including western blot (WB) of cell-derived and recombinant forms of the antigens, immunoprecipitation, indirect IF and enzyme-linked immunosorbent assay (ELISA), are used for the identification of target antigens [4]. Several ELISA systems using recombinant fragments of BP180, BP230, desmoglein 1 (Dsg 1), desmoglein 3 (Dsg 3), envoplakin, and type COL7 have become commercially available and are highly valuable diagnostic tools. Furthermore, BIOCHIP mosaics consisting of different antigen substrates allow polyvalent immunofluorescence (IF) tests and provide antibody profiles in a single incubation [13].

Finally, some AIBD, such as mucous membrane pemphigoid (MMP) with autoantibodies against laminin-332 and paraneoplastic pemphigus, (may) point to an underlying malignancy.

Group	Immunobullous disease	Target antigen	Predominant Ig Isotype(s)
Pemphigus	PV	Dsg 1, Dsg 3	IgG1-4, IgA
	PF	Dsg 1, Dsg 3	IgG1, IgG4
	PNP	envoplakin, periplakin, Dsg1 and 3, BP230, desmoplakin I/II, a2 macroglobulin-like 1	IgG1, IgG2
Pemphigoid	BP	BP180, BP230	IgG1-4, IgE
	PG	BP180, BP230	IgG1, IgE
	LP pemphigoides	BP180, BP230	IgG4, IgE
	MMP	Laminin 332, BP180, BP230, α6β4 integrin	IgG1, IgG4
	Linear IgG/A disease	LAD-1 (BP180 ectodomain), BP230	IgG, IgA
	Anti-p200 pemphigoid	Anti-laminin g1	IgG1, IgG3
	EBA	Type VII collagen	IgG, IgA

Table 1: Pemphigus and pemphigoid diseases.

Desmoglein (Dsg), Pemphigus foliaceus (PF), Pemphigoid gestationis (PG), Pemphigus vulgaris (PV), bullous pemphigoid (BP), Lichen planus (LP), Paraneoplastic pemphigus (PNP), Mucous membrane pemphigoid (MMP), linear IgA dermatosis antigen-1 (LAD-1) .

1.2.4. Treatment

Differentiation of the various types of the disorders is crucial as treatment options are diverse. Accurate diagnosis is the key standard of treatment success [14]. As AIBD are heterogeneous diseases, treatment differs greatly among the different AIBD. Up to date treatment of AIBD mainly relies on general immunosuppressive therapy and due to a low number of data from

controlled clinical trials, election of treatment is mostly based on the treating physician's clinical experience. Most commonly, treatment with topical steroids is the mainstay for BP [8]. Treatment of other subepidermal AIBD consists of systemic corticosteroids, although side effects such as systemic infections, diabetes mellitus, osteoporosis, thrombosis and gastrointestinal ulcer are reported upon high doses [15]. However, together with immunosuppressive agents such as azathioprine, mycophenolate mofetil, cyclophosphamide, and methotrexate to treat pemphigus as corticosteroids, doses can be decreased. Alternatively, tetracycline or dapsone combined with topical or systemic corticosteroids is preferred. In some poor treatment responder cases second line therapies are required. These include intravenous immunoglobulins, immunoadsorption, and rituximab [16, 17].

1.3. Epidermolysis bullosa acquisita (EBA)

The term EBA was first introduced by Elliott in 1904 to describe patients with adult onset and features resemble hereditary dystrophic epidermolysis bullosa. In 1971, Roenigk [18], based on distinctive clinical and histological features, was the first to distinguish EBA from other bullous diseases, suggesting the first diagnostic criteria for this disease. These are: 1) clinical lesions resembling epidermolysis bullosa dystrophica, 2) adult onset of disease, 3) a negative family history of epidermolysis bullosa dystrophica, and 4) exclusion of other bullous diseases. Currently, on suspected EBA upon clinical examination, histological and serological tests are used to confirm the initial diagnosis. More details about clinical manifestation, diagnoses, pathogenesis and treatment of EBA are presented in the following sections.

1.3.1. Clinical presentation

EBA is a clinically heterogeneous disease and patients may present with an inflammatory or non-inflammatory phenotype. The inflammatory type is characterized by cutaneous inflammation resembling other AIBD, such as BP, linear IgA disease, mucous membrane pemphigoid or Brunsting–Perry pemphigoid [19]. In contrast, patients with non-inflammatory or mechanobullous EBA, show skin fragility, trauma-induced blisters and erosions localized to the extensor skin surface, healing with scars and milia [14, 18]. According to clinical manifestations five variants of EBA have been described: (1) a classical presentation; (2) a BP-like presentation; (3) a cicatricial pemphigoid (CP)-like presentation; (4) a presentation reminiscent of Brunsting-Perry pemphigoid with scarring lesions predominantly localized to the head and neck; (5) a presentation similar to linear IgA bullous dermatosis (LABD) or chronic bullous disease of the childhood [20]. EBA is a rare disease with an incidence of

approximately 0.2 million people per year, mainly in elderly although some juvenile cases were reported [21, 22]. There is not known gender and racial predilection and it is not a genetic disease with a Mendelian inheritance pattern [23-25].

1.3.2. Pathogenesis

In EBA, like in all other AIBD, autoantibodies targeting antigens located within the skin mediate tissue injury. Discovery of COL7 as the autoantigen in EBA aided the development of model systems duplicating several aspects of the human disease and these models have significantly contributed to our current understanding of the diseases' pathogenesis [36]. Using several model systems and *in vivo* experiments have identified several cellular and molecular requirements for antibody-induced tissue injury in EBA such as: neutrophils, fragment crystallizable (Fc) receptors (FcRn), complement activation, and cytokines. Although the contribution of each of these cells and molecules has been well documented, the exact sequence of events leading to the formation of blisters is not specified in detail. Based on current information of the pathogenesis of EBA, tissue damage caused by autoantibodies can be explained by following events: (a) binding of the antibody to its target antigen, (b) fragment antigen-binding (Fab) and Fc-dependent formation of a blister, including the release of several cytokines, (c) integrin-dependent neutrophil extravasation into the skin, (d) activation of neutrophils, the release of reactive oxygen species (ROS) and MMP [36].

1.3.2.1. Antigenic target

EBA is a subepidermal blistering disease characterized by antibodies against a 290 kDa dermal protein, COL7 (Figure 4), the main component of anchoring fibrils at the DEJ. In 1984, Dr. Woodley and colleagues identified a 290 kDa protein located at the basement membrane of human skin [37]. Four years later, the same group identified the carboxyl terminus of COL7 as the autoantigen in EBA [38]. In most EBA patients, the autoantibodies are IgG. In addition to IgG, IgA anti-COL7 autoantibodies are observed either as an additional major Ig class. IgA autoantibodies against COL7 may occur alone or in combination with IgG autoantibodies [36].

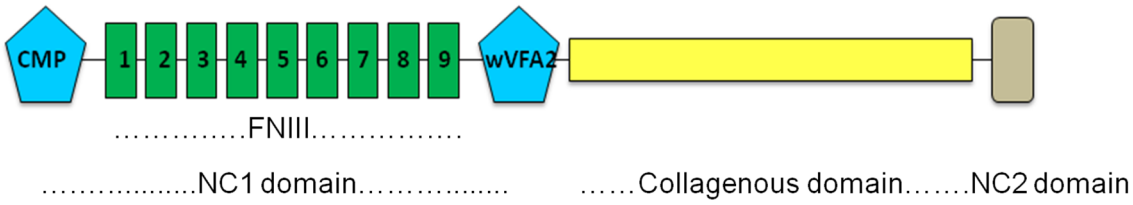

Figure 4: Scheme of one α-chain of COL7.

Three identical-chains build up COL7 forming anchoring fibrils. Each chain consists of one central collagenous domain (C), flanked by two non-collagenous domains (NC). The N-terminal NC-1 domain consists of several subdomains with high homology to adhesion proteins: cartilage matrix protein (CMP)-like domain, nine fibronectin like domains III FNIII-(1–9) and one C/N-terminal von-Willebrand-factor-A-like domain 2 (vWFA2), (Adopted from [39]).

COL7 is a trimmer with a helical structure consisting of 3 identical α1 polypeptide chains. Each of the chains consists of a 145 kD central C domain (Figure 4). The C domain is flanked at the N-terminal by a large, 145 kD NC domain, the NC-1, and at the C-terminal end by a smaller, 20 kD NC domain, NC-2 [40, 41]. Epitope-mapping of the COL7-specific B-cell immune response in EBA patients identified the NC-1 domain of COL7 as the major antigenic site [32, 42, 43].

In general, sera from EBA patients bind to many epitopes located within the NC-1 domain, but pathogenicity has only been demonstrated for few of these epitopes. Further epitope mapping of EBA patients' sera identified 4 major antigenic epitopes within the NC-1 domain [19, 32, 44-46]. However, it remained unclear if the specificity of the anti-COL7 antibodies is associated with certain clinical EBA phenotypes. The antibodies, specific to different epitopes were postulated to cause different phenotypes, although the relationship between epitopes and clinical manifestations were not detected [47]. In addition, experimental EBA can also be induced in mice by transfer of antibodies directed against epitopes located within the 6^{th}-9^{th} fibronectin-3 like repeat, or by immunization with the same antigen [48, 49]. Furthermore, transfer of patient antibodies affinity-purified against the CMP domain also induced EBA after transfer into mice [44]. Recently, pathogenicity of anti-vWFA2 antibodies has been demonstrated, by transfer of autoantibodies, as well as by immunization of mice with vWFA2 [50]. Collectively, detailed knowledge of the skin architecture and the role COL7 are still sparse and no high resolution structural information at atomic level is available.

1.3.2.2. Loss of tolerance in COL7

Different factors have been identified to be important for the loss of tolerance in COL7. Genetic studies in EBA patients point towards a genetic control of EBA, which can also be confirmed in animal models of the disease. Regarding cellular requirements for the induction of autoantibody production, CD4 T cells have been identified to be crucial in experimental EBA [36].

1.3.2.2.1. Genetic control of EBA susceptibility

Different EBA studies demonstrated a critical role of the genetic background. Several studies have been reported an increased occurrence Human Leukocyte Antigen (HLA)-DR2 in patients with EBA and bullous systemic lupus erythematosus [51, 52] and another later study showed HLA-DRB1*15:03 to be associated with EBA [53]. Common HLA haplotype in EBA patients and major histocompatibility complex (MHC) association in experimental EBA points towards a genetic control of EBA within the MHC locus [54]. However, the major histocompatibility complex genes alone are apparently not the only EBA susceptibility genes in experimental EBA [53]. In our department, in order to find EBA susceptibility genes, an advanced autoimmune-prone intercross mouse line has been generated. More specifically, immunization-induced EBA-resistant and EBA-susceptible mice were intercrossed at an equal strain and gender distribution [54]. Mice of the 4th offspring generation (G4) were then immunized with glutathione S transferase (GST) - murine type VII collagen C (mCOL7C) and 33% developed clinically EBA. Single-nucleotide polymorphisms (SNPs) genotyping led to the identification of several non-MHC quantitative trait loci (QTL) controlling EBA susceptibility [54].

1.3.2.2.2. T cells

Regarding cellular requirements for the induction of autoantibody production, it has been shown that T-cell-deficient SJL^{nude} mice are completely protected from induction of immunization-induced EBA [55]. In these mice, disease susceptibility could be restored by transfer of T cells from WT SJL/J mice that had been immunized with COL7 indicating that T cells are required to induce autoantibody production [55]. To further define T cell subsets involved in generation of anti-COL7 antibodies in experimental murine EBA, Dr. Iwata and colleagues at the Department of Dermatology in Lübeck established a novel EBA model by immunization with vWFA2 fused to intein (lacking the GST-tag). In this model they showed the requirement of APC-induced CD4 T cells to induce experimental EBA. All tested mouse strains developed autoantibodies, but blisters were exclusively developed in mice carrying *H2s*. In immunized mice, CD4 T cells specific for vWFA2 were detected, and their induction required

presence of B cells, dendritic cells, and macrophages (as antigen-presenting cells). Absence of CD8 T cells at time of immunization had no effect [50].

1.3.2.3 Autoantibody production and circulation

In immunization-induced EBA, antigen-specific B cells can be detected (almost) exclusively in peripheral lymph nodes. However, in human EBA patients there is no information regarding the localization of antigen-specific B cells. In other AIBD antigen-specific B cells are found in the circulation. Comparing the autoantibody responses of clinically healthy versus diseased mice after COL7 immunization, showed that IgG2 antibodies are associated with clinical EBA manifestation, indicative of Th1 polarized immune response [36].

Interestingly, IgG autoantibody half-life is controlled by the neonatal FcRn. The FcRn is a MHC class I-like molecule that, among other functions, protects IgG from catabolism [56]. In line, blockade of the FcRn leads to an enhanced clearance of all IgG, including autoantibodies. Therefore, maintenance of IgG autoantibody is controlled by FcRn. In animal models of AIBD, including pemphigus, BP and EBA, FcRn-deficient mice are completely or partially blocked from disease induction [57, 58].

1.3.2.3. Antibody-induced tissue injury

Well-established animal models suggest that EBA is a typical antibody mediated disease. The pathogenicity of autoantibodies specific to COL7 was first demonstrated in our group using an *ex vivo* model [59]. In this model, autoantibodies were shown to induce dermal-epidermal separation when incubated on human skin sections in the presence of human leukocytes from healthy donors. Interestingly, it was shown that leukocytes localization to the skin-bound immune complexes and their subsequent activation was dependent on the presence of the Fc portion of the antibodies. Later on, it was shown that autoantibodies generated against murine or human COL7 in rabbits or isolated from EBA patients could induce blister formation when passively transferred into mice [60-62]. Moreover, immunization of susceptible mice strains with the recombinant form of mCOL7 results in blistering diseases reproducing clinical, histopathological, and immunopathological findings in EBA patients [63].

Autoantibodies generated against COL7 bind to their target antigen, a large variety of epitopes located with the NC-1 domain of COL7. The binding of activating Fc gamma receptor (FcgR) to the immune complexes located in the skin is a key feature for autoantibody mediated blister formation in EBA [64].

Subsequent, release of pro-inflammatory cytokines followed by complement activation is crucial for antibody-transfer induced EBA. Complete protection of C5-deficient mice was

observed, while partial protection in C1q-, Factor B-, or C5aR-deficient mice has been reported. The pro-inflammatory milieu in EBA leads to a CD18-dependent recruitment of neutrophils into the skin [65] and activation of FcgR- complexes in mice and humans [64]. This activation leads to the release of ROS and proteases including elastase and gelatinase-B from the neutrophils, causing tissue damage [59, 65, 66].

1.3.3. Diagnosis

The diagnosis of EBA is based on the clinical presentation, histological as well as serological tests. At a minimum, this includes obtaining a lesional biopsy for histology and a perilesional biopsy for direct IF microscopy. In addition, serum analysis for the detection of antibody reactivity should be performed. Furthermore, tests such as transmission electron microscopy or antigen mapping may be performed in unclear cases.

For histopathology, the biopsy has to be obtained from lesional skin, where in most cases, subepidermal blister is observed. However, the histology in EBA is not pathognomonic but adds to the overall clinical picture, and thus, a skin biopsy should be obtained if there is EBA suspicion. On the other hand, electron microscopy shows specific pattern, where blister is situated in the dermis leaving the basal lamina in the roof of the blister [26]. However, one should bear in mind that transmission electron microscopy is used only in unclear cases and in specialized centers. In addition, direct immunoelectron microscopic on EBA skin biopsies shows distinct localization immune deposits, located in the anchoring fibril zone, just beneath the lamina densa [26, 27]. Immunoelectron microscopy is, by some authors, considered the gold standard for EBA diagnosis, but for practical reasons other methods are used in clinical laboratory practice [28, 29].

The detection of a linear IgG and/or IgA deposition along the basement membrane in a perilesional skin lesion from the patient is observed in almost all EBA cases. At high magnification, u-serrated is observed. Detection of circulating anti-COL7 can be used alternatively [30]. In indirect IF, binding of autoantibodies to the blister floor in salt-split skin indicates the presence of anti-COL7 antibodies. However, in the later cases, reactivity to laminin gamma-1 and laminin-332 has to be excluded [14]. For the specific detection of anti-COL7 IgG antibodies, commercially available ELISAs can be used [30, 31]. Finally, reactivity with a 290 Kilodalton (kDa)-sized protein of dermal extract can be detected by WB [32].

However, in approximately 1/3 of the EBA cases, circulating autoantibodies are not detected [33]. In these cases, the diagnosis can be established by either immunogold-electron microscopy or by pattern analyses of the direct IF microscopy sections [34]. In the latter case,

an u-serrated pattern is exclusively observed in EBA patients, and hence allows do diagnose EBA [35].

1.3.4. Treatment

Due to the low prevalence of EBA, no controlled treatment clinical trials have been performed. Therefore, recommendations for EBA treatment are solely based on the clinical experience of the treating physician(s) [67]. Usually, EBA patients are treated with systemic corticosteroids. In most cases corticosteroid treatment is combined with other immunosuppressive modulatory strategies to lower the corticosteroid dose. These include methotrexate azathioprine, cyclosporine, high dose intravenous Immunoglobulin (IVIG), dapsone, cyclophosphamide, rituximab, plasmapheresis immunoadsorption and colchicine in mild cases [36].

1.4. Cytokines in AIBD

Cytokines, during an inflammatory stimulus, are rapidly expressed and act as a network of molecules with additive, synergistic and opposite effects, which combine to remove the hazardous stimuli, initiate the healing process and maintain homeostasis. The balance between the production pro-inflammatory and anti-inflammatory cytokines is the key to the outcome of the inflammatory response. Therefore it seems obvious that uncontrolled production of these mediators is closely linked to several pathologic conditions [68].

Since cytokines are of most importance in homeostasis, it is not surprising that their activity is regulated at multiple levels. First, a stimulus is required to control the transcription of the majority of cytokine genes. Second, several cytokines are produced as larger biologically inactive precursor molecules and need to be proteolytically cleaved to gain their function. Third, soluble receptors which bind to cytokines can antagonize or agonize their activity. Finally, cytokine activity is regulated at receptor level and more specifically by modulating the number and the function of membrane receptors. Receptor number can be modulated by controlling gene expression, internalization, or cleavage, while receptor function is usually modulated by cytokine receptor antagonists.

In AIBD patients an increased cytokine expression has been well documented [69]. However, with one study pointed to the involvement of IL-1 and TNF-α in the pathogenesis of pemphigus vulgaris [70], no functional data on the contribution of cytokines to the pathogenesis of AIBD is currently available. Previously, data from expression profiling in the Department of Dermatology in Lübeck identified interleukin-1 receptor antagonist (IL-1Ra) as one of 33 gene products differentially expressed in the skin of BALB/c mice with experimental EBA. IL-1Ra

expression in diseased mice was closely linked to IL-1β [64], and its' local and systemic expression is controlled by IL-6. Furthermore, we recently found increased IL-1α and IL-1β serum levels in C57BL/6 mice after the induction of experimental EBA [71]. Our group also noted a higher expression of IL-1α and IL-1β in EBA patients, which, most likely due to the high variation in the patients samples, was however not statistically different (unpublished).

Moreover, in patients with pemphigoid diseases, elevated IL-1 expression was first observed in blister fluids of patients with BP; with the most striking increase in expression in early blisters [72]. Subsequent work showed that IL-1β, but not IL-1α, is elevated in blister fluids from BP patients [73, 74]. Using the patients´ number of lesions of the patients as a marker for disease severity, a significant correlation with blister fluid IL-1β was observed [73]. Given that IL-1 serum levels were not elevated in BP patients, this increased IL-1 expression appeared to be restricted to the affected skin sites [73]. In patients with cicatricial pemphigoid serum levels of IL-1α and IL-1β were significantly higher in untreated patients with active disease compared to patients in prolonged clinical remission and healthy controls [75].

1.4.1. Altered cytokine profile in autoimmune blistering diseases

Generally, a cytokine disease specific profile for one single disease does not exist and differential expressed levels of several different molecules are usually found in the majority of inflammatory diseases. In line with this, differential cytokine profile has been reported for the sera, skin and blister fluids of patients with autoimmune blistering diseases. However, this cytokine profile is not robust over the disease course and varies depending on disease severity, clinical phenotype and applied treatments. Most of the studies regarding cytokine profile in autoimmune blistering diseased regard BP or PV.

For BP, a review by D'Auria, and colleagues summarizes published data about the presence and levels of different cytokines and chemokines in patients with BP. The list of the analyzed cytokines includes 20 molecules, namely IL-1, IL-2, IL-3, IL-4, IL-5, IL-6, IL-7, IL-8, IL-10, IL-11, IL-12, IL-13, IL-15, granulocyte macrophage colony-stimulating factor (GM-CSF), interferon (IFN)-gamma, oncostatin-M, RANTES, Transforming growth factor (TGF)-β 1, TNF-α and Vascular endothelial growth factor (VEGF) (Table 2) [76]. The authors concluded that most of the molecules are found differentially expressed at the lesional skin and therefore they argued for a local synthesis model. Furthermore, they suggested that those molecules have multiple roles in disease development, including modulating the expression of the BP autoantigens, inducing humoral and cellular immune responses against those autoantigens, activating complement, regulating endothelium and keratinocytes and recruiting effector cells.

Cytokine	Method	Serum Det.	Serum Corr.	Blister fluid Det.	Blister fluid Corr.	BF/S
IL-1α	ELISA	BDL	ND	↓ vs NSBF	ND	↑
	Bioassay	ND	ND	↑ vs NSBF	ND	ND
IL-1β	ELISA	BDL	ND	↑ vs NSBF	ND	↑
	ELISA	BDL	ND	yes	yes	↑
IL-2	ELISA	BDL	ND	yes	no	↑
	ELISA	BDL	ND	ND	ND	ND
	Bioassay	ND	ND	↑ vs NSBF	ND	ND
IL-3	ELISA	BDL	No	yes	no	↑
	ELISA	Yes	ND	yes	ND	↔
IL-4	ELISA	BDL	no	yes	no	↑
	ELISA	BDL	no	ND	ND	ND
	ELISA	↑ vs NS	ND	ND	ND	ND
IL-5	ELISA	BDL	ND	↑ vs NSBF	ND	↑
	ELISA	Yes	yes	yes	yes	↑
	ELISA	Yes	yes	ND	ND	ND
IL-6	ELISA	↑ vs NS	ND	↑	ND	↑
	ELISA	↑ vs NS	yes	yes	no	↑
	ELISA	↑ vs NS	Yes	ND	ND	ND
IL-7	ELISA	↑ vs NS	yes	yes	yes	↓
IL-8	ELISA	BDL	no	yes	yes	↑
	ELISA	Yes	ND	↑ vs NSBF	ND	↑
	ELISA	Yes	ND	ND	ND	ND
IL-10	ELISA	↑ vs NS	no	yes	no	↑
	ELISA	BDL	ND	↑ vs NSBF	ND	↑
IL-11	ELISA	BDL	no	BDL	no	ND
IL-12	ELISA	BDL	no	BDL	no	ND
IL-13	ELISA	↔	no	ND	ND	ND
IL-15	ELISA	↑ vs NS	yes	yes	no	↑
GM-CSF	ELISA	↔	ND	↔	ND	ND
IFN-γ	ELISA	ND	ND	yes	ND	ND
	ELISA	BDL	ND	yes	no	↑
RANTES	ELISA	↔	ND	yes	yes	↑
TGF-β 1	ELISA	↔	no	yes	ND	↓
TNF-α	ELISA	Yes	ND	↑ vs NSBF	ND	↑
	ELISA	↑ vs NS	yes	yes	yes	↑

Table 2: Cytokines and chemokines in patients with BP.

Det.= detectability; BF/S blister fluid/serum ratio; Ref.= references; Corr= correlation with disease intencity "↑"= increased; "↓"= decreased; "—"= no significant difference; "ND"= not done; "BDL"= below detection limit; "NSBF"= normal suction blister fluid; "NS"= normal sera; (Adopted from [76]).

As a pioneer in the field of interleukins in AIBD Dr. Grando was the first to provide data on the presence of IL-1 in BP patients in more detail [72]. Recent data from our group shed light on IL-1 biology in BP. This data showed that at the site of blisters in BP, IL-1β, L-1 receptor antagonist and to a lesser extent, of IL-1α are released [74]. Indeed, IL-1β is major cytokine regulating inflammation and thus its local increase is not surprising. Of note, the reported release of IL-1 receptor as a compensatory mechanism was a puzzle until our discovery that linked its presence with IL-6 [71]. A more detailed description of IL-1 biology is provided below, as I focused on the role of IL-1 in experimental EBA.

IL-2, the first of a series of lymphocytotrophic hormones to be recognized and completely characterized, is a T lymphocyte product which also stimulates T cells to undergo cell cycle progression [77]. Unaltered IL-2 concentrations in the serum of BP patients has been reported independently by several groups. On the other hand, its increased presence in blister fluid of BP patients has been consistently reported, indicative of a lesional synthesis and rapid serum clearance by catabolic mechanisms [76]. Interestingly enough, Schaller et al. showed an increased IL-2 production in properly stimulated lymphocytes isolated for BP patients with active disease [78]. T cell derived IL-3, often in synergism with other pro-inflammatory mediators is involved in the survival, proliferation and differentiation of pluripotent hemopoietic cells [79]. This aforementioned cytokine were found elevated in the blister fluid but not the serum of BP patients [80].

IL-4 and IL-5 are related to the production of immunoglobulin E (IgE), whose levels are significantly increased in the skin, serum and blister fluid of BP patients, while IL-5 is also a potent eosinophil differentiation and activation factor, eosinophils participation in the blistering processes is well known. The majority of the studies failed to show elevated IL-4 levels. In contrast, in BP blister fluid IL-4 concentrations were consistently higher. Regarding IL-5, elevated levels have been described in both sera and blister fluid of BP patients [76].

An increased level of IL-6 in the serum and blister fluid of BP subjects has been reported by several groups. Notably, the high ratio between IL-6 concentrations in blister fluid compared to serum points to a local production of this molecule [76]. Recently, our group, using an animal model of passive EBA, has uncoupled IL-6 with disease enhancement. It was shown that in both IL-6-deficient mice and WT mice treated with anti-IL-6, clinical EBA severity was significantly increased compared to the respective controls [71]. On the contrary, administration of recombinant IL-6 dose-dependently impaired the induction of experimental EBA by the transfer of anti-COL7 IgG. These effects were at least partially due to an induction of IL-1Ra by IL-6 and exclusively mediated by classical IL-6 signaling [71].

Epidermal keratinocytes, under IFN-gamma control, constitutively produce IL-7, thereby supporting the growth of epidermal gamma-delta T cells [81]. Normal serum possesses significantly lower serum IL-7 concentrations than BP. However, surprisingly enough, IL-7 has been reported to be lower in the blister fluid compared to serum, an observation that remains still elusive [82].

A recent report suggests that collagen XVII, via NF-κB signaling can modulate keratinocyte expression of the pro-inflammatory IL-8 [82]. Increased serum IL-8 levels in BP patients are found when compared to controls. Regarding blister fluid, IL-8 concentrations are higher than those found in the serum. Notably, IL-8 in blister fluid positively correlates with the area of lesional skin [76]. CD4+ T cells, activated monocytes and subsets of B cells are major sources of IL-10. This cytokine inhibits the antigen-presenting functions and down-regulates class II MHC expression. High IL-10 levels have been described in BP blister fluid and sera. The high ratio between blister fluid and serum IL-10 concentrations indicates a lesional synthesis of IL-10 [76]. Regarding IL-11, a pleiotropic cytokine with both inflammatory and anti-inflammatory functions, which drives the T-dependent B-cell activation, there are no detectable levels at neither the serum nor the blister fluid in BP patients. This was also the case for IL-12 [76].

IL-13 is a pleiotropic cytokine that induces B-cell proliferation and enhances IgE and IgG4 secretion. There are no significant differences in the IL-13 serum levels between BP patients and controls [76].

IL-15 is constitutively expressed in both, immune and non-immune cell types, including monocytes, macrophages, dendritic cells, keratinocytes, fibroblasts and other [83]. It regulates T and NK cell activation and proliferation. Interestingly, in the absence of antigen, survival signals that maintain memory T cells are provided by IL-15. Furthermore, an important mechanism mediating IL-15 responses in lymphocytes during the steady state is transpresentation. More specifically, in transpresentation, cell surface IL-15, bound to IL-15Rα is delivered to opposing lymphocytes [84]. Recently, it was shown that IL-15 induces chromatin remodeling of the interleukin 12 receptor, beta 1 (IL-12Rβ1) promoter and thereby increasing IL-12Rβ1 messenger Ribonucleic acid (mRNA) expression [85]. Not only are NK cells particularly sensitive in IL-15, but an enhancement of NK cells has been reported in BP, as well. Interestingly, there are data showing that low doses of IL-15 may act as an inhibitor of pro-inflammatory cytokines and enhance the release of anti-inflammatory cytokines. However, high IL-15 doses stimulate the release of both anti-inflammatory and pro-inflammatory cytokines. Notably, bullous diseases are also characterized by autoantibodies produced by B

cells, known to be stimulated by IL-15. Research has shown that IL-15 serum levels in BP patients are higher than in those in the serum of healthy controls [86].

GM-CSF was initially characterized by its ability to generate *in vitro* granulocyte and macrophage colonies from bone marrow precursor cells. However, it is interesting to mention that recent data showed that even in the absence GM-CSF and other known myeloid colony-stimulating factors, additional growth factor(s) can stimulate myelopoiesis and acute inflammatory responses [87]. GM-CSF can be produced by a number of different cell types, such as T cells, B cells, macrophages, mast cells, endothelial cells, fibroblasts, and adipocytes. On mature hematopoietic cells, it acts as a survival signal and activates the effector functions of innate immune cells [88]. Our group has tested GM-CSF levels in the blister fluid from BP patients and compared them with those in suction blister fluid from healthy volunteers and concluded that there were no detectable differences [89].

IFN-gamma, a product of activated T cells and natural killer cells, regulates keratinocyte growth and differentiation. Regarding epidermal cell biology, this cytokine promotes the expression of intercellular adhesion molecule (ICAM)-1 and HLA-DR on keratinocytes. Furthermore, IFN-gamma has a direct inhibitory effect on keratinocyte growth and induces terminal differentiation, by up-regulating the expression of differentiation-specific genes, including transglutaminase type I and a variety of proteins involved in the formation of the cornified envelope [90]. IFN-gamma has been reported to play a role on BP keratinocyte specific antigen expression [91]. More specifically, an IFN-gamma-dependent altered expression of different keratinocyte antigens recognized in the sera of patients with BP has been identified. Yet, there was a variability of the expression of BP antigens, depending on the skin donor, which suggests a differential sensitivity to IFN-gamma in different keratinocytes [91]. Even more important, the 230 BP antigen specifically was found up-regulated at both, protein and mRNA level, upon IFN-gamma stimulation in keratinocytes [92]. However, subsequent studies showed that IFN-gamma, on the contrary, inactivates the transcription of 230 BP antigens [93-95]. Interestingly, IFN-gamma is also implicated in the expression of complement components, known to be involved in blistering processes [96-98]. In blister fluid and histological sections of BP patients IFN-gamma is differentially found up-regulated which suggest a local synthesis of IFN-gamma [76].

Oncostatin-M, a cytokine produced by T cells, monocytes and macrophages was originally recognized by its unique activity to inhibit the proliferation of tumor cells. However, the trend notion is that oncostatin-M exhibits many unique biological activities in inflammation, hematopoiesis, and development [99]. Regarding BP, it was found higher lesional levels than

those observed in sera, showing the same pattern as the majority of the cytokines involved in bullous diseases [76].

RANTES, a C-C motif chemokine, has been shown to be able to attract T cells, eosinophils and basophils and to play an active role in recruiting leukocytes into site of inflammation [100]. Published data have indicated that serum RANTES levels in BP do not differ from those in normal subjects. However, RANTES levels in blister fluid were reported to be lower, compared in those in serum [76].

TGF-β 1, is a multifunctional polypeptide growth factor produced by many cell types, with anti-inflammatory properties [101]. Interestingly enough, it has been shown to inhibit the expression of BP antigens. The serum levels of this cytokine in BP patients do not differ when compared to healthy control, while lower levels in blister fluid than in sera have been detected. It has further been found that blister fluid level of this molecule in BP patients is higher than in controls [76]. As regards mRNA TGF-β levels, has been found up-regulated in BP biopsies, in studies conducted by Fabbri's groups [102]. Noteworthy, TGF-β has strong fibrogenic effects and BP is a non-scaring disease [103]. Therefore, it has been suggested that in BP, it could dampen the activity of inflammatory mediators and act as cutaneous blistering stop signal [102].

Once TNF was cloned, allowing its specific analysis in serum and neutralization *in vivo*, the involvement of this cytokine in infectious disease pathology was established. TNF-α induces the synthesis of IL-1, IL-6, IL-8, GM-CSF, leukotrienes and prostaglandins, thereby amplifying the inflammatory reaction [104]. This molecule is produced by most cells present in the histological infiltrate of BP, including keratinocytes, monocytes, macrophages, eosinophils, mastocytes, and T cells. Since, in synergy with IL-5, it can effectively recruit and activate eosinophils, it is believed to have a crucial role in disease progress. TNF-α is elevated both locally and in the sera of BP patients as compared to normal sera [76]. Add data from Liu on mast-cell derived TNF and elute on its role in BP pathogenesis

1.4.2. Targeting cytokines in inflammatory diseases

The possibility of exploring the behavior of cytokines during the evolution of pathological conditions represents a valuable approach in understanding the inflammatory mechanisms that specifically characterize the different diseases. A thorough understanding of cytokine interactions not only can be helpful in understanding the pathophysiology of such diseases, which also can lead in targeted therapies [105]. Indeed, several inhibitors of cytokines are considered as successful biologics and have proven to be clinically efficacious at reducing inflammation associated with several autoimmune diseases. As a result, attention is focusing

on the therapeutic potential of additional cytokines. As possible targets for modulating inflammatory diseases, many of these are now in clinical or preclinical stage.

For example, infliximab (remicade) is a chimeric TNF-α monoclonal antibody consisting of the human constant and mouse variable regions of the IgG. It is currently Food and Drug Administration (FDA)-approved for psoriasis, psoriatic arthritis, rheumatoid arthritis, ankylosing spondylitis, Crohn's disease, and ulcerative colitis [335].

Etanercept, a dimeric fusion protein consisting of the extracellular ligand-binding domain of the human TNF-α receptor fused to the Fc domain of human IgG1, is currently approved by the FDA for the treatment of psoriasis, psoriatic arthritis, rheumatoid arthritis and ankylosing spondylitis [336].

Adalimumab is a fully human TNF-α monoclonal IgG1 antibody that blocks TNF-α. It is currently FDA-approved for treating psoriasis, psoriatic arthritis, rheumatoid arthritis, ankylosing spondylitis, and Crohn's disease [337].

Ustekinumab, a human IgG1κ monoclonal antibody that binds with high affinity and specificity to the p40 protein subunit used by both the IL-12 and IL-23 cytokines, is currently FDA-approved for treating psoriasis [338].

Anakinra is an intravenous recombinant, nonglycosylated form of human interleukin-1 receptor antagonist (IL-1Ra). IL-1 blockade by anakinra is dramatically effective in systemic-onset juvenile idiopathic arthritis, it has been FDA approved for arthritis in 2001 and since 2013 it has specifically been indicated for Neonatal-Onset Multisystem Inflammatory Disease (NOMID) [339-340].

The blockade of IL-1 has been shown to ameliorate disease in preclinical studies. Biological agents that target IL-1 have demonstrated efficacy in patients with rheumatoid arthritis, NOMID and further agents targeting IL-1 neutralization are in clinical development. Therefore, IL-1 can be a good study target for controlling blistering in antibody-transfer induced EBA.

1.5. IL-1

The skin contains cells with different ontogenic origins, including keratinocytes, melanocytes, Langerhans cells, Merkel cells, and "resident" T cells (dendritic epidermal T cells) in which keratinocytes represent the majority of cell types. Cytokines produced by epithelial cells maintain normal homeostatic mechanisms in these structures and can induce proliferative changes caused by injury. Skin and mucosal cytokines can have pro-inflammatory as well as anti-inflammatory function, and dysfunction in the cytokine balances can contribute to inflammatory diseases in these organ systems. Keratinocytes synthesize and secrete a wide variety of cytokines in respond to trauma, UV irradiation, and bacterial products [106].

IL-1 is produced constitutively by keratinocytes and it has many properties and functions therefore it is a primary mediator in inflammatory skin diseases [107]. Indeed, it has long been known that human keratinocytes are a potent source of the proinflammatory cytokine IL-1, both α and β, which are activated and released in response to UV irradiation. However, the pathways for IL-1 processing in keratinocytes remain obscure. One possible theory is that the UVB-mediated enhancement of cytoplasmic Calcium (Ca^{2+}) is required for activation of caspase-1 [108]. Interestingly, Watanabe and his collogues by inducing danger signals made keratinocytes to secret caspase-dependent IL-1β showing that the inflammasome is indeed present and can be activated in keratinocytes [109]. These findings support the notion that keratinocytes are immunocompetent cells under physiological and pathological conditions. This raises the possibility of a direct involvement of keratinocytes in situations characterized by aberrant IL-1 signaling in the skin. Yet, the intracellular pathways, which regulate maturation and secretion of IL-1 in keratinocytes, are still unknown.

1.5.1. Biology of IL-1

Recent advances in our understanding of the inflammatory machinery have focused attention on the central role of IL-1 in inflammatory phenotype, from Familial Mediterranean Fever to Inflammatory Bowel Disease and Rheumatoid Arthritis.

In 1972 it was widely accepted that the interaction of exogenous pyrogens, such as bacteria or bacterial products, with host phagocytic cells, activates these cells to release a protein, which stimulates the hypothalamus and results in fever. At that time it was known under several names such as leukocytes endogenous mediator hematopoetin, endogenous pyrogen, catabolin and osteoclast activating factor [110]. In 1974 Dinarello characterized two distinct endogenous pyrogens with similar physiological activity; they would later be determined to be IL-α and IL-β [111]. Since then, much has been learned about the

physiological activity and biological process of these molecules and their fundamental role in inflammatory conditions [112].

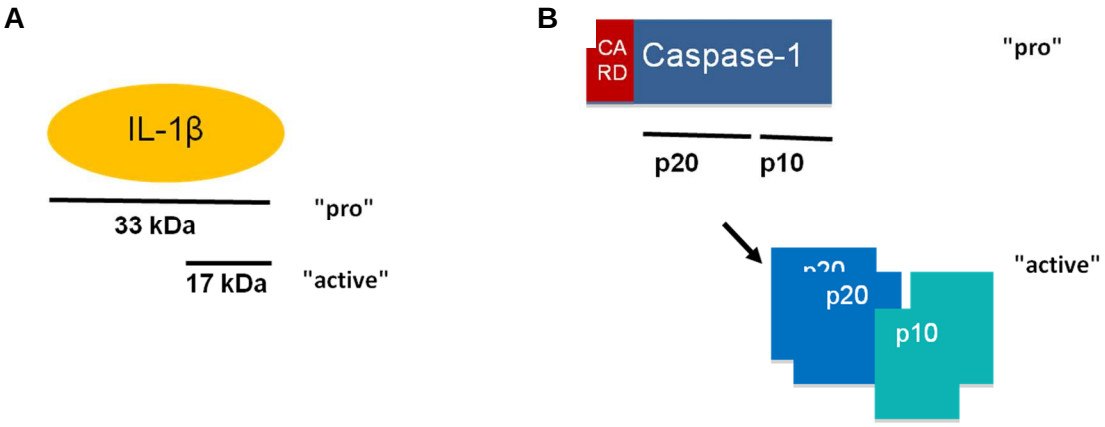

Figure 5: IL-1β and caspase-1 should be cleaved in order to become active.

A) *The immature IL-1β is synthesized as a 33 kDa precursor in the cytoplasm and makes the 17 kDa mature form after cleavage. B*) *The cysteine protease, caspase-1, is synthesized as a zymogen in the cytoplasm. A multimeric complex cleavages it to make its active form which is compose of two p20 and two p10 subunits [113].*

Both IL-1α and IL-1β are processed proteolytically, generating a 17 KDa fragment; IL-1α is cleaved mainly by calpain [114] and IL-1β primarily by caspase-1. Unlike IL-1β, which must be cleaved to generate an active molecule [115], both cleaved and uncleaved IL-1α forms can be biologically active [116].

Regarding production and processing of IL-1β, a large body of recent work has greatly enhanced our understanding on the mechanisms involved in. However, it is just start casting light on the mechanisms of IL-1β secretion. The difficulty is raised by the unconventional secretory pathway used cells to export this leaderless cytokine. So far, five different mechanisms have been proposed, namely a) release from shedding plasma membrane microvesicles, b) exocytosis of IL-1β-containing secretory lysosomes, c) fusion of multivesicular bodies with the plasma membrane and subsequent release in exosomes, d) export through the plasma membrane with specific membrane transporters, and e) release upon cell lysis [117].

The effects of IL-1 are exerted via its binding to IL-1 receptor complex, a heterodimer comprised of the interleukin-1 receptor type I (IL-1RI) and interleukin-1 receptor accessory protein (IL-1RAcP). Interestingly, IL-1RAcP has no affinity on its own for IL-1, but when the cytokine binds IL-1RI, AcP is recruited to form the high-affinity receptor complex. Upon signal

transduction initiation, the adaptor protein myeloid differentiation primary response gene 88 (MyD88) is recruited to the intracellular Toll-IL-1 receptor (TIR) domain of the receptor, resulting in phosphorylation of several kinases. After a cascade of reactions, NF-κB translocates to the nucleus, where it activates the transcription of a large portfolio of inflammatory genes. On the other hand, IL-1Ra binds to IL-1RI but fails to nucleate a functional complex with IL-1RAcP, thus the pro-inflammatory signal is not initiated. Since IL-1Ra can occupy IL-1RI with a slightly higher affinity than IL-1, it can apparently act as a potent receptor antagonist.

An additional regulatory mechanism of IL-1 activity is achieved by a decoy receptor, named interleukin-1 receptor type II (IL-1RII). This receptor lacks signal capacity because its short cytoplasmic tail does not contain the TIR domain, where MyD88 can dock. Since IL-1β binds IL-1RII with greater affinity compared to IL-1RI and IL-1RAcP can be recruited to IL-1RII–IL-1β complex, IL-1RII can sequester both, IL-1 and IL-1RAcP from IL-1RI. Since IL-1Ra and IL-1RII serve to regulate IL-1 signaling, it can be anticipated that IL-1RII shows low affinity for IL-1Ra, if IL-1Ra could strongly bound IL-1RII, these two molecules would negate each other's action. Interestingly, IL-1RII can be released from the cell surface, in a regulated way. This soluble form of IL-1RII is believed to block the systemic actions of IL-1 leaking from inflamed sites, without affecting responsiveness in situ [118-122].

1.5.2. IL-1 maturation and secretion

Caspases (Cysteine requiring ASPartate protease) are cysteine proteases that are expressed as inactive precursor enzymes with an N-terminal prodomain followed by a two-subunit effector domain. Based on their physiologic roles, caspases are classified in two functional groups. Those involved in apoptosis (caspase-2, -3, -6, -7, -8, -9, and -10) and those involved in cytokine processing (caspase-1, -4, -5, -13, and -14, as well as murine caspase-11 and -12).

Caspase-1 is the cysteine protease that converse the inactive precursor of IL-1β to the active "mature" cytokine, by cleaving 116 aa from the N-termin of precursor molecule. Caspase-1 is synthesized as a pro molecule of 45 kDa, which is not active. Its active form is a tetramer of two 20 kDa and two 10 kDa subunits that come from the C-termini of at least two separate molecules (Figure 5). For caspase-1 to be activated, adenosine triphosphate (ATP) should bind to $P2X_7$ purinergic receptor, with a subsequent rapid exit of potassium from the cell. The fall in intracellular potassium is believed to trigger the oligomerization of inflammasome, a multiprotein complex, which can convert procaspase-1 to an active enzyme. Active caspase-1 then cleaves the IL-1β precursor, which is secreted in its active state (Figure 5).

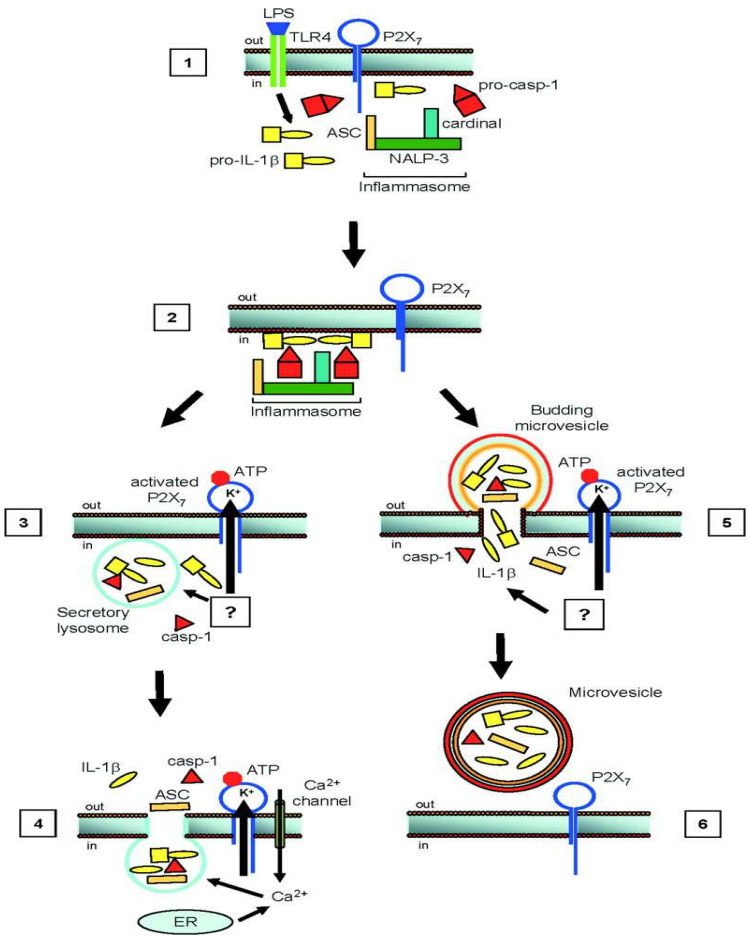

Figure 6: The secretory lysosome content.

1). Following toll like receptors (TLRs) activation by its cognate ligands, pro IL-1β accumulates in the cytoplasmic and inflammasome is formed. 2). Then, pro-L-1β and inflammasome are localized to the plasma membrane. First Hypothesis: 3). The loading of the inflammasome to secretory lysosomes is driven by K^+ efflux, triggered by $P2X_7R$ activation. In parallel, procaspase-1 is cleaved to active caspase-1 and pro-IL1β is cleaved to mature IL-1β produced. 4). Finally, the secretory lysosome content is released into the pericellular space, through a process requiring $P2X_7R$-dependent K^+ efflux and Ca^{2+} increase. Alternative hypothesis: 5). After localization of the inflammasome to the plasma membrane, activation of the $P2X_7R$ and K^+ efflux triggers budding of small membrane blebs that trap the inflammasome. In parallel, pro-IL-1β is converted into mature IL-1β. 6). *Finally, plasma membrane blebs pinch off and diffuse into the pericellular space. Figure is adopted from [123].*

The best-characterized inflammasomes are the *NOD*-like receptor family, pyrin domain containing NLRP1, Aim2, NLRP3 and NLR family CARD domain-containing protein NLRC4 inflammasomes, although more have been described. The NLRP1 inflammasome is activated by muramyl dipeptide, the Aim2 by binding to viral and bacterial double-stranded DNA and

NLRC4 by flagellin resulting from intracellular pathogens. Regarding NLRP3, although is known to response in a variety of PAMPs and DAMPs direct interaction with these molecules has not been shown so far. Lysosomal rapture by an unknown mechanism possibly involving cathepsins has been proposed to activate NLRP3. Resting NLRP3 inflammasome component localizes to endoplasmic reticulum structures, whereas on its induction, both NLRP3 and its adaptor ASC redistribute to the perinuclear space where they co-localize with endoplasmic reticulum and mitochondria organelle clusters [124-127].

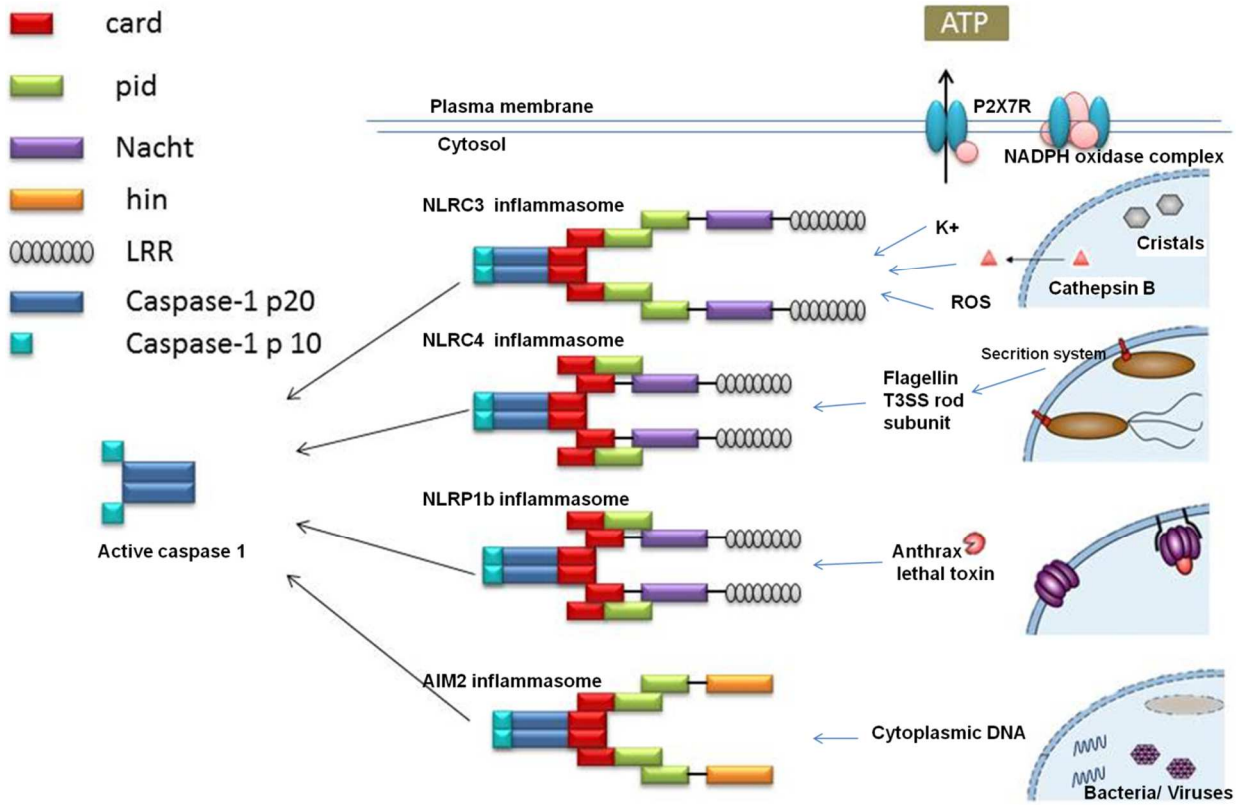

Figure 7: All inflammasomes activate caspase-1, which leads to processing of pro-IL-1β and pro-IL-18, and host cell death.

NLRC3 responds to numerous stimuli including pore-forming toxins, extracellular ATP, and crystalline compounds. The exact mechanism of activation is unknown but may involve potassium efflux, membrane damage, and generation of ROS. NLRC4 responds to bacterial flagellin and the type III secretion systems (T3SS) rod subunit. NLRP1b responds to anthrax lethal factor. Absent in melanoma 2 (AIM2) binds cytosolic Double-stranded -DNA (dsDNA) from bacterial, viral, mammalian, and synthetic sources. Complexes are formed through homotypic interactions, leucine rich repeats (LRR); hemopoietic IFN-inducible nuclear proteins (HIN); PYD, pyrin; CARD, caspase activation and recruitment domain) (Adopted and modified from [128]).

Interestingly, monocytes have constitutively activated caspase-1, and thus the release of mature IL-1β occurs after a single stimulation event, which can be bacterial ligands such as LPS. In contrast, macrophages and dendritic cells need 2 distinct stimuli: The first stimulus induces transcription and subsequent translation of IL-1β, while a second stimulus, that can trigger $P2X_7$ receptor, is needed for caspase-1 activation, leading to IL-1β processing and secretion. Since monocytes, in contrast to the other cells, can release endogenous ATP, they

do not require a second stimulus. However, blood monocytes also respond to ATP challenge, leading to a greater release of IL-1β. Specific environmental adaptations can explain these fundamental differences between these cells types. Since monocytes circulate in a pathogen free environment, they should respond promptly whenever encounter a danger signal. On the other hand, macrophages are constantly exposed to several danger signals. To avoid overwhelmed inflammatory reactions, a second stimulus that could confirm the alarming situation is required. Such second stimulus is available at sites of infection, trauma, or necrosis where elevated ATP levels can trigger $P2X_7$ receptor. Of note, cathelicidin-derived peptide LL37 from infiltrating neutrophils, IFN-γ or bacterial toxins can serve as second stimulus as well [129].

It has been proposed that ROS can induce IL-β secretion. Indeed, data suggest that ROS can prime but not activate inflammasome [130]. Inflammasome activators induce the dissociation of thioredoxin interacting protein (TXNIP) from thioredoxin in a ROS-sensitive manner that allows it to bind and activate NLRP3 [131, 132]. In this case, the predominant source of ROS generated by danger signals is most probably the mitochondria [133]. However, in cells with defective Nicotinamide adenine dinucleotide phosphate (NADPH) activity, where ROS levels are low or absent, IL-1β levels are high. Correspondingly, cells deficient in super oxide dismutase-1 (SOD1), where ROS levels are high, caspase-1 is suppressed and IL-1β levels are found low. Notably, decreased cellular redox potential can specifically inhibit caspase-1 by reversible glutathionylation of the redox-sensitive cysteines residues of the molecule. In line with these, humans with chronic granulomatous disease due to defective NADPH activity have increased inflammation with granulomatous lesions and a form of colitis indistinguishable from that found in Crohn's disease [134, 135].

Recently, it has been suggested that caspase-1 activation results not only in the production of activated cytokines but also to a special form of programmed cell death, called pyroptosis, More specifically, during pyroptosis a rapid plasma-membrane rupture occurs and thus, pyrogenic interleukins are released. This is in marked contrast to the packaging of dangerous cellular contents during apoptosis. However, cleavage of chromatin that is considered as a hallmark of apoptotic cell death also occurs during pyroptosis [136].

A better understanding of up- and down-stream IL-1 events is of great therapeutic relevance since it could pave the way for the development of novel approaches aiming at targeted control of inflammatory responses.

1.5.3. IL-1 function

IL-1 is a pro-inflammatory and anti-apoptotic agent that induces cytokine production by activating nuclear factor kappa-light-chain-enhancer of activated B cells (NF-κB) and activator protein 1 (AP-1) and Mitogen-activated protein (MAP)-Kinase signaling which in turn, induce other significant mediators that orchestrate various immune and inflammatory responses. AP-1 and NF-κB activate transcription of genes that encode mediators and suppressors of inflammation (cytokines, chemokines, inducible nitric oxide synthase (iNOS), adhesion molecules, etc), as well as costimulatory molecules such as CD40, CD80 and CD86 involved in adaptive immune response. Furthermore, these signal transduction pathways are also known to influence; cytoskeleton reorganization, Ca_2^+ or K^+ fluxes, release of chemokines, phospholipases and prostaglandins [137, 138].

NF-κB is a member of the Rel family of transcription factors and is composed of two groups of structurally related, interacting proteins that bind DNA as dimers. The one group of NF-κB/Rel family members includes NF-κB1 and NF-κB2, which are synthesized as precursor proteins of 105 and 100 kDa, respectively. The other group includes Rel A (p65), Rel B, and c-Rel, which are synthesized as mature proteins with at least one activation domains. In resting cells, NF-κB is bound on NF-κB inhibitor proteins, named I-κB. IL-1, but other molecules as well that can activate NF-κB result in the Ser-phosphorylation of I-κB, a modification that tags those inhibitors for ubiquitination and subsequent proteolytic degradation by the ATP-dependent 26S proteasome complex. After this event, NF-κB can translocate to the nucleus, bind to its recognition site, and activate gene transcription. An alternative activation pathway for NF-κB independent of I-κB degradation involves the tyrosine phosphorylation of I-κB. Phosphorylation of I-κB requires the sequential phosphorylation of NF-κB inducing kinase (NIK) and IKK [139, 140].

IL-1 signaling is initiated after IL-1 binding to its cognate receptor. Subsequently, MyD88 is recruited, which interacts with interleukin-1 receptor-associated kinase 1 (IRAK-1) and interleukin-1 receptor-associated kinase 4 (IRAK-4). IRAK-1 is recruited to the receptor independently of MyD88. By contrast, IRAK-4 is recruited to the receptor through binding of MyD88. Once bound to the receptor complex, IRAK-1 becomes phosphorylated by IRAK-4 and subsequently autophosphorylated [141]. These phosphorylation steps result, the dissociation of kinases from the receptor complex and the interaction with the TNF receptor associated factor 6 (TRAF6). Indeed, lessons from knockout mice indicate that IRAK-4 plays an essential role in the activation of this pathway, as responses to IL-1 are abolished in those mice [142]. By contrast, other kinases, possibly interleukin-1 receptor-associated kinase 2

(IRAK-2), can substitute for IRAK-1 since activation of TRAF6 is only attenuated in IRAK-1 deficient cells [143].

TRAF6 activates a heterodimer composed of two ubiquitination proteins called Uev1A and Ubc13 [144]. Significantly, unlike the classical ubiquitination in which ubiquitination occurs on Lysine 48 and the subsequent degradation of the modified protein by the proteasome, upon activation of TRAF6, noncanonical ubiquitin chains are extended on Lysine 63, which trigger association with the MAP3 kinase TAK1 [145]. More specifically, TRAF6, through its RING domain, which is an E3 ubiquitin ligase, conjugates Lys63-linked polyubiquitin chains to itself, IRAK-1, and NF-κB Essential Modulator (NEMO). Interestingly, Lys-209 at TAK1 is a site-specific acceptor of TRAF6 catalyzed Lys-63-linked polyubiquitinated chains in IL-1 treated cells. Binding of TAB2 and TAB3 to the polyubiquitin chains of TRAF6 and the binding of NEMO to the polyubiquitinated chains of IRAK-1, leads to the activation of TAK1 and the IKK complex. Phosphorylation of Thr-178 and Thr-184 residues within the kinase activation loop of TAK1 is essential for both, NF-κB and AP-1 activation [146, 147]. Activated TAK1 can directly phosphorylate and activates the kinase IKKβ a part of a large protein complex named signalosome, which contains also NEMO [148]. IKKβ phosphorylates the NFκB cytoplasmic inhibitor IκB. After IκB polyubiquitination and degradation NFκB is released and translocated to the nucleus. Activated TAK can also phosphorylate MKK6, which in turn phosphorylates JNK and leads to activation of AP-1, an important stress-responsive transcription factor [145].

However, several lines of evidence have shown that another Mitogen-activated protein kinase (MAPK), mitogen-activated protein kinase kinase kinase 3 (MEKK3), can act downstream of TRAF6 and activate the IKK complex, p38 MAPK and JNK and therefore activate of NF-κB and AP-1. Actually, critical roles for TAK1 and MEKK3 in IL-1–induced TRAF6 signaling has been shown and it has been proposed an IL-1 signaling model where two mechanistically and temporally distinct MEKK3-dependent pathways diverge at TRAF6 and cooperatively activate NF-κB to produce proinflammatory cytokines [149].

1.5.4. IL-1 and ICAMs

One of the effects of IL-1 to the skin is the expression of endothelial adhesion molecules [150], including E-selectin, ICAM-1, CD45 and vascular cell adhesion molecule (VCAM)-1, as well as chemotactic and activating chemokines [151].

Interestingly, Dustin et al. have shown that IL-1, in a process that involves de novo mRNA and subsequent translation, induces the expression of ICAM-1 on cell surface of dermal fibroblasts, in a concentration dependent manner [152].

ICAM-1 is present constitutively on the cell surface of both hematopoietic and non-hematopoietic cells and can be up-regulated upon stimulation with inflammatory mediators. IL-1-mediated expression of ICAM-1 occurs in endothelial cells, epithelial cells, leukocytes hepatocytes, and fibroblast, while in keratinocytes and smooth muscle cells IL-1 does not mediate the-up-regulation of ICAM-1 [153]. The induction of ICAM-1 mRNA synthesis occurs rapidly, as fast as less than 1 hour, upon cytokine stimulation [154].

The major intracellular signaling events leading to IL-1 dependent ICAM-1 expression are based on complex cooperative interactions. IL-1 binding to its cognate receptor recruits TRAF6, which activates NIK and subsequently the IKKα/β kinase. This heterodimeric kinase phosphorylates the inhibitor of kappa B (I-κB), a modification that targets I-κB for ubiquitin mediated proteolysis. NF-κB translocates into the nucleus and binds the proximal promoter, ~200bp upstream of ICAM-1 [153, 155, 156]. Furthermore, data suggest that CCAAT-enhancer-binding proteins (C/EBP) b and d might be involved in IL-1β-mediated ICAM-1 induction [157]. Albeit PCK activation is capable of inducing ICAM-1 expression, PKC seems to be dispensable for IL-1 dependent ICAM expression [158]. Finally, the role of p42/p44 MAPK and JNK in IL-1-induced ICAM-1 expression remains still controversial [159].

Although a number of cis-elements in both, distal and proximal regions exist on ICAM-1 promoter, the proximal NF-κB binding site located about 200 bp upstream has been shown to be of most importance for the induction of ICAM-1 transcription. The NF-κB element within the proximal ICAM-1 promoter is a variant NF-κB binding site. Immediately upstream of and adjacent to the variant NF-κB site is a C/EBP site that in concert with the NF-κB site forms a cytokine response element. In addition, the ICAM-1 promoter contains several AP-1 binding sites. AP-1 is a basic leucine zipper (bZip) factor and is composed of dimers of the Jun and Fos transcription factor families [153, 160].

Recruitment of immune cells to the skin is a highly complex process that involves adhesion to the endothelial lining, extravasation, migration through the connective tissue, and finally localization to the epidermis. All the aforementioned steps are mediated by interacting sets of cell adhesion molecules (CAMs) and chemoattractant activator molecules.

The roles of adhesion molecules in acute and chronic inflammation have been thoroughly investigated and appear to be of prime importance in various inflammatory skin conditions ICAM-1 or CD54 and VCAM-1 or CD106, expressed by vascular endothelium, act as counter-receptors for leukocyte integrins. ICAM-1, one of the major ligands for the leukocyte b2-integrins such as linear IgA dermatosis antigen-1 (LFA-1) also known as CD11a/CD18 and Macrophage-1 Ag (Mac-1) also known as CD11b/CD18 is a member of the immunoglobulin

superfamily of adhesion molecules and contains five Ig like domains. In line with this, ICAM-1 knockout mice show significantly impaired neutrophil migration into an inflamed sites [161, 162] while ICAM-1 antibodies reduce acute and chronic inflammation in a number of animal models [163]. *In vitro*, ICAM-1 antibodies reduce cytokine-activated transmigration of neutrophils by over 85% [164, 165] and chemotactic transmigration by ~55% [166]. VCAM-1 contains six to seven Ig like domains and is expressed on both large and small vessels after cytokine stimulation. VCAM-1 promotes the adhesion of lymphocytes, monocytes, eosinophils, and basophils [167].

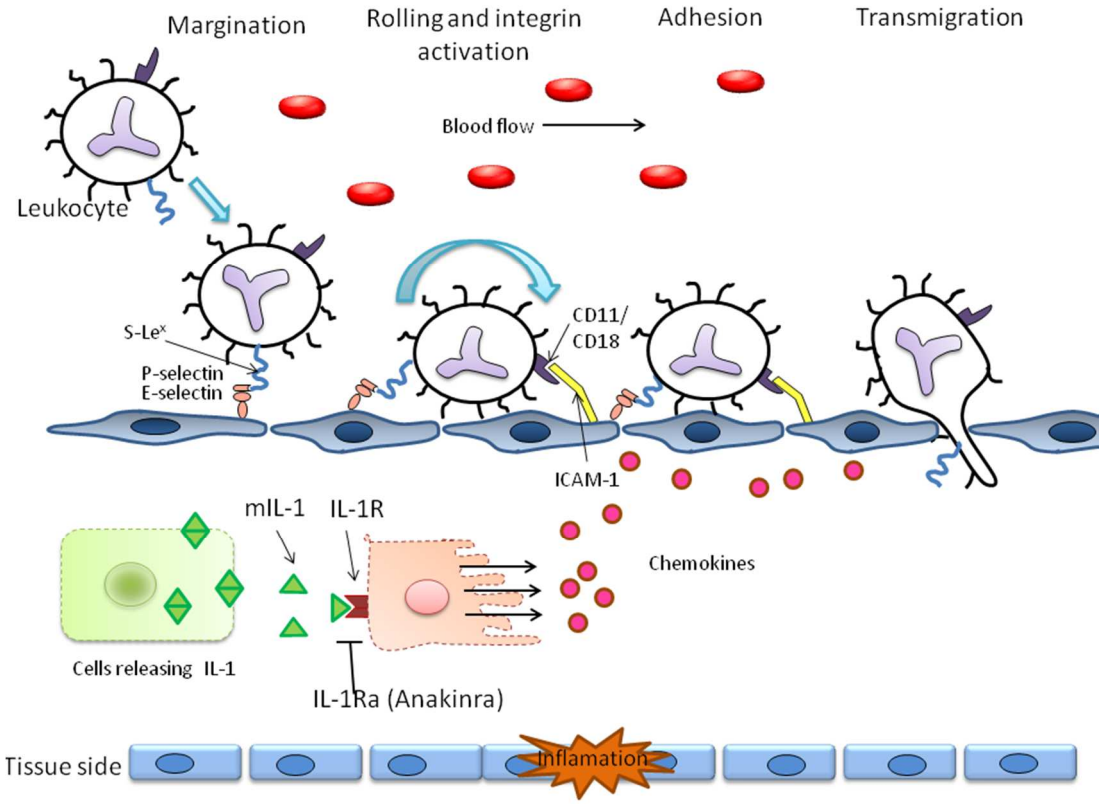

Figure 8: Interactions among adhesion molecules and cytokines.

Cytokine stimulation activates membrane-bound adhesion molecules and induces chemokines cause leukocytes to move into various tissue sites by inducing the adherence of these cells to the vascular endothelium lining the walls of blood vessels. After migrating into tissues, leukocytes move by chemotaxis toward the higher localized concentrations of chemokines. (Adopted and modified from [168]).

1.5.5. IL-1 in autoimmune diseases

IL-1β plays an orchestrating role in both, inflammatory and immune responses. Indeed, IL-1β is characterized by its ability to enhance the expression of some adhesion molecules. In

addition, IL-1β through the induction of other cytokines, such as TNF-α, IFN-gamma, IL-2, IL-6, and IL-8 can trigger and amplify the inflammatory cascade. Notably, IL-1 has the capacity to regulate the synthesis of some complement components. The significant role of IL-1β in immunity can be observed in IL-1β knockout mice, which have severely impaired bacterial clearance. On the other hand, high levels of IL-1β have been linked with numerous chronic inflammatory disease. For example, in arthritis, IL-1α is believed to be involved in cartilage degradation [169].

In a mouse model of arthritis, levels of membrane-bound IL-1α, but not serum IL-1α or IL-1β, correlate with disease severity [170], while in collagen-induced mouse models of arthritis, overexpression of sIL-1RAcP significantly ameliorates disease activity [171]. Synoviocytes from joints of RA patients have high levels of IL-1α mRNA [172], and patients who produce anti- IL-1α antibodies get a less destructive disease [173]. Furthermore, compared to WT mice, mice deficient for IL-1 have decreased number of osteoclasts in trabecular bone, while they increased femur mineral density, trabecular bone mass and cortical thickness [174].

In the skin, IL-1 is mainly produced by the keratinocytes where it is stored as pro-IL-1α and pro-IL-1β (31 kD precursors). Grando *et al.* provided the first data concerning the presence of IL-1 in the BP blister fluid [72]. Subsequent studies found increased local concentrations only of IL1β as compared with normal suction blisters, while IL-1α showed the opposite behavior [74]. Although there is still no plausible explanation for this finding, similar observations have been recorded for psoriatic lesions [175]. More recent publications reported a positive correlation between IL-1β and the number of skin lesions observed in the patients, and therefore support a possible pathogenic role for this cytokine in BP [69].

1.5.6. Therapies targeting IL-1

During the past year, it becomes clear that aberrant IL-1 signaling is linked to several inflammatory conditions, including periodic fever syndromes, systemic-onset juvenile idiopathic arthritis, adult Still's disease, and crystal-induced arthritis. Therefore, at the horizon of innovative therapies, several inhibitors of IL-1 signaling have been developed. Some of these compounds have been used only in experimental models of disease, others have been tested in clinical trials, and only a few are currently available for clinical use. These include anakinra, which is very effective in patients with Schnitzler’s and in adult-onset Still's disease. Not satisfactory clinical data of IL-1 blockade with anakinra in RA have raised the questions whether anakinra is not a “good enough drug” to block IL-1 in RA or whether targeting IL-1 in RA is the wrong cytokine [176, 177]. ACZ885, a human anti-IL-1β monoclonal antibody, and was approved for the treatment of cryopyrin-associated periodic syndromes (CAPS) by FDA

on 2009. It is effective in a proof-of-concept study in patients with rheumatoid arthritis. Clinical trial of AMG 108, a fully human monoclonal antibody to IL-1RI, on RA or osteoarthritis of the knee showed moderate disease improvement. PRAL, an orally-active interleukin-1β converting enzyme (ICE) inhibitor, and the casase-1 inhibitor VX-765 are two other new compounds already in phase II of clinical trials.

2. Aim of study

Autoimmune diseases are an apt example of complex diseases, and, as discussed before treatment most commonly relies on general immunosuppression, which in most cases controls symptoms, but rarely leads to complete remission [36]. Interestingly, at the horizon of innovative therapy in inflammatory conditions, biological targeting cytokines have emerged.

Until now, little to no data on the functional role of cytokines in AIBD, including EBA, have been published. A few studies have shown the role of cytokines in disease pathogenesis using animal models. The main problem in such studies is lack of well established models which recapitulate the multifactorial pathogenesis, the histopathological features and the clinical phenotype of AIBD [70, 71, 178]. EBA was selected in our group as a laboratory established animal model, which in contrast to other models of AIBD, reflects the entire pathogenesis of the diseases, including loss of tolerance and antibody-induced tissue injury. This allows investigating the effect of cytokine modulating therapies at all stages of disease.

The aim of this study was to evaluate the functional relevance of IL-1 in experimental EBA and whether IL-1 blocking could be a promising therapeutic option in EBA patients. Thus, in the first part of my thesis I evaluated the role of IL-1 in the pathogenesis and treatment of experimental EBA by:

- Investigating IL-1 expression in experimental EBA
- Addressing the effects of genetic and pharmacologic IL-1 inhibition in antibody-transfer induced EBA
- Addressing the effects of genetic and pharmacologic IL-1 inhibition in already established immunization-induced EBA
- Dissecting IL-1 effects at cellular level using *in vitro* systems
- Investigating alternative routes of IL-1 processing during inflammatory conditions
- Identifying potential sources of IL-1

Although IL-1 blockade was effective in both, passive and active models of EBA, the disease could not be fully cured. Hence, the 2nd aim of my study focused on the identification of novel

therapeutic targets. One possible approach was to build-up potential pathways for pharmacological modulation though the identification of genetic susceptibility loci. This was addressed by:

- A genome-wide association study using 600,000 SNPs in 16 genetically well characterized inbred strains in an antibody transfer EBA model to identify disease susceptibility genes
- Expression profiling to narrow down the number of potential susceptibility genes
- STRING database to build up IL-1 related genes network
- *In vivo* studies of the selected gene in knockout mice

3. Materials and methods

3.1. Materials

3.1.1. Equipment in laboratory

Name of equipment	Provider
Bio-photometer 8,5 mm	Eppendorf AG, Hamburg, Germany
Centrifuge (BIOFUGE Fresco)	Haereus Instruments GmbH, Hanau, Germany
Centrifuge (Varifuge 3.0 R)	Haereus Instruments GmbH, Hanau, Germany
Cold room(4°C)	Viessmann GmbH & Co. KG, Allendorf, Germany
Cryostat (Leica CM 3050S)	Leica Mikrosysteme Vertrieb GmbH, Wetzlar, Germany
Deep freezer-C660 (-80°C)	New Brunswick Scientific (UK) Ltd, England
Dry heat sterilizer	Binder GmbH, Tuttlingen, Germany
ELISA plate reader	Perkin Elmer, Inc., CA, USA
ELISA plate washer	Tecan Group Ltd., Maennedorf, Switzerland
Pipettes	Eppendorf AG, Hamburg
Microscopy (Olympus BX40)	Olympus Deutschland GmbH, Hamburg, Germany
Microtome	Leica Mikrosysteme Vertrieb GmbH, Wetzlar, Germany
pH-meter (ph526)	WTW GmbH, Weilheim, Germany
SDS ABI 7900 system	Applied Biosystems Deutschland GmbH, Darmstadt, Germany
Vortex	Scientific Industries, Inc., Bohemia, New York, USA

3.1.2. Consumable materials

Name	Provider
1.5ml/2.0ml tubes	Sarstedt AG & Co. KG, Nuembrecht, Germany
Cover glasses (24x60mm)	Gerhard Menzel, Glasbearbeitungswerk GmbH & Co. KG, Braunchweig, Germany
Disposable cuvets	BRAND GmbH, Wertheim, Germany
Disposable needle (BD Microlance 3, 26Gx1/2)	Becton Dickinson GmbH, Heidelberg, Germany
Disposable syringe-1ml (BD PlastipakTM)	Becton Dickinson GmbH, Heidelberg, Germany
Disposable syringe-20ml (BD DiscarditTM II)	Becton Dickinson GmbH, Heidelberg, Germany
EDTA-syringes	Sarstedt AG & Co. KG, Nuembrecht, Germany
ELISA plate (Maxisorb®)	Nunc A/S, Roskilde, Norway
ELISA plate seal	Sarstedt AG & Co. KG, Nuembrecht, Germany
Fliter Minisart-Sterile (0.20 µm)	Sarstedt AG & Co. KG, Nuembrecht, Germany
feeding syringes	Fuchigami, Tokio, Japan
Protein G sepharose columns	Amersham Biosciences Europe GmbH, Freiburg, Germany
SuperFrost/Plus- slide glasses	Gerhard Menzel, Glasbearbeitungswerk GmbH & Co. KG, Braunschweig, Germany
Tissue-Tek® O.C.T. Compound	Sakura Finetek Europe B.V., Alphen aan den Rijn, Netherland
Tissue-Tek® Cryomold	Sakura Finetek Europe B.V., Alphen aan den Rijn, Netherland

3.1.3. Chemicals, biological and kits

Name	Provider
1-step Turbo ™- ELISA	Thermo Fisher Scientific, Inc., Rockford, USA
ABC Peroxidase Staining Kit	Thermo Scientific Scientific, Inc., Rockford, USA
BCA™ Protein Assay	Thermo Scientific Scientific, Inc., Rockford, USA
Murine IL-1β Standard ELISA Development Kit	Pepro Tech, Inc, Hamburg, Germany
Amersham ECL Prime Western Blotting Detection Reagent	GE Healthcare Europe GmbH, Freiburg, Germany
Biotin-free BSA	Carl Roth GmbH & Co. KG, Karlsruhe, Germany
BSA	Sigma-Aldrich Biochemie GmbH, Hamburg, Germany
Dako Dual Endogenous Enzyme Block	Dakocytomation GmbH, Hamburg, Germany
DAPI (4',6-Diamidino-2-Phenylindole, Dihydrochloride)	Life Technologies GmbH, Germany
Distilled Water	UKSH Pharmacy, Campus Lübeck, Germany
DMSO	Sigma-Aldrich Biochemie GmbH, Hamburg, Germany
Eosin	Merck KGaA, Darmstadt, Germany
Ethanol	UKSH Pharmacy, Campus Lübeck, Germany
Glycerol	Carl Roth GmbH & Co. KG, Karlsruhe, Germany
Haematoxylin	Merck KGaA, Darmstadt, Germany
Human IL-1β Standard ELISA Kit	Bioscience, Inc., San Diego, USA
Hydroxy Ethyl Cellulose	Sigma-Aldrich Biochemie GmbH, Hamburg, Germany
InnuPrep RNA Mini Kit	Analytic Jena AG, Germany
Ketamine hydrochloride	Sigma-Aldrich Biochemie GmbH, Hamburg, Germany
Kineret® (Anakinra)	Biovitrum AB, Stockholm, Sweden

Peroxidase substrate, HistoGreen(TM)	LINARIS GmbH, Wertheim-Bettingen, Germany
protease inhibitor cocktail set III	Merck KGaA, Darmstadt, Germany
protein A/G PLUS-Agarose beads	Santa Cruz Biotechnology, Inc., Heidelberg, Germany
Quantikine® mouse IL-1Ra ELISA kit	R&D Systems GmbH, Wiesbaden-Norderstadt, Germany
QPCR Master Mix Plus	Eurogentec GmbH, Cologne, Germany
TaqMan probeTM	Biomers.net GmbH, Ulm, Germany
TiterMaxTM	Enzo Life Sciences GmbH, Lörrach, Germany
T-PER (Tissue Protein Extraction Reagent)	Thermo Fisher Scientific, Inc.,IL, USA
Tween-20	Sigma-Aldrich Biochemie GmbH, Hamburg, Germany
Tween-80	Sigma-Aldrich Biochemie GmbH, Hamburg, Germany
VECTA MOUNTTM permanent mounting medium	Vector Laboratories, Inc., CA, USA
Vector, pGEX-6P-1	Amersham Biosciences Europe GmbH, Freiburg, Germany
VX-765 (Belnacasan)	MedKoo Bioscience, Inc., NC, USA
Xylazine hydrochloride	Sigma-Aldrich Biochemie GmbH, Hamburg, Germany
Xylene	Sigma-Aldrich Chemie GmbH, Deisenhofen, Germany

3.1.4. Antibodies

Antibody name	Provider
goat anti-mouse complement C3 (FITC)	Cappel Organon-Teknika Corp., NC, USA
Polyclonal rabbit anti-mouse IgG (FITC)	DAKO Deutschland GmbH, Hamburg, Germany
polyclonal goat anti-rabbit antibody (HRP)	DAKO Deutschland GmbH, Hamburg, Germany
Polyclonal goat anti-mouse IgG for IL-1α	R&D Systems, Wiesbaden, Germany
Polyclonal goat anti-mouse IgG for IL-1β	R&D Systems, Wiesbaden, Germany
Polyclonal donkey anti mouse (HRP)	Jackson ImmunoResearch, PA, USA
Monoclonal armenian hamster anti-mouse IgG for ICAM	Abcam, Cambridge, UK
Polyclonal rabbit anti-armenian hamster IgG (HRP)	Abcam, Cambridge, UK
polyclonal rabbit anti-mouse IgG antibody (HRP)	DAKO Deutschland GmbH, Hamburg, Germany
Polyclonal swine anti rabbit (TRITC)	DAKO Deutschland GmbH, Hamburg, Germany
Goat anti rabbit antibody (FITC)	Dakocytomation GmbH, Hamburg, Germany
Goat anti-rat secondary antibodies (HRP)	BioLegend GmbH, Germany
Goat anti-mouse IgG (HRP)	Santacruz Biotechnology, Inc., CA, USA
Normal rabbit serum	C.C.Pro GmbH, Oberdorla, Germany
Monoclonal mouse IgG for actin	Santacruz Biotechnology, Inc., CA, USA
Polyclonal Rabbit anti goat (HRP)	DAKO Deutschland GmbH, Hamburg, Germany

3.1.5. Buffers

Name of buffer	Preparation
Phosphate buffered saline (PBS)	8g/L NaCl, 0.2g/L KCl, 1.44g/L Na2PO4K2HPO4 in distilled water, adjust pH at 7.2 with phosphate acid
Phoshphate buffered saline-Tween 20 (PBST 20)	PBS with 0.05% Tween 20, pH 7.2
Glycine buffer	7.52g of glycine in 1L of distilled water. Adjusted pH to 2.8 with 1N HCl
TRIS-buffer	181.71g of TRIS base in 1L of distilled water. Adjusted pH to 8.8 with 1N HCl
NaCl	58.44g of NaCl in 1L of distilled water
Carbonate buffer	5.3g of Na2CO3, 5.04g of NaHCO3 dissolved in 1L of distilled water. Adjusted pH to 9.6 with 1N HCl
20% Ethanol	20ml of absolute ethanol in 80ml of distilled water

3.1.6. List of media for cells

Horse serum (Gibco)	Life Technologies, Karlsruhe, Germany
Keratinocyte Growth medium	PromoCell, Heidelberg, Germany
Fetal calf serum (FCS)	Biochrom, Berlin, Germany
RPMI 1640 Medium	Life Technologies, Karlsruhe, Germany
DMEM	Life Technologies, Karlsruhe, Germany

3.1.7. Mice

All inbreed (A/J, AKR/J, B10.S-H2s/SgMcdJ, BALB/cJ, BXD2/TyJ, C3H/HeJ, C57BL/6J, Cast/EiJ, CBA/J, DBA1/J, FVB/NJ, MRL/MpJ, NOD/ShiLtJ, NZM2410/J, PL/J, PWD/PhJ, SJL/J and WSP/EiJ) mice used in this study were obtained from Jackson Laboratory (Bar Harbor, Maine, USA). Mice of the 6th generation of, autoimmune-prone advanced intercross mouse line (AIL) has been established by Prof. Saleh Ibrahim (Dept. of Dermatology, University of Lübeck) and kindly provided for this study. In brief, parental mouse strains (MRL/MpJ, NZM2410/J, BXD2/TyJ, Cast/EiJ) were intercrossed at an equal strain and sex distribution. Parental origin of first generation (G1) offspring mice was considered when setting up mating for the second generation (G2) mice in order to maintain an equal distribution of the original strains. This procedure was also followed for intercrossing G2 mice. At least 50 breeding pairs were used as parental for the next generation of mice.

Heterozygous Retinoid-related orphan receptor (ROR) α mice on the C57BL/6 genetic background (ROR-/+) were kindly provided by Prof. Jean Mariani (Laboratoire Développement et Vieillissement du Système Nerveux, Institute des Neurosciences, Université P. and M. Curie, Paris, France). For experiments with RORα deficient mice, mice aged 2-3 weeks were used.

Caspase-1/11 knockout with a mixed C57BL/6 × 129Sv/J background were kindly provided by Prof. Arturo Zychlinsky (Max-Planck-Institut für Infektionsbiologie Berlin).

Mice used in this study were held at specific pathogen free conditions, and also standard mouse chow and acidified drinking water ad libidum was fed to them. All biopsies, clinical examinations and bleedings were done under anesthesia by intraperitoneal administration of a mixture of ketamine (100µg/g) and xylazine (15µg/g). At the endpoint of experiments mice were killed by cervical dislocation and samples were collected. All animal experiments had approval by the Animal Rights Commission Ministry of Agriculture and Environment, Schleswig-Holstein.

A brief descriptions of mice used in this thesis, and the rational to use these mice are given below. All mice were obtained from commercial suppliers or kindly provided by cooperation partners (see above).

3.1.7.1. C57BL/6J mice

There are two major substrains of C57BL/6 mice, known as 6J and 6N. The original strain was initially derived as C57BL in 1921 by Dr. CC Little from mating of female 57 with male 52 from Miss Abbie Lathrop's stock. Substrains C57BL/6 and C57BL/10 were separated prior to 1937

[179-182]. C57BL/6N is a C57BL/6 subline originated at NIH that was separated from C57BL/6J in 1951. Further C57BL/6 substrains, J or N, were developed as breeding stock by various investigators and vendors [179]. It is important to distinguish the exact background because of the possible effects on phenotype [183, 184].

C57BL/6J have an increased preference for alcohol and are used in studies of the genetics of substance preference [185, 186]. Other characteristics are their susceptibility to diet-induced obesity [187], diabetes II type [188] and atherosclerosis [189]. Susceptible to induction of autoimmune prostatisis (contrast BALB/c) [190]. It needs also to be mentioned that these mice are highly susceptible to induction of antibody-transfer induced EBA [54].

3.1.7.2. Caspase-1/11 -/- mice

Caspase-1/11 -/- mice are also known as ICE knockout mice. They lack exons six and seven of the *caspase-1* gene and fail to process pro-IL-1β or pro-IL-18 [191]. In addition, caspase-1 deficiency leads to a reduction of IL-1α secretion [192]. It is confirmed that caspase-1 is involved in particular cell death pathways including pyroptosis. Caspase-1 deficient cells demonstrate reduced lysis upon infection with certain pathogens [193]. It has recently been confirmed that these mice are caspase-1/caspase-11double knockout mice [194-196]. Homozygous caspase-1/11 targeted mutant mice prove to be viable, fertile with no gross abnormalities in appearance, body weight or organ size in their first 16 weeks of life. Homozygotes are born at predicted Mendelian frequencies and reverse transcription (RT) - polymerase chain reaction (PCR) analysis confirms the absence of mRNA. To investigate the role of caspase-1 in induced EBA, 6-8 weeks old caspase-1/11 -/- were used for these thesis. C57BL/6 was used as negative control.

3.1.7.3. IL-1R -/- mice

IL-1R -/-mice are knockout for IL-1R on C57BL/6 background, showing defects which fail to respond to IL-1. These mice have normal vigor and exhibit no overt phenotype. Some effects including defective responses to certain inflammatory agents such as turpentine and altered response to various pathogenic organisms such as *S. aureus* and *C. pneumonia* are seen from knocking out this receptor [197]. Mice have been produced with a genetically disrupted IL-1RI gene. After S. aureus infection, mice exhibit severe septicemia, increased weight loss and increased susceptibility to induced arthritis compared with wild-type mice [198]. Interestingly, serum levels of IL-18 in IL-1R -/- mice were significantly lower than wildtype mice 24 hours after inoculation of S. aureus, but serum level of both IL-18 and IL-1β were significantly increased in IL-1R -/- vs wildtype 4 days after the bacterial inoculation [198]. In this thesis role of IL-1 in EBA severity is investigated by inducing EBA in IL-1R -/- mice.

3.1.7.4. RORα -/- mice

The staggerer mutation occurred spontaneously in a stock of obese mice at the Jackson Memorial Laboratory in 1955. The segregation data given later in this report prove the mutation to have been due to a single recessive gene [199]. Staggerer mice were found to carry a deletion within the RORα gene that inhibits translation of the ligand-binding homology domain [200]. More specifically, this deletion removes an exon encoding part of the ligand binding domain of the putative receptor, generating a RORα truncated protein [200]. These mice are first distinguishable from normal littermates between postnatal days 8 and 12 but they are identified most readily in the second postnatal week by their lower weight, abnormal gait, which is more shuffling and hesitant than the gait of normal littermates while a mild tremor sometimes accompanies the initiation of motor activity [199]. During the third week the impairment of gait and balance becomes even more pronounced, especially in contrast to the increasing motor facility of the normal littermates [199]. More than 50% of the mutant mice die in the fourth week and those that survive show little or no further progression of symptoms but remain lighter in weight than their littermates [199]. In these mice the cerebellar cortex is grossly underdeveloped, with too few granule cells and unaligned Purkinje cells [199].

However, the group of Becker-André M. to better study the physiological role of RORα gene generated a null-mutant mice by targeted insertion of a lacZ reporter gene encoding the enzyme β-galactosidase The genetic background of these mice was C57BL/6, 129/Ola [201]. In heterozygous RORα mice they found β-galactosidase activity, indicative of RORα protein expression to the central nervous system, skin and testis [201]. Interestingly, other organs such as liver, heart, spleen, lung, and leukocytes, which have been shown to express significant to high levels of RORα mRNA did not display any detectable enzyme activity [201]. In particular, peripheral blood leukocytes, such as T cells, B cells and neutrophils containing highest amounts of RORα mRNA were negative in the β-gal assay [201]. In this thesis, the effect of RORα blockade on EBA susceptibility has been evaluated.

3.1.7.5. A/J mice

The A/J strain was developed in 1921 by L.C. Strong from a cross between Cold Spring Harbor and Bagg albino random-bred stocks [179-182]. This inbred strain is widely used in cancer and immunology research and is also highly susceptible to cortisone-induced congenital cleft palate. It shows to have a high incidence of spontaneous lung adenomas [202, 203]. In contrast to B6 mice, A/J mice are resistant to diabetes, obesity, insulin resistance, and glucose intolerance [204]. A/J mice are known to be deficient in complement factor C5 [205, 206]. Furthermore, abnormal neutrophil physiology has been reported for this mouse strain [207,

208]. A/J mice show highly diminished neutrophil infiltration into hepatic sinusoids compared with C57BL/6J controls. Having abnormal neutrophil physiology make them a good candidate to check their susceptibility to EBA as the later is neutrophil dependent [65].

3.1.7.6. AKR/J mice

The AKR strain was developed from 1928 to 1936 , by J. Furth, and then inbred randomly for several generations by C. Lynch at the Rockefeller Institute [179-182]. Because of their high leukemia incidence (60-90%) and in immunology as a source of the Thy1.1 (a thymocyte antigen) such mice are widely used in cancer research [209-211]. They are proved to be viremic from birth, and express the ecotropic retrovirus AKV in all tissues [212-214]. There is no report showing this strain developing autoimmune diseases. Susceptibility of this strain to EBA was previously unknown and has been checked in this thesis.

3.1.7.7. BALB/cJ mice

These mice were developed by Halsey Bagg in 1913. They designated BALB for Bagg ALBino, while c refers to their albino allele [179-182]. Being particularly well-known for the production of plasmacytomas following injection with mineral oil, these mice form the basis for the production of monoclonal antibodies [215, 216]. Although not all BALB/c substrains have been examined for plasmacytoma induction, sub-strains derived from the Andervont (An) lineage (which includes BALB/cByJ) are typically susceptible, while those descended from BALB/cJ prove to be resistant [217]. Later in life, BALB/c mice develop cancers such as reticular neoplasms, primary lung tumors, and renal tumors [218]. Besides, pathological and clinical evidence suggesting cutaneous allergy and wasting syndrome in BALB/c mouse [219]. BALB/cJ has been used in different models to support immunology, autoimmune, inflammatory, and infectious disease research. Susceptibility of this strain to EBA has been systemically compared to other stains in this thesis. Previously, we had incidental indications for a lower susceptibility to antibody-transfer induced EBA [64].

3.1.7.8. BXD2/TyJ mice

BXD2/TyJ mice are derived from multiple crosses on C57BL/6J and DBA1/J mice to generate BXD stains to identify genetic susceptibility. These recombinant inbred are used to study the genetics of behavioral phenotypes including alcohol and drug addiction, stress, and locomotor activity [220]. 50% of females by eight months of age and 90% of males greater than 12 months BXD2/TyJ mice develop spontaneous arthritis in such mice [221]. These mice are suggested as a strain which can be used in immunology and inflammation and auto immunity. They have been used for the genetic variation. Furthermore, they are chosen as one of the

parental strain to generation of the four-way intercross and they were checked for susceptibility to immunization-induced EBA.

3.1.7.9. B10.S-H2s/SgMcdJ mice

In this congenic strain, the H2 complex derived from A.SW (*H2s*) was introgressed onto the C57BL/10SnSg background [222]. The *H2s* haplotype is s at the class I (K,D) loci and the class II loci (A, E) and b at T18 [223]. Mice congenic for H2 haplotypes are widely used in immunologic research and often vary in immune response and pathogen susceptibility from the recipient strain [224]. This mice are suggested as a strain which can be used in immunology and inflammation and autoimmunity disorders. Susceptibility of this strain to antibody-transfer induced EBA has been checked in this thesis. Previously susceptibility of this strain in immunization-induced EBA has been checked in our group [54].

3.1.7.10. C3H/HeJ mice

C3H/HeJ is the most common substrain of C3H. They have high lung volume and alveolar size compared to other inbred strains, about 50% more lung volume than C57BL6 [225, 226]. In a wide variety of research areas including cancer, immunology and inflammation, sensorineural, and cardiovascular biology have been used [227-229]. C3H/HeJ mice spontaneously develop the autoimmune disease alopecia areata [230]. These mice because of having TLR deficiency are interesting for immunology and autoimmunity researches. Susceptibility of this strain to antibody-transfer induced EBA has been checked in this thesis.

3.1.7.11. Cast/EiJL mice

This strain first time in Thailand was derived from wild trapped mice. Wild-derived mice and common laboratory mice are genetically defined because of number of complex phenotypic characteristics common laboratory strains are often with CAST to generate F1 hybrids with high levels of heterozygosity for use in genetic mapping [231]. Cast mice as a wild strain are untapped natural resources for genetic studies [232] and therefore they have been used for the genetic variation. Furthermore, they are chosen as one of the parental strain to generation of the four-way intercross and they have been checked in this thesis for susceptibility to immunization-induced EBA.

3.1.7.12. CBA/J mice

CBA/J was developed from a cross of an unpedigreed Bagg albino female and an early DBA1/J progenitor male. They are known for their longevity and low tumor incidence. These inbred mice are widely used as a general-purpose strain. CBA/J strain is the only CBA sub-strain carrying the *Pde6b*^{rd1} mutation, *Pde6brd1* causes blindness by wean age [233, 234].

The CBA/J inbred mouse strain is widely used to study granulomatous experimental autoimmune thyroiditis (G-EAT). They also develop a mild hearing loss late in life [235]. Susceptibility of this strain to EBA has been systemically compared to other stains in this thesis.

3.1.7.13. DBA1/J mice

This strain is the oldest of all inbred strains of mice initiated by CC Little in 1909 during coat color experiments from stock segregating for recessive coat color genes: *d, b, a*: dilute, brown, non agouti, and was named for those genes, now *Myo5ad*, *Tyrp1b*, *a*. Substrains DBA/1J and DBA/2J were developed later in 1929. DBA/1J are susceptible to type II collagen induced arthritis [236, 237], and the susceptibility is linked to the expression of specific MHC class II molecules [238]. In response to challenge, DBA/1J mice develop immune-mediated nephritis characterized by proteinuria, glomerulonephritis and tubulointerstitial disease [239]. DBA/1J has been used in different models of immunology, autoimmunity, inflammatory and infectious diseases. Susceptibility of this strain to EBA has been checked in this thesis.

3.1.7.14. FVB/NJ mice

This strain is inbred for the *FV1b* allele confers sensitivity to the Friend leukemia virus B strain compared to many other inbred strains [240]. FVB/NJ is highly susceptible to asthma-like airway responsiveness with significant generation of antigen-specific IgE [241]. FVB/NJ is resistant to collagen-induced arthritis despite having the *H2q* MHC haplotype [242]. These mice are genetically deficient in complement C5 [243]. Complement deficiency in these mice make them good candidate to check their susceptibility in our EBA model.

3.1.7.15. MRL/MpJ mice

Despite carrying the normal Fas gene, MRL/MpJ mice also exhibit autoimmune disorders but symptoms are manifested much later in life compared to those the MRL/MpJ-Faslpr mice. As a strain developed as the control for MRL/MpJ-Faslpr, MRL/MpJ mice are useful in the study of their comparable defects and diseases. Females develop spontaneous pancreatitis in over 22 weeks of age [244]. This strain has been used to support research in many areas including inflammation and autoimmunity such as sjogren syndrome, autoimmune pancreatitis, sialoadenitis experimentally induced rheumatoid arthritis and lupus erythematosus. They have been used for the genetic variation. Furthermore, they are chosen as one of the parental strain to generation of the four-way intercross and they were checked for susceptibility to immunization-induced EBA.

3.1.7.16. NOD/ShiLtJ mice

NOD (non obese diabetic) mice derive from Japanese ICR outbred stock selected for high fasting blood glucose (diabetes) without cataract [245]. Immunophenotypes include defective antigen presenting cell immunoregulatory functions, defects in T lymphocyte regulation, defective NK cell function, and defective cytokine production from macrophages [246]. The major component of diabetes susceptibility in NOD mice is the unique MHC haplotype ($H2^{g7}$= Kd, Aad, Abg7, Enull, Db). In NOD mice multiple aberrant immunophenotypes such as defective antigen presenting cell immunoregulatory functions, defects in the regulation of the T lymphocyte repertoire. They also lack hemolytic complement, C5 [243]. Susceptibility of this strain to EBA has been checked in this thesis.

3.1.7.17. NZM2410/J mice

This inbred strain develops severe lupus nephritis at an early age [247]. The NZM2410/J strain is derived from the NZB/WF1 model. Both males and females show early onset of severe lupus nephritis [247]. They have been used for the genetic variation. Furthermore, they are chosen as one of the parental strain to generation of the four-way intercross and they were checked for susceptibility to immunization-induced EBA.

3.1.7.18. PL/J mice

This inbred strain widely used in studies of retinal degeneration. PL/J mice show a moderate susceptibility to experimental autoimmune encephalitis (EAE) with late onset and high mortality [248]. PL/J mice also were used as a model of psoriasis [249]. Susceptibility of this strain to EBA has been checked in this thesis.

3.1.7.19. PWD/PhJ mice

They are an inbred mouse strain of the subspecies Mus musculus musculus (M.m.m.). M. m. m. is estimated to have diverged approximately 1 million years ago from M. m. domesticus that is the subspecies from which derives most of the genome of practically every laboratory mouse strain. PWD/PhJ mice are distinct from common laboratory mice in body mass, distribution of adipose tissue, serum concentrations of intermediary metabolites, susceptibility to type I diabetes and various behavioral traits. For the reason that this strain is an inbred mouse strain derived from wild mice therefore is an excellent tool for mapping both single-gene (Mendelian) traits and QTL. Susceptibility of this strain to EBA has been checked in this thesis.

3.1.7.20. SJL/J mice

This inbred albino strain derived in 1955 from three different sources of Swiss Webster mice. They are popular for high incidence of lymphomas (formerly called reticulum cell sarcoma type B) that resemble Hodgkin's disease [250, 251]. This strain is also characterized by susceptibility to EAE for multiple sclerosis research [252]. This strain presents with severe EBA symptoms after immunization with COL7. It has been shown that susceptibility to EBA was strongly associated with *H2s* in this strain [253]. Susceptibility of this strain to antibody-transfer induced EBA has been checked in this thesis.

3.2. Methods

3.2.1. Generation and purification of anti-COL7 immune sera

Recombinant non-collagenous NC1 domain was expressed and purified according to the established protocol [49] by Claudia Launderer in Dermatology Laboratory of Lubbock. Rabbit Immune sera were commercially generated (Eurogentec GmbH, Belgium). In detail, rabbits were injected with recombinant non collagenous fragment of mCOL7 twice (at 15-day interval) subcutaneously with 200 µg of an equimolar mixture of the 3 purified recombinant proteins in Freund´s complete adjuvant. Collected sera were delivered to dermatology laboratory and were analyzed by indirect IF on cryosections of murine skin in order to confirm the ability of IgG to bind to COL7 in dermal-epidermal junction. I regularly purified the IgG for the experiments in passive transfer EBA using Protein-G sepharose fast flow affinity column chromatography (Amersham Biosciences). Antibodies were eluted with 0.1M glycine buffer (pH 2.8) and neutralized with 1M Tris-HCl (pH 9). Obtained antibody fraction was concentrated in extensive washing with PBS (pH 7.2) using 30kD Millipore filters (Millipore). Purified IgG was later filter-sterilized (pore size, 0.22 µm; Millipore) and the protein concentration was measured spectrophotometrically at 280 nm. Reactivity of IgG fractions was analyzed by IF microscopy on murine skin. As a control, normal rabbit (NR) IgG was used which was also purified from rabbit sera using same protocol mentioned above.

3.2.2. Expression and purification of vWFA2

The C-terminal subdomain of NC-1 shows high homology with vWFA, and was therefore termed vWFA2. vWFA2 of Col7 is recognized by autoantibodies in about 80% of EBA patients. Additionally, it has been suggested that vWFA2 is responsible for type I collagen binding [254]. However, the importance of this interaction is subject of controversial discussions. Seeger et al. showed in their study that murine vWFA2 binds not only to type I collagen, but also interacts

with type III collagen and type IV collagen [39]. This implies that vWFA2 recognizes the collagen triple helix. Chemical modification and mutations of vWFA2 lead to abrogation of the interaction with type I collagen thus allowing the localization of the binding interface for collagens at vWFA2 [39, 50, 254]. vWFA2 which I used in this study for immunizing mice in the active model was prepared in the group of Prof. Seeger in the Institute of Chemistry, University of Lübeck.

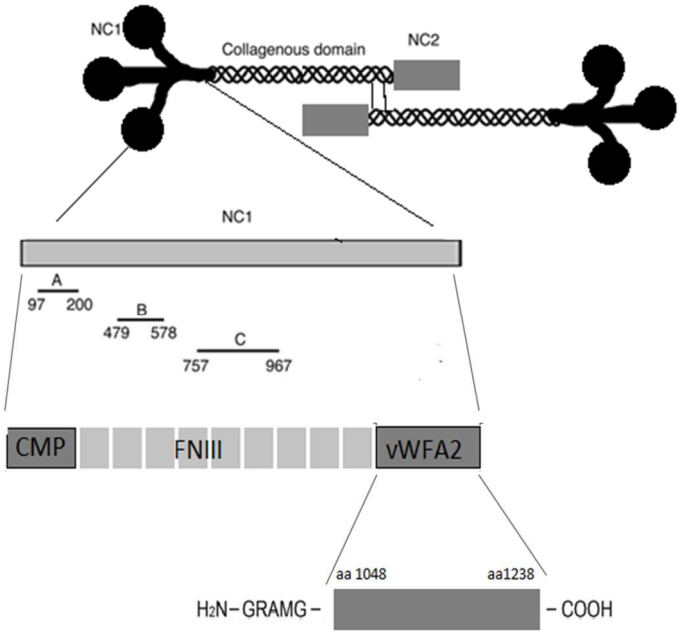

Figure 9: Schematic model of mCOL7. COL7 is composed of 3 identical chains, each one consisting of a central triple helical C domain, flanked by a large amino-terminal NC-1 domain and a smaller carboxy-terminal NC-2 domain. Two molecules form antiparallel tail-to-tail dimers stabilized by disulfide bonding through a carboxy-terminal overlap between NC-2 domains. Within the murine NC-1 domain, the vWFA2 domain is located at amino acids 1048–1238 [49].

3.2.3. Animal experiments

3.2.3.1. Induction of experimental EBA

In this thesis, antibody-transfer (passive) and immunization-induced (active) EBA mouse models were used. Both models have been developed and subsequently optimized in the laboratory [48, 62, 255].

3.2.3.1.1. Passive transfer models of EBA

Induction of antibody-transfer was performed as previously described, with minor modifications [49]. Briefly, 6-8 week old mice of the indicated strains were injected every second day subcutaneously in abdominal skin with purified rabbit IgG from mCOL7 immune sera, for 5 times in total. Normal rabbit IgG in the same concentration served as a negative control. Every four days mice were examined for any evidence of lesions (i.e. erythema, blisters, erosions, and crusts). To evaluate circulating antibody levels, sera were obtained from mice. On day 12, mice were killed to obtain samples for further analysis (Figure 10). Regarding RORα -/- mice different age and frequency due to premature death has been used (details below).

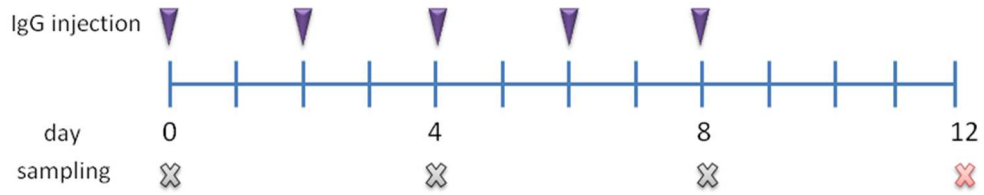

Figure 10: Induction of experimental EBA by transfer of anti-COL7 IgG.

Polyclonal antibodies against mCOL7 were generated in rabbits by immunization with recombinant mCOL7. The IgG fraction from immune rabbit sera was purified by protein G chromatography and, subcutaneously injected into mice every second day for a period of 12 days. At day 12 the mice were sacrificed. Crosses indicate the sampling or scoring days and arrows represent the injection days. The red cross indicates the end of the experiment.

3.2.3.1.2. Immunization-induced EBA mouse model

In the immunization-induced model, eight weeks aged SJL mice were immunized with 60 µg of purified recombinant protein (vWFA2) emulsified in adjuvant (TiterMax®, Alexis, Lörrach, Germany). Briefly, 60 µg of recombinant protein, emulsified in adjuvant TiterMax in a volume ratio 1:1, (Hiss, Freiburg, Germany), was subcutaneously injected into the hind footpads of mice. For immunization of 10 mice, 600 µL of protein was mixed with 600 µL of TiterMax™ on

vortex for 20 minutes until emulsions were fully formed. Of this mixture, 60 µL was injected per mouse as described [256]. Besides, control mice were immunized with PBS and TiterMax. Extend of clinical EBA manifestation was determined on a weekly basis. If at least 2% of the body area surface was affected, mice were randomly allocated to PBS, anakinra or VX-765 (see below for details). All mice were observed for two weeks after allocation to treatment.

From every mouse, serum and tissues samples were obtained at the end of treatment period. Serum samples were assayed for autoantibody level by ELISA using recombinant protein. Biopsies of ear were collected at the end of the observation period and prepared for examination by histopathology, and direct IF microscopy.

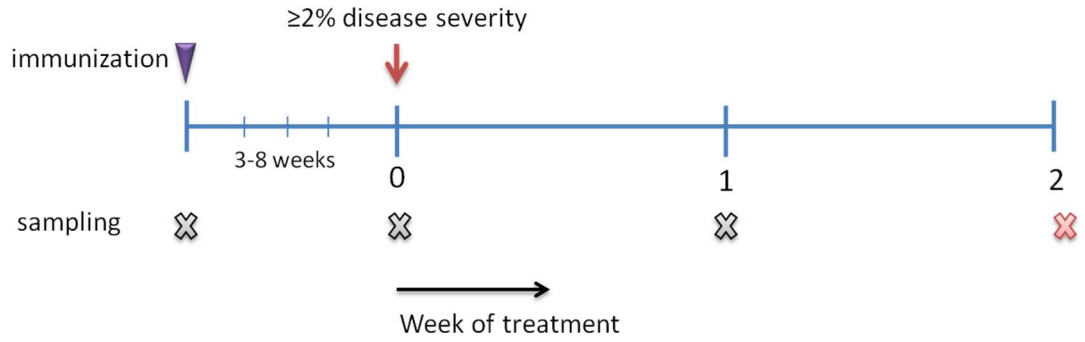

Figure 11: mCOL7-GST and vWFA2 immunization plan.

Mice were immunized with 60 µg recombinant protein (vWFA2). Violet arrow indicates the immunization time points. Crosses indicate the scoring sampling time points and red cross indicates sacrificing. After disease severity of each mouse reached to 2%, each mouse got to a treatment group. Treatment duration was for two weeks and after, mice were sacrificed and samples were collected.

3.2.3.2. Calculation of disease severity

Disease severity was expressed as percentage of body surface area affected by skin lesions and determined at three time points (day 4, 8, 12) in antibody-transfer induced EBA and weekly in immunization-induced EBA. Affected body surface area was calculated by allotting individual fraction to each part of the body (ear (left)-2.5%, ear (right)-2.5%, eye (right)-0.5%, eye (left)-0.5%, snout-2.5%, oral mucosa-2.5%, head&neck-9%, front leg (left)-5%, front leg (right)-5%, rear leg (left)- 10%, rear leg (right)-10%, tail-10% and trunk-40%)) to get total body surface area in percentage. An example of calculation table is shown below in table 3.

Date:		
Mouse nr.	**Type of lesion**	**Lesion**
Ear (left)	Erosion	10
Ear (right)	Crust	10
Eye (right)	Crust, Erosion	25
Eye (left)		0
Snout		0
Oral mucosa		0
Head&neck		0
Front leg (left)	Alopecia	20
Front leg (right)	Erythema	3
Rear leg (left)		0
Rear leg (right)		0
Tail	Crust	7
Trunk		0
Overall score		2,5

Table 3: Mouse clinical scoring calculation table.

Each body part of the mouse was assigned with individual percentage and total effected body surface was calculated as overall score of lesion on individual body parts. Filled example table shown with overall score after final calculation. The area under the curve (AUC) was calculated using scores in different time points, taking both disease onset and maximal disease severity into account. Blood and tissue samples were collected on day 12. This antibody transfer EBA duplicates the clinical, histological, and immunopathological findings of the inflammatory variant of the human disease.

3.2.3.3. Sample handling

Biopsied tissue was immediately embedded in with Tissue-Tek® O.T.C. (Sakura Finetek Europe B.V.) and frozen in liquid nitrogen. These cryoblocks were kept at -80°C. For histopathology, biopsies of ear were fixed in 4% buffered formalin. Blood was obtained by cardiac puncture under terminal anesthesia. Serum was prepared by allowing blood to clot and centrifuging (BIOFUGE fresco, Heraeus Instruments GmbH, Hanau, Germany) at 13,000 g for 15 minutes at 4°C. All samples were then stored at −80°C until further use.

3.2.3.4. Treatment

3.2.3.4.1. VX-765

Deionized water containing 0.5% Hydroxy Ethyl Cellulose (Sigma) and 0.1% tween-80 (Sigma) was prepared as vehicle and store at 2-8°C and was used for making the formulation without waiting for the vehicle to warm up. Having the vehicle cold minimize bubble formation. VX-765 dissolved in prepared vehicle according to Table 4. The dosing for each mouse was done by volume adjustment of the initial VX-765 preparation at 20 mg/ml (20 mg/ml formulation

concentration in vehicle). VX-765 starting material was kept in room temperature (rt) for 1 hour. Weighed material placed into clean glassware and a homogenizer with appropriate size based on volume used for mixing particles for ten minutes with speed of 2,500 rpm speed increased gradually to about 7,000 rpm. Water bath sonicator used for 20 minutes to reduce the foam. The formulation made is milky-white suspension formulation.

In immunization-induced EBA, VX-765 at 100 mg/kg was administered p.o. by oral gavage once or twice per day according to the treatment group and throughout the duration of the experiment. In antibody-transfer induced EBA, C57BL/6 mice were treated daily for 12 days.

Group	**Dose level in VX-765 (mg/kg/day)**	**Dose volume (ml/kg/day)**
1*VX	100	5
2*VX	200	10

Table 4: Dose of VX-765 used in treatment groups.

3.2.3.4.2. Anakinra

Kineret® (Anakinra, Biovitrum AB, Stockholm, Sweden) was injected i.p. into mice at either 100 or 200 mg/kg per day. In the passive EBA mouse model, mice were treated daily. In the active EBA mouse model, anakinra treatment was started when at least 2% of the body surface area were affected by skin lesions and was continued on a daily basis for a total of two weeks. PBS treatment as served as control.

3.2.4. *In vitro* experiments

3.2.4.1. Determination of human serum cytokine concentrations

Serum from EBA patients and normal controls were analyzed for expression of 23 cytokines (TNF-α, Macrophage inflammatory protein (MIP)-1α, MIP-1β, GM-CSF, G-CSF, IL-1α, IL-1β, IL-2, IL-3, IL-4, IL-5, IL-6, KC, IL-9, IL-10, IL-12p40, IL-12p70, IL-13, IL-17, Eotaxin, RANTES, IFN-γ and monocyte chemotactic protein-1 (MCP-1) using bioplex (Bioglobe GmbH, Hamburg, Germany). In addition, serum concentrations of all the above cytokines or their corresponding homologs were determined in mice with experimental EBA and appropriate controls at the indicated time points using bioplex (Bioglobe GmbH).

3.2.4.2. Hematoxylin and Eosin staining

In order to microscopically view a sectioned tissue specimen, the specimen must be stained in order to be visible. The basic nature staining in histology is to stain the sections with one or more dyes that highlight specific areas. The most standard staining is hematoxylin and eosin (H&E). Hematoxylin, a dark purplish dye stains the nucleus, while eosin, an orangish-pink to red dye stains the cytoplasm and connective tissue, including collagen [257]. Murine specimens were stained for H&E using protocols established in the routine histology laboratory of the Department of Dermatology in Lübeck. Skin samples were fixed in 4% buffered formalin and processed into paraffin blocks. Four µm sections were prepared and stained with H&E according to standard protocols [253]. Extend of leukocyte infiltration in these sections were scored semi-quantitatively in at least ten optical fields at the area of DEJ by an observer unaware of the mouse strain and (if applicable) treatment.

3.2.4.3. Immunohistochemistry

Immunohistochemistry (IHC) is a wide-used biological technique and is usually used for the characterization of normal and pathologic tissue. Immunohistochemistry is used to detect antigens in a highly sensitive and specific way in tissue sections by means of immunological and chemical reactions [258]. The fundamental principle in IHC is the optical visualization of antigens within tissue sections by means of specific antibodies. The stable antigen–antibody complex is demonstrated with a colored histochemical reaction visible by light microscopy or fluorochromes by fluorescent microscopy. The procedure was first introduced by Dr. Albert Coons in 1941 [259].

3.2.4.4. Determination of cutaneous IL-1 and ICAM-1 protein expression

IL-1 expression in skin was determined by immunohistochemistry. Six µm cryosections of lesional skin obtained from vWFA2-immunised C57BL/6 mice were fixed in acetone and kept

at -20°C for 10 minutes. Next, dried sections were washed with PBS for five minutes three times, and then were incubated with Dako Dual Endogenous Enzyme Block (DakoCytomation, Hamburg, Germany) for 30 minutes at rt for blocking endogenous peroxydase. To reduce non-specific binding of secondary antibody, sections were incubated with 5% normal rabbit serum for 20 minutes at rt, for both IL-1α and IL-1β staining, cryosections were incubated at rt for one hour with primary antibody goat anti-mouse IL-1α and goat anti-mouse IL-1β antibody (1:200, R&D Systems, Wiesbaden, Germany), respectively. As secondary antibody, rabbit anti-goat antibody (1:1000, Dako, Hamburg, Germany) was used. Incubation with HistoGreen (LINARIS, Germany), counterstaining with haematoxylin and dehydrating were subsequently done before mounting slides. Intensity of IL-1 expression was scored semi-quantitatively in at least ten optical fields at the area of DEJ, by two observers, and the mean value was calculated. The second observer was unaware of the nature of the specimen.

To estimate the relative levels of ICAM-1 on skin, frozen sections were immunostained. In brief, 6-µm thick mice's ear sections were fixed in acetone at minus 20°C for ten minutes. Air dried sections were washed with PBS for five minutes three times and incubated with Dako Dual Endogenous Enzyme Block (DakoCytomation, Hamburg, Germany) for 30 minutes at rt to block endogenous peroxidase. To reduce non-specific binding of secondary antibody, sections were incubated with 5% normal rabbit serum for 20 minutes at rt. Next, excess serum was washed out, and sections were incubated with the pre-diluted primary antibody, Armenian hamster anti-mouse served as primary antibody (1:200, BD), at rt for one hour. Slides were washed with PBS followed by incubation with rabbit anti-armenian hamster (1:1000 Abcam, Cambridge, UK) as secondary antibody for 45 minutes at rt. To develop the peroxidase reaction, sections were incubated in HistoGreen solution (LINARIS, Wertheim-Bettingen, Germany) until appropriate color developed. Excess solution was washed in tap water, followed by counterstaining with haematoxylin before mounting slides. Intensity of ICAM-1 expression was scored semi-quantitatively in at least 10 optical fields at the area of DEJ by two observers, and the mean value was calculated [260]. The second observer was unaware of the nature of the specimen.

3.2.4.5. Direct IF microscopy

Direct IF microscopy aims to identify the presence and the location of tissue bound IgG and murine C3 in experimental EBA by the use of a fluorescent-labeled specific antibody. IF microscopy on 6 µm frozen sections prepared from tissue biopsies using fluorescein isothiocyanate (FITC)-conjugated polyclonal goat anti-rabbit IgG (1:100 dilution in PBS; all obtained from BD Pharmingen) was used to detect antibodies bound on the DEJ, or murine

C3 (1:50 dilution in PBS; Cappel MP Biomedicals LLC, OH, USA). The presence of fluorescence in the upper layer of the epithelium indicates that IgG was deposited in the skin prior to the biopsy [48]. ImageJ software is a Java-based image processing program which used to evaluate Fluorescence intensity of IgG and C3 deposition [343].

3.2.4.6. Indirect IF microscopy

Indirect IF microscopy used to detect serum autoantibodies in mice. Six µm frozen sections of mouse skin were prepared, and they were incubated with appropriately diluted rabbit serum (and mouse serum for active model). Later, FITC-labeled polyclonal swine anti-rabbit IgG (1:100, DAKO), or FITC-conjugated rabbit anti-mouse IgG (dilution 1:100 in PBS; DakoCytomation) was added, respectively. After 45 minutes incubation at rt slides were washed with PBS and mounted in buffered glycerol. Normal rabbit IgG or normal mouse serum were used as negative controls [48].

3.2.4.7. Detection of circulating COL7-specific autoantibodies in mice sera

For detection of COL7-specific autoantibodies in mice sera, ELISA, has been performed, as explained before [261-263]. In detail, 96-well microtiter plates (Maxlsorb": Nunc, Roskilde, Denmark) were coated with vWVFA2 at concentration of 5 µg/ml (250 ng/well) in 0.05 M carbonate-bicarbonate buffer, pH 9.6. After overnight incubation at 4°C plates were washed three times with PBST 20 using an automatic microplate washer (Columbus Pro, Tecan, Crailsheim, Germany) and blocked with PBST 20 containing 1% bovine serum albumin (BSA) (Sigma-Aldrich, Hamburg, Germany) at rt for 90 minutes. The mice' sera dilutions were done in PBST 20 containing 1% BSA and ranged from 1:5,000 to 1:125,000. After washing with PBST 20 three times with the automatic microplate washer, wells were incubated with 100 µL rabbit anti-mouse IgG conjugated with horse radish peroxidase (HRP) (BD Pharmingen, Germany); dilution 1:10,000 with PBST 20 containing 1% BSA for 1 hour at rt. Then, plates were washed with PBST 20 three times with PBST 20 with the automatic microplate washer and 100 µL i-step Turbo TM-ELISA (Thermo Scientific, Rockford, USA) substrate was added for visualization of antibody binding. The reaction was terminated with the addition of 50 µL H_2SO_4 and the OD450nm was measured using a VICTOR3 Wallac 1420 microplate reader. All sera were tested in duplicates. From the mean optical density (OD) value for each serum sample, the mean OD value of the blank was subtracted.

3.2.4.8. Detection of circulating rabbit anti-mouse COL7 IgG in mice sera

For the detection of circulating anti-mCOL7 rabbit IgG, ELISA was used. 96-well microtiter plates (Maxlsorb: Nunc, Roskilde, Denmark) were coated with GST-mCOL7 at concentration

of 5 µg/ml (250 ng/well) in 0.05 M Carbonate-Bicarbonate buffer, pH 9.6. After overnight incubation at 4°C plates were then washed three times with PBST 20 using an automatic microplate washer (Columbus Pro, Tecan, Crailsheim, Germany), and blocked with PBST containing 1% BSA, (Sigma-Aldrich, Hamburg, Germany) at rt for 90 minutes. Plates were next incubated with 100 µL mice sera diluted 1:1000 in PBST containing 1% BSA at rt for 90 minutes. After washing with PBST, wells were incubated with 100 µL antibody conjugated with HRP (BD Pharmingen, Germany); dilution 1:10,000 with PBST containing 1% BSA for one hour at rt. Development was performed by 1-Step adding 100 µL Turbo TMB-ELISA solution. The reaction was terminated with the addition of 100 µL H_2SO_4. The OD450nm was measured using a VICTOR3 Wallac 1420 microplate reader. All sera were tested in duplicates. From the mean OD value for each serum sample, the mean OD value of the blank was subtracted.

3.2.4.9. IL-1β detection by ELISA

For analysis of human and mice IL-1β levels, ELISA was performed using a kits from e-bioscience (San Diego, USA) or PeproTech (Hamburg, Germany), respectively. Experiments were performed according to manufacturer's protocols. The dilutions for mice sera was 1:4 and for cells supernatant 1:2.

3.2.4.10. Determination and semi-quantification of active IL-1β concentration in the skin

Ear specimen from mice were excised, and immediately snap frozen in liquid nitrogen and stored at -80 °C until further analysis. For preparation of total protein skin extracts, frozen ears were grinded in liquid nitrogen, homogenized in T-PER reagent (Thermo Scientific, Darmstadt, Germany; 1:6), with the addition of protease inhibitor cocktail set III (Calbiochem, Darmstadt, Germany; 1:100). Tissue homogenates were centrifuged at 10,000g for 10min at 4°C to pellet debris and supernatants were collected. Next, samples were incubated with protein A/G PLUS-Agarose beads (Santa Cruz Biotechnology, Heidelberg, Germany; 5:1) at 4° C on rotating device, overnight. Beads were pelleted by centrifugation at 1,000g for 5 min at 4° C, and supernatants were collected and stored at −80 °C until use. Total protein concentration was determined according to BCA method (Thermo Scientific). Protein samples were separated by SDS-PAGE under reducing conditions on a 15% polyacrylamide gel and transferred to a 0.2 µm-pore size nitrocellulose membrane for western blotting. Membranes were blocked with 5% w/v skim milk powder in Tris-Buffer Saline-0.1% v/v Tween-20 (TBS-T) for 1 h at room temperature (RT). Between each step membranes were washed 5 times for 10 min in TBS-T. All antibodies were diluted in blocking buffer. Goat polyclonal IgG against murine IL-1β (R&D SYSTEMS) and mouse monoclonal IgG against actin (Santa Cruz Biotech) were used at 1:400 and 1:3000 dilutions, respectively, overnight at 4°C. HRP-labeled

secondary antibodies for goat (Dako, Hamburg, Germany) and mouse (Jackson ImmunoResearch, Suffolk, UK) were applied at 1:20,000 and 1:50,000 dilutions, respectively, for 1h at RT and detected by Amersham ECL Prime reagent (GE Healthcare).

3.2.4.11. RT-PCR from mouse skin

For analysis of cytokine mRNA expression, cryosections of ear skin were dissolved in 700µl lysis buffer. Total RNA was isolated according to the manufacturer's protocol (InnuPrep RNA Mini Kit, Analytic Jena AG) and reverse transcribed. The cDNA was added to quantitative polymerase chain reaction (QPCR) Master Mix Plus (Eurogentec GmbH, Cologne, Germany) and amplified using the SDS ABI 7900 system (Applied Biosystems, Darmstadt, Germany). TaqMan probes, forward and reverse primers were designed using the computer software CloneManager (version 7.01; Sci Ed Central). The same batch of cDNA (20µl) was used to determine the cycles of threshold. The amount of cDNA copies was normalized to the housekeeping gene metastatic lymph node 51 (MLN51). Optimal primer concentrations used were 900nM each for the forward and reverse primers and 200nM for the TaqMan probe (Biomers.net, Ulm, Germany). For IL-1Ra primers, sequences were kindly provided by Prof. Cem Gabay and Dr. Celine Lamacchia (Division of Rheumatology, University Hospitals of Geneva, Geneva, Switzerland). All the data expressed as relative expression x 100 in relation to MLN51. All used primers are listed in table 5. All RT-PCR experiments were performed by Dr. Kathrin Kalies (Institute of Anatomy, University of Lübeck). I obtained the samples from mice, prepared samples for RT-PCR and analyzed the data generated by Dr. Kalies.

Name	**Primer sequence**
mIL-1Ra (soluble)	5‘ TTGC TGTG GCCT CGGG ATGG 3‘
mIL-1Ra (intracellular)	5‘AGAC ACTG CCTG GGTG CTCC T 3‘
mIL-1Ra rev	5‘GTTT GATATTTGGTCC TTGTAAG 3‘

Table 5: List of primers used in RT-PCR from mouse skin.

3.2.4.12. Preparation of Phorbol myristate acetate (PMA) and LPS

To prepare stock solution of Phorbol 12-myristate 13-acetate (PMA) (Sigma) was diluted in DMSO (Sigma) in a concentration of 1mg/ml. Aliquots were stored at −20°C until use. To prepare stock solution of LPS (Sigma), LPS was diluted in the culture medium in a concentration of 1mg/ml. Aliquots were stored at −20°C until use.

3.2.4.13. Optimization of stimuli and inhibitor concentrations

P-388D1 (murine macrophages cell line which produces IL-1) were cultured in RPMI-1640 growth medium (Lonza), supplemented with heat inactivated (56°C for 30 minutes) 20% horse serum (Gibco), at 37°C in 5% CO_2 atmosphere. Cells were seeded on 12-well plates (Greiner Bio-One, Solingen, Germany) and allowed to grow until ~80% confluence. In order to stimulate cells for IL-1β release, cells were first incubated with different concentrations (50 ng/ml, 100 ng/ml, 150 ng/ml, 200 ng/ml and 250 ng/ml) of LPS or PMA for two hours, followed by treatment with 5 mM ATP for 20 minutes. These treatments were performed in the presence of different concentrations of VX-765 (5 µg/ml, 10 µg/ml, 15 µg/ml and 20 µg/ml), which was added to the cell cultures together with the treatment with either LPS or PMA. Cells treated with the vehicle only, served as negative controls. At the endpoint of experiment, supernatants were harvested and stored at −20°C for further analysis.

3.2.4.14. Human keratinocyte line (HaCaT) cells experiments

HaCaT cells were cultured in serum-free keratinocyte growth medium (Promo Cell, Heidelberg, Germany) at 37°C in 5% CO_2 atmosphere. Cells were seeded on 12-well plates (Greiner Bio-One, Solingen, Germany) and allowed to grow until ~80% confluence. In order to stimulate cells for IL-1β release, cells were first primed with 150 ng/ml LPS or 50 ng/ml PMA, followed by treatment with 5 mM ATP for 20 minutes. These treatments were performed in the absence or presence different concentrations of VX-765, ranging from 5 to 20 µg/ml, which was added to the cell cultures during the priming. P-388D1 served as controls and HaCaT cells treated with the vehicle only served as a negative control. At the endpoint of experiment, supernatants were harvested and stored at −20°C for further analysis.

3.2.4.15. Human endothelial cells

Human umbilical vein endothelial cells (HUVEC; PromoCell, Heidelberg, Germany) were cultured in Endothelial Cell Growth Medium (PromoCell) at 37 °C in a humidified atmosphere containing 5% CO_2. Four hours prior to activation, the medium was replaced by Endothelial Cell Basal Medium (PromoCell) supplemented with 10% FCS. In order to induce adhesion molecule expression, endothelial cells were activated with recombinant human IL-1β (5 ng/ml) or TNFα (25 ng/ml) for four hours. These treatments were performed either in the presence or absence of anakinra (5 µg/ml), which was added to the cell cultures one hour before treatment with either TNFα or IL-1β Non-treated cells served as negative controls (these experiment have been performed by the group of Prof. M. Schön, University of Göttingen).

3.2.5. Genetic studies for EBA susceptible genes

For mapping EBA susceptibility genes, experimental EBA was induced in female mice by antibody transfer to inbred mouse strains (A/J, AKR/J, B10.S-H2s/SgMcdJ, BALB/cJ, BXD2/TyJ, C3H/HeJ, C57BL/6J, Cast/EiJ, CBA/J, DBA1/J, FVB/NJ, MRL/MpJ, NOD/ShiLtJ, NZM2410/J, PL/J, PWD/PhJ, SJL/J and WSP/EiJ) and then a two-stage case-control association study was performed using tagging SNP (tSNP) selection.

3.2.5.1. Tagging SNPs

The use of tSNPs is a method to greatly reduce the number of polymorphisms required to be genotyped. This is achieved by selecting a minimal subset, which act as proxies for the others, and capture all of the variation contained within the full set. Polymorphisms are able to act as proxies for each other through linkage disequilibrium (LD). Loci on the same chromosome are in LD when they are inherited together more often than expected by chance following independent assortment. Genetic recombination during meiosis results in random-assortment of the parental variant combinations in the offspring. Theoretically, the physically further apart loci are on the chromosome, the greater the chance that recombination will have occurred. This would result in a steady decrease of LD over distance. However, recombination rates are not constant over the genome, with regions known as recombination hot spots, having much higher recombination rates than the rest of the genome. Regions of high LD separated by regions of no LD are seen across the genome, giving rise to a block-like pattern of LD (The International HapMap Consortium, 2005). Because there is not a consistent correlation between distance and LD, it is therefore necessary for LD relationships between pairs of polymorphisms to be determined empirically.

3.2.5.2. SNP dataset

SNP data for 7.8 million genomic locations for 16 inbred murine strains was accessible from Jackson mice database [344]. Association was calculated independently for each genomic location thus assuming a single gene model for the control of the trait. The second statistical approach to calculate association between traits and SNPs was based on the local structure of neighboring SNPs flanking each tested genomic location; therefore, the latter method addressed the bias between trait and local haplotype structure in the genome that is important for the effective suppression of noise and ultimate specificity of calculations.

3.2.5.2.1. SNP selection

The Jackson laboratory offers SNP data from full genome sequencing of the mouse strains used in this study. 549683 SNPs were derived and subject to both association tests (Chi square) directly in R and haplotype sharing analysis with Haploview [264]. Eight SNPs were found significant after correction for multiple testing (Bonferroni). Two of these SNPs were confirmed as associated with disease severity 300 G7 (generation 7, for details refer to 3.2.5.2.2) antibody-mediated EBA (linear model in R).

3.2.5.2.2. Four-way autoimmune-prone intercross mouse line

EBA-susceptible (BXD2 and Cast) and EBA-resistant (NZM2410/J and MRL) mice and the offspring of each generation were intercrossed following an equal strain and sex distribution. At each time, 50 breeding pairs were used to generate the next generation. A total of 300 mice from the seventh generation (G7) of this autoimmune-prone intercross mouse line were tested for antibody-transfer induced EBA susceptibility in this thesis. These mice were kindly provided by Prof. Saleh Ibrahim. The genetic diversity of this so termed four-way, intercross mouse line is reflected through different morphological traits, such as fur color.

3.2.5.2.3. SNP Genotyping

DNA was extracted from mice tail biopsies using DNeasy® Blood & Tissue kit (Qiagen, Hilden, Germany) according to the manufacturer's instructions. For the genotyping of SNPs (rs27019283, rs29179064, rs3666934, rs4212464, rs33217114, rs29543297, rs31459209, rs30860794, rs13479871, rs13480247, rs13459110), the TaqMan® SNP Genotyping Assay (Applied Biosystems, CA) was used. The amplification mixtures were prepared using 10ng DNA, 1xTaqMan® Genotype PCR Master Mix (Applied Biosystems), 1xTaqMan® SNP Genotyping Assay (Applied Biosystems) including allele specific probe and primers, labeled with the two allele specific fluorescent reporter dyes VIC (green) and FAM (blue) (table 6) and Milli-Q water in a 10 µl reaction. The PCR reactions were performed on Mastercycler ep realplex, using 96 well plates. The PCR profile was as follows: Two negative controls were included on each plate.

SNP	VIC Probe	Allel VIC	FAM Probe	Allel FAM
rs27019283	TAGACAGTGACAAAGTCT	A	ACAGTGACCAAGTCT	C
rs29179064	AGTCACTGGTTGTTTGC	T	TCACTGGCTGTTTGC	C
rs3666934	ATCAGTTCACCCTGTGAGAT	T	AGTTCACCCCGTGAGAT	C
rs4212464	CCTAAGCCCTATAACACTT	A	CCTAAGCCCTATTACACTT	T
rs33217114	CTACCAGGACAAGGAT	G	CTACCAGAACAAGGAT	A
rs29543297	TTGCCAAGCGTTCCT	G	TGCCAAGCATTCCT	A
rs31459209	CTAAGAGGGCTTATCTC	C	TCTAAGAGGGTTTATCTC	T
rs30860794	ATATTTTATTTCTCCCTTTTGCT	T	ATTTTATTTCTCCCCTTTGCT	C
rs13479871	CTCAGATCACAGGGATCAAACACTC	A	CTGGGGACTTTGTACACAACATCTA	G
rs13480247	TGACAGCCTATCTGCATTTCCATAG	A	CTTCAGAAAAGTTCATTAGCTTTCC	C
rs13459110	TGGCTCGCATTTCTAGCACTTTCAT	A	TAATGAGGCTTCTTAGGAGTCTCAC	G

Table 6: List of SNPs and probes used in this study.

3.2.5.2.4. Genotyping for RORα mice

DNA was extracted from tail biopsies using DNeasy® Blood and Tissue kit (Qiagen, Hilden. Germany). The PCR was performed in a total reaction volume of 20 µL. A master mix was prepared as indicated below:

Component	Volume
5X Phusion HF Buffer	1.25 µl
dNTPs	0.4 µl
ROR S primer (10 µM)	0.2 µl
ROR As primer (10 µM)	0.2 µl
Bgal As primer(10 µM)	0.2 µl
Phusion DNA polymerase	0.2 µl
Nuclease-free water	up to 20 µl
Template DNA	~1 µl (<60 ng)

Table 7: PCR master mix for RORα amplification.

The reactions were run in a thermal cycler GeneAmp PCR System 9700 (Applied Biosystems, Darmstadt, Germany). Briefly, initial denaturation was conducted at 95°C for five minutes, followed by 40 cycles of (denaturation at 94°C, annealing at 53°C, extension72 ºC) each for 30 seconds. Final extension 72 ºC for 10 minutes.

The primers used were as follows:

ROR S: *5′-TTCAGGAGAAGTCAGCAGAGC-3′*,

ROR As: *5′-TCACCGGCTAGTTGGCTGATTCC -3′*,

Bgal As: *5′-TGTGAGCGAGTAACAACCCGTCGGATTCT -3′* (Biomers, Ulm, Germany).

PCR products were separated by 2% agarose gel electrophoresis, stained with SYBR Green (Qiagen) and photographed under UV-light. WT (Wild Type) should get a product of about 318 bps, and ROR-Bgal will get a band of 450.

3.2.6. Statistics and computer programs

Unless otherwise noted, data is presented as mean ± standard error. For comparisons of two groups, t-test was used, whenever appropriate. For comparison of more than two groups, ANOVA or likelihood ratio test was used. For equally distributed data one-way ANOVA, followed by Bonferroni t-test for multiple comparisons, were used; if data was non-parametric, ANOVA on ranks (Kruskal-Wallis) was applied, followed by Bonferroni t-test for multiple comparisons. Pearson Product Moment Correlation was used to test for correlations. In all tests, a $p<0.05$ was considered significant. Comparisons or differences in the extent of clinical phenotypes were performed using SigmaPlot (Version 12, Systat Software Inc., Erkrath, Germany) and/or R statistical package version 3.0 [341]. Applied tests are also indicated in the figure legends. A p-value of <0.05 was considered statistically significant.

Whole-genome genotyping data were collected from the Jackson laboratory [342]. Single SNP association tests were performed using PLINK, and haplotypes were investigated using Haploview [264]. Genotyping data from the selected SNPs that were evaluated in animals from the advanced intercross line were analyzed using ANOVA on linear models, with the maximum disease score as the dependent variable and SNP data and the gender of the animals as covariates. Each SNP was analyzed separately. The obtained p values were corrected using the Benjamini-Hochberg method. To determine differentially expressed genes in the skin of mice with evident blistering after the transfer of anti-COL7 IgG compared with mice injected with control IgG, a previously published dataset was used [64]. From these data sets, all genes with a two-fold or greater change in expression that

were expressed by the regions characterized by the SNP in the validation experiment were considered.

To build up interactions among EBA-associated genes and the possible susceptible genes, identified by forward genomics, STRING was used. STRING'S algorithm proposes several.protein–protein or protein-gene association, and any known biological function or pathway [265].

4. Results

4.1. IL-1 expression in EBA

4.1.1. Increased IL-1α and IL-1β serum concentrations in antibody-transfer induced EBA

Given the pivotal role of IL-1 in the development of antibody-induced tissue, injury in the EBA model levels of circulating IL-1 were determined in both BALB/c and C57BL/6 mouse strains 12 days after the injection of either anti-COL7 or NR-IgG. In BALB/c mice by injection of anti-COL7 IgG, IL-1β, but not IL-1α, serum concentrations showed significant increase compared with mice injected with normal rabbit IgG (NR-IgG) (almost 8 fold change)(Table 8). Nonetheless, C57BL/6 mice had increase of both IL-1β, IL-1α, serum levels compared to control mice injected with NR-IgG. This experiment has been done by Dr. Kathrin Kalis (Institute of Anatomy, University of Lübeck) before I started my thesis.

In a previous study, we showed that IL-1α and IL-1β serum concentrations correlates with the extent of blistering in antibody-transfer EBA in C57BL/6 mice [71].

Cytokine	**BALB/c**		**C57BL/6**	
	NR-IgG	**anti-COL7 IgG**	**NR-IgG**	**anti-COL7 IgG**
IL-1α (pg/ml)	1373 ± 520	974 ± 433	40 ± 10	1,520 ± 221*
IL-1β (pg/ml)	18 ± 11	151 ± 47*	860 ± 260	5,861 ± 3,897*

Table 8: Induction of experimental EBA leads to an increased IL-1β expression in serum.

Induction of experimental EBA by injections of anti-COL7 IgG increases serum concentrations IL-1β but not L-1α, in BALB/c mice. In contrast both IL-1α and L-1β are increased in the serum of C57BL/6 mice. Data is based on five mice injected with normal rabbit (NR) IgG and eight mice injected with anti-COL7 IgG mice and are presented as mean ± SEM. *$p<0.05$ (Rank Sum Test). *Values are in pg/ml.*

4.1.2. Determination of serum cytokine concentrations in patients

To test if increased IL-1α and IL-1β in experimental EBA mice sera is also differentially changed in the EBA patients and to see if the mouse model can recapitulate human disease, I measured concentrations of IL-1α, IL-1β in serum of 26 EBA patients and 52 healthy controls normal human serum (NHS) using BioPlex (Bioglobe GmbH). Both, IL-1α and IL-1β were elevated in EBA patients compared to healthy controls (Table 9).

	NHS	EBA
IL-1α (pg/ml)	14,32 ± 11,8	32,61 ± 8,4
IL-1β (pg/ml)	0,77 ± 0,8	2,40 ± 4,7

Table 9: significant increased of IL-1α and IL-1β expression in serum of EBA patients.

4.1.3. Increased IL-1α IL-1β and IL-1Ra expression of skin in antibody-transfer induced EBA

To investigate if increased IL-1α and IL-1β expression is also differentially expressed in the skin, the target tissue in EBA, I determined cutaneous IL-1β and IL-1α expression in antibody-transfer induced EBA. Harvested skin tissues from diseased and healthy mice were evaluated for the presence of IL-1β and IL-1α at protein level by immunohistochemistry. Despite with elevated IL-1β in serum concentrations, both cutaneous IL-1α and IL-1β expression was found increased at protein level in antibody-transfer induced EBA mice compared to healthy controls (Figure 12).

Recently we published data regarding significantly increased mRNA level of IL-1β in lesional compared to healthy mouse skin. In detail, six days after the first IgG injection, IL-1β mRNA expression was significantly increased in anti-COL7 IgG injected animals compared to mice injected with normal rabbit IgG [71].

In separate experiment analysis of IL-1R antagonist IL-1Ra mRNA expression in skin was performed. Interleukin-1 receptor antagonist (soluble) was significantly increased in mice with experimental EBA compared with mice injected with normal rabbit IgG (fold change 0.1). But in the case of interleukin-1 receptor antagonist (intracellular) there was interestingly decreased in anti-Col7 treated mice (This experiment has been performed by Dr. Kathrin Kalies (Institute of Anatomy, University of Lübeck) and Unni Samavedam (Dept. of Dermatology, University of Lübeck)) [71].

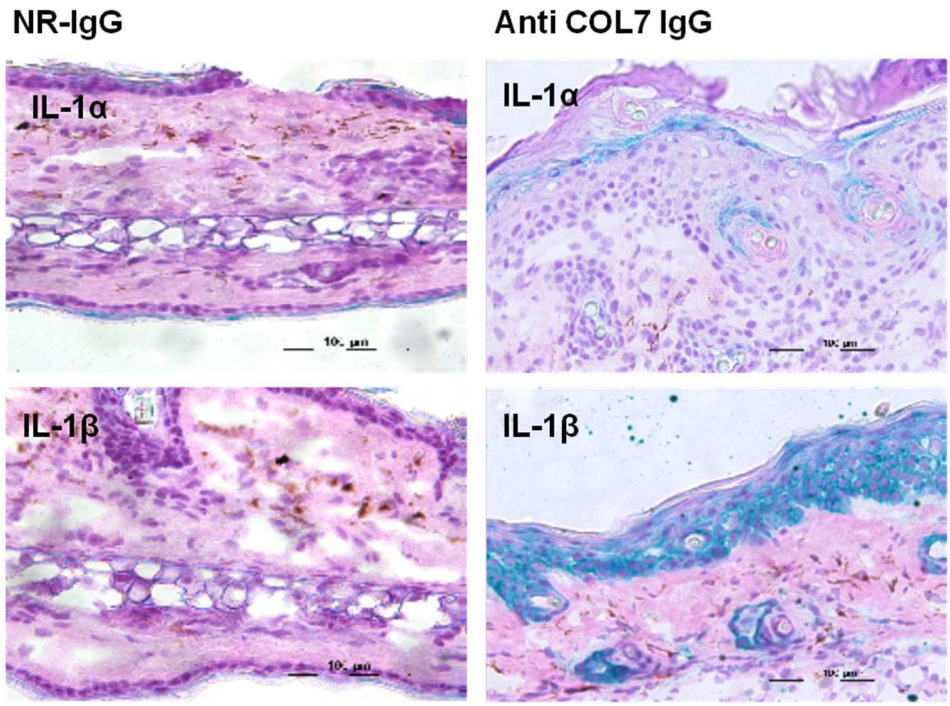

Figure 12: Skin expression of IL-1α and IL-1β is increased in experimental EBA.

Representative staining from skin specimens obtained from mice injected with normal rabbit-IgG or anti-COL7 IgG (out of 20 slides per group), 12 days after the initial IgG injection. IL-1α and IL-1β were stained using anti- IL-1α and anti-IL-1β antibodies with HRP labeled secondary antibodies. Color was developed using HistoGreen. IL-1α and IL-1β were shown in blue (Insert: isotype control staining of anti-COL7 injected mouse). Scale bar, 100 µm.

4.2. IL-1 contributes to blister formation in antibody-transfer induced EBA

4.2.1. The induction of experimental EBA is impaired in mice lacking IL-1R expression

To test if the detected increased IL-1 expression in experimental EBA is of functional relevance *in vivo*, I tested if lack of IL-1R expression attenuates blister formation in antibody-transfer induced EBA. EBA was induced in IL-1R -/- deficient (n=11) and WT control mice (n=13) in the same C57BL/6 genetic background. At the end of the 12-day observation period, both strains developed clinical evident EBA skin lesions. Representative clinical pictures are shown in Figure 13A. Clinical disease progression was monitored regularly in both groups. In IL-1R -/- mice, the overall extent of skin blistering was reduced to 52% of control mice ($p<0.001$; Figure 13B). Comparisons of clinical scores between the two strains at 4, 8 and 12 days showed that the affected body surface area was significantly lower in IL-1R -/- mice at all time points (day 4: 1.6% ± 0.4% vs. 0.6% ± 0.2% ($p=0.008$), day 8: 7.4% ± 0.7% vs. 5.2% ± 0.7%

(p=0.04), day 12: 20.7% ± 1.8% vs. 10.1 ± 1.7% (p<0.001), in wild type and IL-1R -/- mice, respectively). These differences in clinical disease manifestation were independent of changes in circulating or tissue bound autoantibodies, and complement deposition at the DEJ, which were similar between both treatment groups (Figure 13C).

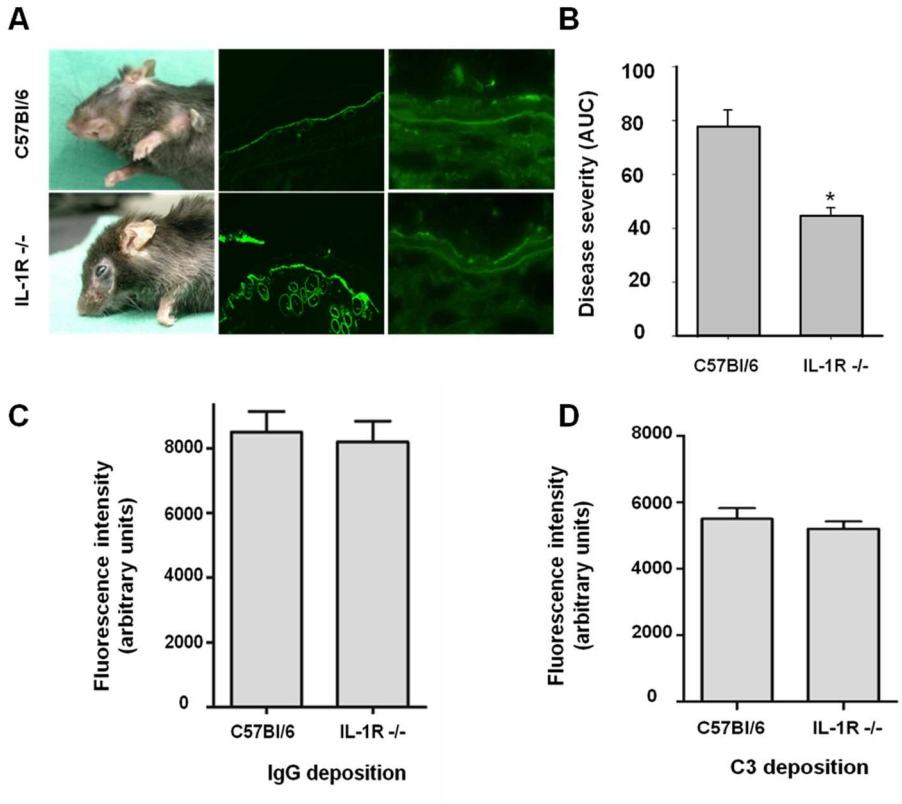

Figure 13: Decreased blister formation in experimental EBA in IL-1R -/- mice.

*Experimental EBA was induced by repetitive injections of anti-COL7 IgG into either IL-1R -/- or C57BL/6 mice. A) Representative clinical pictures 12 days after the initial anti-COL7 IgG injection in the indicated treatment groups. B) Disease severity in the indicated groups is expressed as the AUC calculated from the affected body surface area 4, 8 and 12 days after the initial anti-COL7 IgG injection. IL-1R -/- mice show 48% decrease in disease severity in relation to control. Data is based on a minimum of eight mice per group and is presented as mean ± SEM. (*p<0.05, t-test). C) In both groups, no difference was detected in the IgG and complement (C3) deposition at the DEJ. Fluorescence intensity was measured using ImageJ software and represented as arbitrary units.*

4.2.2. Pharmacologic inhibition of IL-1 function impairs blistering in antibody-transfer induced EBA

To further validate these findings, I investigated if pharmacological inhibition of IL-1 function has similar effects on the blistering phenotype as observed in IL-1R deficient mice. Again, EBA was induced in C57BL/6 mice by repetitive anti-COL7 IgG injections. To block IL-1 function, mice were treated with anakinra (100 mg/kg (n=10) or 200 mg/kg (n=10)). Mice were injected once per day from day 0 until the end point of the experiment (day 12). Control mice were treated with vehicle (PBS). Clinical disease was observed in both, the control and the two anakinra treatment groups. Parallel application of anakinra significantly alleviated clinical disease manifestation (Figure 14A). Calculation of the overall clinical disease activity, taking onset and maximum severity into account, disease activity expressed as the AUC in C57BL/6 mice reached 30% less in anakinra treated mice ($p<0.05$; ANOVA) (Figure 14B).

In contrast to the clinical findings, IgG and C3 deposition along the DEJ was identical in all groups. Circulating rabbit anti-mCOL7C IgG levels were identical in all groups, indicating that the clinical effects were not due to an altered IgG metabolism and/or effects on complement activation (Figure 14A).

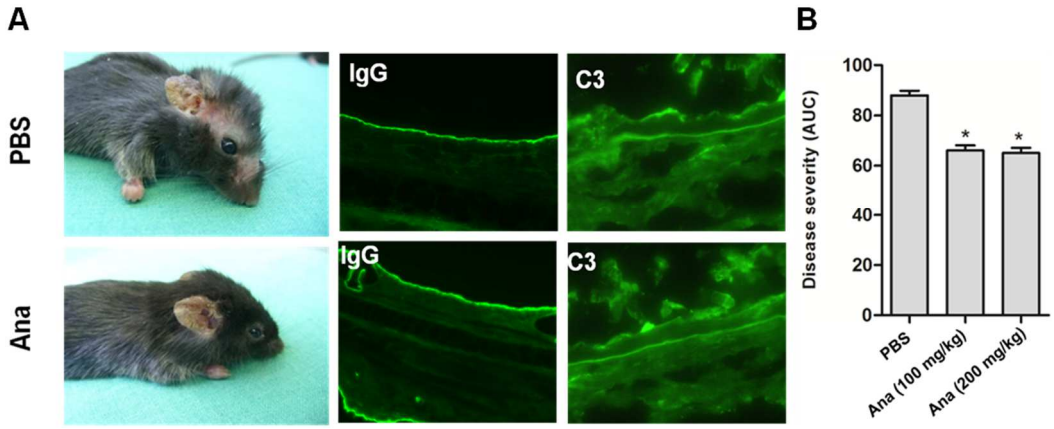

Figure 14: Reduced blister formation in anakinra treated mice after injection of anti-COL7 IgG.

*A) Representative clinical presentation, IgG and C3 deposition of mice 12 days after the initial anti-COL7 IgG injection. B) Disease severity in the indicated groups is expressed as the AUC calculated from the affected body surface area 4, 8 and 12 days after the initial anti-COL7 IgG injection. Data are based on 11-16 mice per group and is presented as mean ± SEM. (*p<0.05; ANOVA), Ana: anakinra*

4.2.3. Inflamatory infiltration is decreased in IL-1R -/- mice

Histopathological examination of the skin sections revealed less dermal-epidermal separation in IL-1R -/- mice compared with the control group. In each section the degree of leukocyte infiltration was ranked as no, medium or strong by an observer unaware of the specimen's treatment (Figure 15).

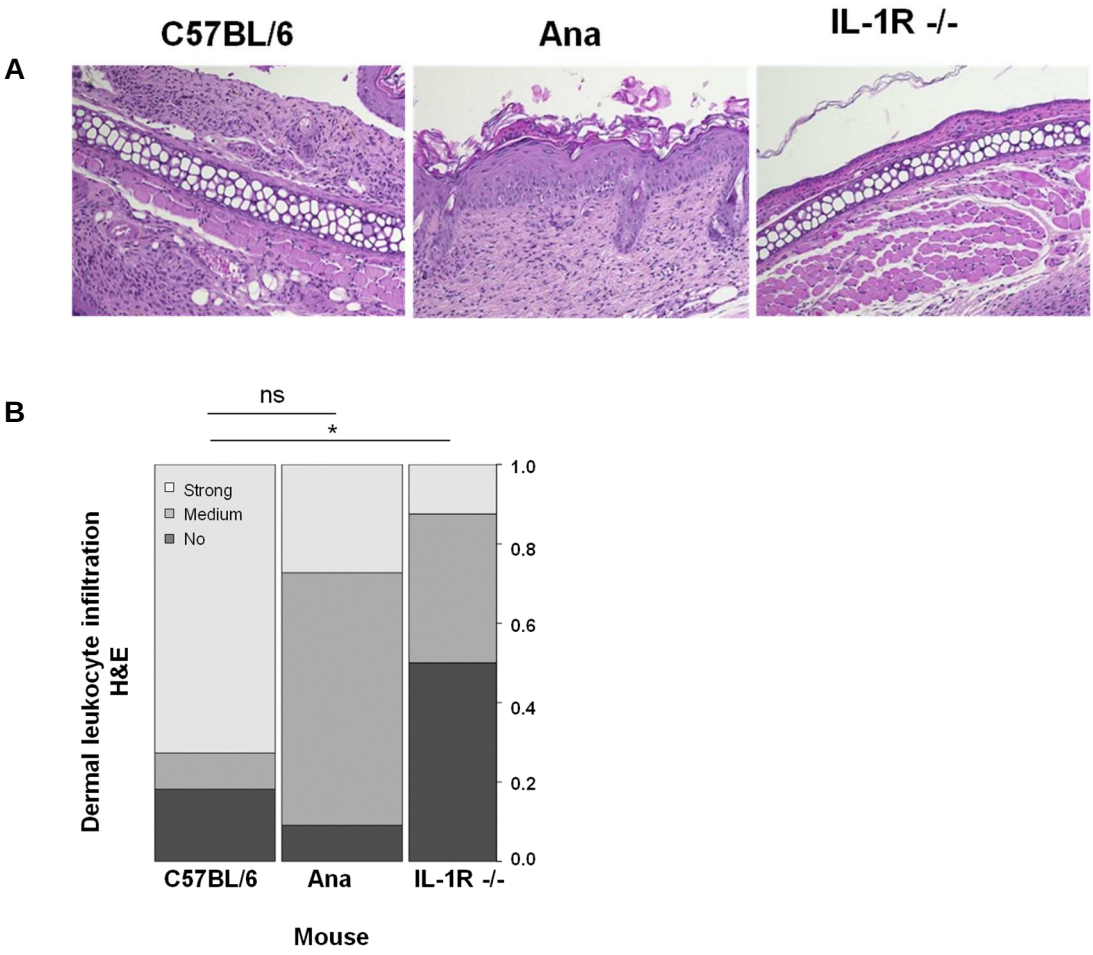

Figure 15: Decreased dermal leukocyte infiltration by blocking IL-1 function in mice after injection of anti-COL7 IgG.

A) Representative H&E stained sections from C57BL/6, anakinra and IL-1R -/- mice injected with anti-COL7 IgG. B) Dermal leukocyte infiltration in H&E stained sections shows a significant decrease in IL-1R deficient mice compared to C57BL/6 control mice (n=16; p=0.02; one-way Ordered logistic regression, likelihood ratio test) 12 days after injection of anti-COL7 IgG. Data is from 16 C57BL/6 and 10 IL-1R -/- scored sections obtained 12 days after the initial IgG injection. Block height represents the amount of mice with the respective ranked as nothing, medium or strong, block width corresponds to the amount of mice in the respective treatment group.

4.2.4. Expression of IL-1α and IL-1β in the anakinra and IL-1R -/- groups are decreased compare with control group

By induction of EBA, increased IL-1α and IL-1β expression was observed in skin section by immunohistochemistry (Figure 16A). To further investigate if blockade of IL-1 function in mice has an effect on cutaneous IL-1 level, sections were stained and scored and ranked to no, medium and strong, [266, 267]. Interestingly I observed that blockade of IL-1 function in experimental EBA lead to a decrease of both IL-1α and IL-1β intensity on the skin of mice. as assessed by immunohistochemistry (Figure 16B).

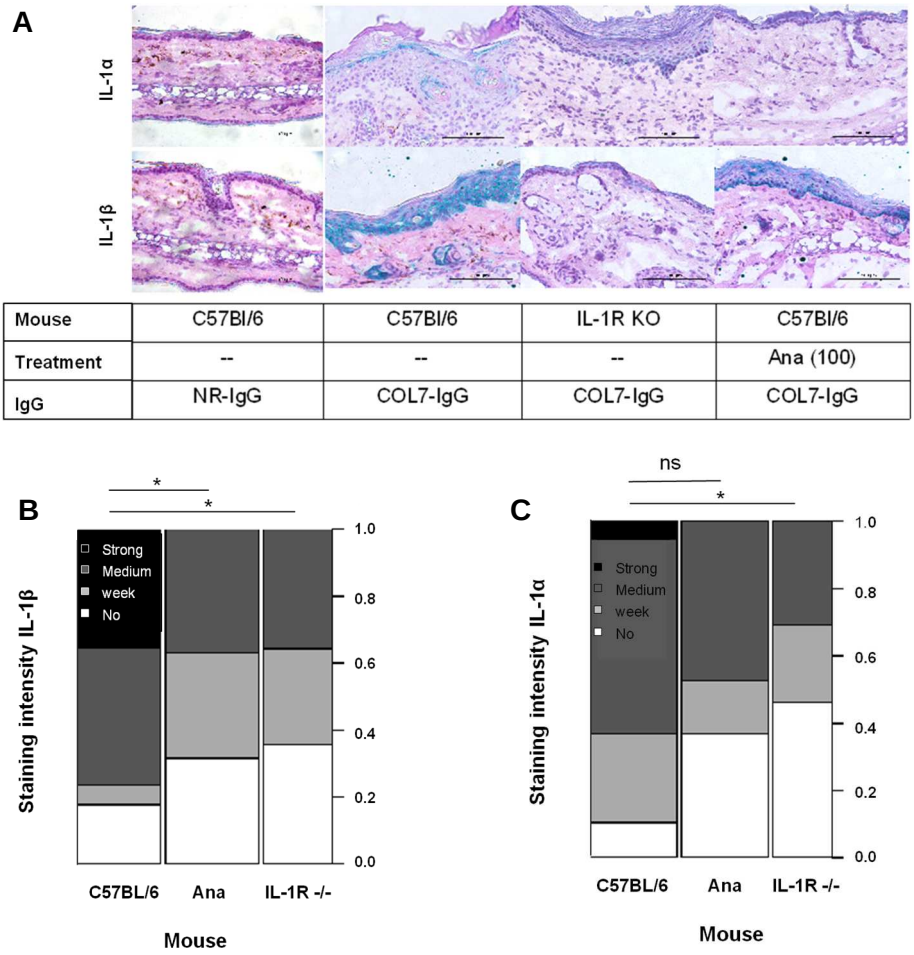

Figure 16: Different dermal IL-1α and IL-1β expression in WT, IL-1R deficient and anakinra treated mice after injection of anti-COL7 IgG.

A) Representative cutaneous expression of IL-1α and IL-1β in the indicated treatment groups compared with negative control and IL-1R -/- group. B).Semiquantitative staining intensities of cutaneous IL-1β expression on anakinra treated and IL-1R -/- mice. Overall, visual assessment of IL-1β staining intensity in mice with experimental EBA showed a significant decrease of IL-1 function in knockout mice (n=16; p=0.0326; one-way Ordered logistic regression, likelihood ratio test) and anakinra (n=16; p=0.0381; one-way Ordered logistic regression, likelihood ratio test), compared to control wild-type mice (n=10). C) Overall, visual assessment of IL-1α staining intensity in mice with experimental EBA showed a significant decrease of IL-1α function in knockout mice (n=16; p=0.041; one-way Ordered logistic regression, likelihood ratio test). No significant effect on IL-1α expression is observed in anakinra mice compared to control wild-type mice. Block height represents the amount of mice with the respective rank to no, medium, week and strong, block width represents the number of mice in the respective treatment group. Ana: anakinra

4.2.5. Caspase-1 independent control of IL-1β expression in experimental EBA

To test if production and processing of IL-1β through caspase-1 activation and to see if the increased serum and cutaneous IL-1β expression in experimental EBA is important, I used caspase-1 inhibitors in blister formation in passive EBA using caspase-1 inhibitor, namely VX-765 [268]. In a separate experiment anti-COL7 IgG was injected into mice lacking caspase-1 expression.

4.2.5.1. The induction of experimental EBA is impaired in mice treated with VX-765

After confirming the protective of effects of blocking IL-1β signaling in EBA, I wanted to exclude the contribution of IL-1α in previous observations. Thus, I thought to test whether inhibiting specifically IL-1β at an upstream level could recapitulate the aforementioned results. Since caspase-1 is a thiol protease responsible for the processing IL-1β from the inactive to an active form, I tested the effects of caspase-1 inhibitors in blister formation in passive EBA using a caspase-1 inhibitor, namely VX-765.

For this reason, EBA was induced in C57BL/6 mice by a total of 10 mg anti-mCOL7C antibodies, given in five equivalent subcutaneously doses, at two days intervals. The treatment scheme was oral doses of 100 mg/kg (n=10) or 200 mg/kg (n=10) VX-765, or PBS (n=15) given daily base from day 0, over a period of 12 days. At four days intervals (day 4, day 8 and day 12), typical EBA lesions in the skin were assessed (Figure 17A). At the end point of the experiment, tissue skin samples were harvested and blood sera were collected.

After 12 days C57BL/6 mice treated with VX-765 demonstrated significantly less disease severity. Disease severity in the indicated groups is expressed as the AUC (Figure 17B). Although different clinical signs were observed between treated and untreated groups, IgG and C3 deposition along the DEJ was identical in all the groups, as tested by direct IF microscopy. Accordingly, circulating IL-1β levels were significantly lower in treated mice compared to controls (more information in section 4.7).

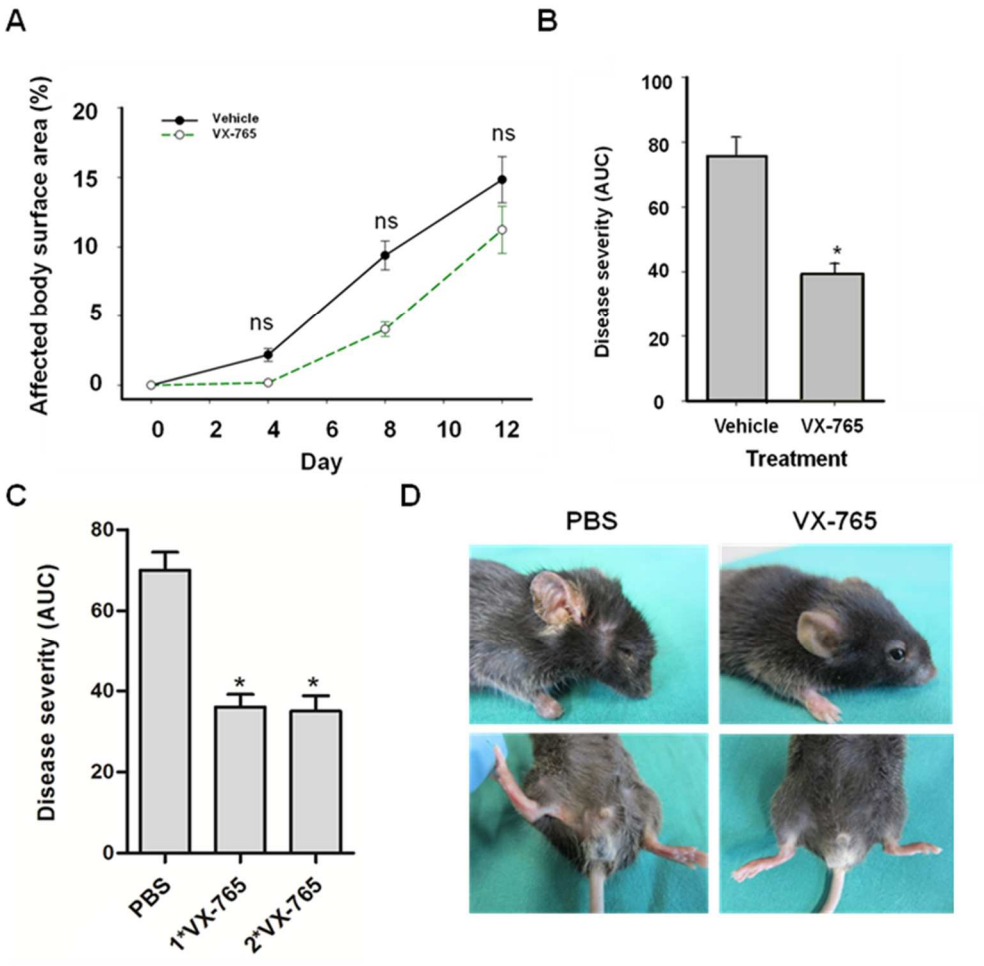

Figure 17: Decreased blister formation in experimental EBA after VX-765 treatment.

*Experimental EBA was induced by repetitive injections of anti-COL7 IgG into either VX-765 or control injected C57BL/6 mice. A) Reduction of affected body surface area in VX-765 treated mice is not significant 4, 8 and 12 days after the initial anti-COL7 IgG injection. B) However, clinical EBA severity assessed by the percentage of body surface area covered by EBA skin lesions in the indicated groups which is expressed as the AUC significantly decrease in VX-765 treated group (n=10 mice/group; *p<0.05; ANOVA). C) Efficacy of VX-765 is, within the tested doses (1*VX-765: 100mg/kg/day, 2*VX-765: 200mg/kg/day), not dose dependent. D) Representative clinical presentations, 12 days after the initial anti-COL7 IgG injection.*

4.2.5.2. Caspase-1/11 deficient mice are fully susceptible to antibody-transfer induced EBA

To confirm the findings from pharmacological caspase-1 inhibition, IL-1β processing, was inhibited, genetically. Unexpectedly, compared to WT animals, caspase-1/11 -/- mice had a

similar clinical phenotype after injections of anti-COL7 IgG. For this purpose I analyzed blister formation in caspase-1/11 deficient (n=9) and WT control mice (n=10) in the C57BL/6 genetic background after EBA induction by transfer of anti-COL7. Overall disease severity (expressed as AUC) was not affected (Figure 18B). However, on day eight a significant lower body surface area was affected in caspase-1/11 -/- compared to wild type mice (Figure 18A).

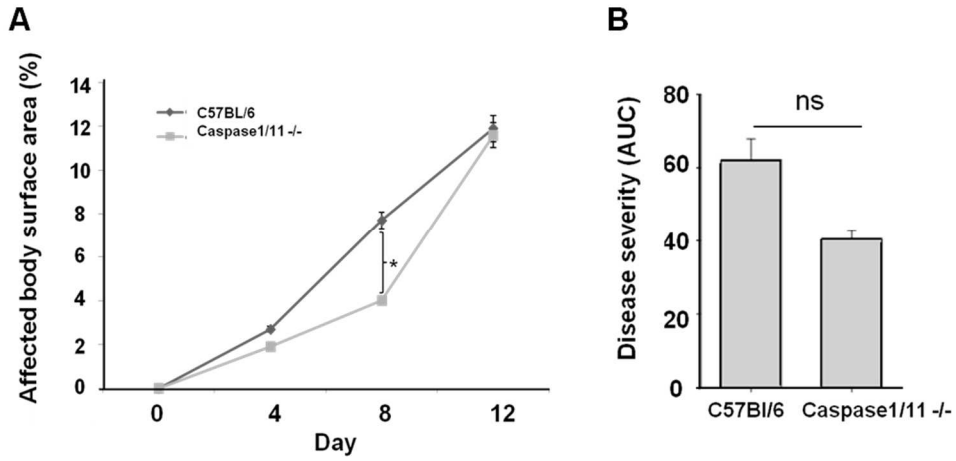

Figure 18: Caspase-1/11 deficient mice are not protected against blistering in experimental EBA.

A) EBA was induced in WT control mice (n= 10) and in caspase-1/11 deficient mice with C57BL/6 genetic background (caspase-1/11 -/-) (n=9). Clinical EBA severity assessed by the percentage of body surface area covered by skin lesions, 4, 8 and 12 days after the initial anti-COL7 IgG injection. In both strains, onset of blistering is observed at day four, and slightly but significantly delayed in caspase-1/11 -/- mice at day eight (indicated by asterix). B) Overall disease severity expressed as the AUC shows no significant difference between WT and caspase-1/11 -/- mice.

4.2.5.3. Increased IL-1 expression in experimental EBA is independent of caspase-1 expression

To address the question why caspase knockout mice are not protected against EBA, I determined the IL-1β concentration by WB in extracts of skin to investigate whether caspase knockout mice have the capacity to process IL-1β. In both strains, a similar IL-1β protein expression was observed (Figure 19). This pointed to a non-caspase-1 extracellular processing of the IL-1β precursor, e.g. elastase, or cathepsion G, in EBA [269, 270].

Therefore, blocking IL-1 signaling rather than processing can better attenuate disease manifestations.

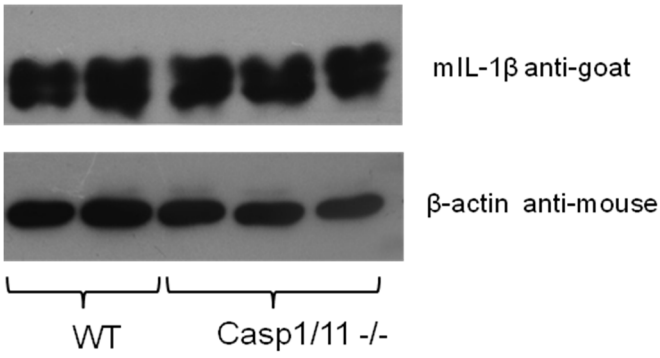

Figure 19: IL-1β is cleaved in antibody-transfer induced EBA even in the absence of caspase-1. WB analysis of completely cellular proteins for β-actin as housekeeping protein, and IL-1β expression in skin of C57BL/6 and caspase knockout mice after EBA induction.

4.3. Inhibition of IL-1 function is associated with a reduced expression of ICAM-1

As IL-1 regulates expression of the respective endothelial ligands for LFA-1 (CD11a/CD18), Mac-1 (CD11b/CD18), and integrin CD11c/CD18 [271], the expression of intercellular adhesion molecule (ICAM)-1 (CD54) in the skin was evaluated in experimental EBA with and without impaired IL-1 function. In mice with antibody-transfer induced EBA, ICAM-1 expression was detected both on endothelial cells and on basal keratinocytes. In contrast, ICAM-1 expression was almost absent in mice injected with normal rabbit IgG. In line, genetic or pharmalocologic blockade of IL-1 function in mice with experimental EBA reduced ICAM-1 expression (Figure 20).

A

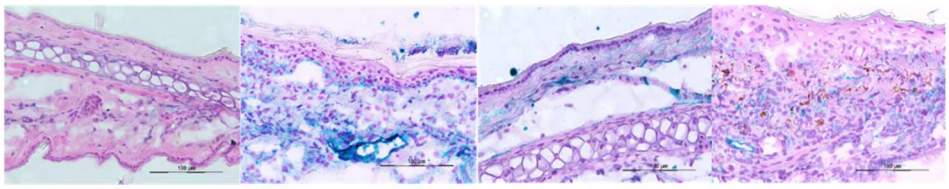

Mice	C57Bl/6	C57Bl/6	IL-1R KO	C57Bl/6
Treatment	--	--	--	Ana (100)
IgG	NR-IgG	COL7-IgG	COL7-IgG	COL7-IgG

B

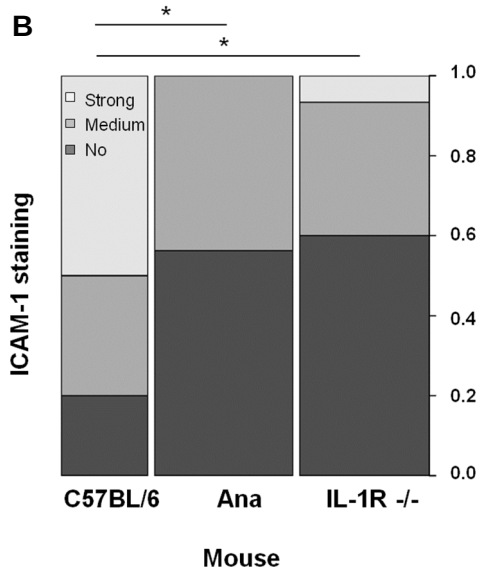

Figure 20: Decreased dermal ICAM-1 in IL-1R deficient and anakinra treated mice after injection of anti-COL7 IgG.

A) Representative ICAM-1 expression 12 days after the first injection of anti-COL7 IgG into mice of the indicated treatment groups. While ICAM-1 is almost completely absent in mice injected with normal rabbit (NR) IgG, ICAM-1 is expressed in keratinocytes and around the vasculature in mice with experimental EBA. B) Overall, visual assessment of ICAM-1 staining intensity in mice with experimental EBA showed a significant decrease if IL-1 function is blocked in knockout mice (n=15; p=0.0252; one-way Ordered logistic regression, likelihood ratio test) or anakinra (n=16; p=0.025; one-way Ordered logistic regression, likelihood ratio test), compared to control wild-type mice (n=10). Block height represents the amount of mice with the respective ranked to no, medium and strong, block width the amount of mice in the respective treatment group. Ana: anakinra 100mg/kg/day.

4.4. IL-1 blockage results in reduced expression of endothelial adhesion molecules in human umbilical vein endothelial cells (HUVEC)

To test, whether inhibitory effect of IL-1 blockade on ICAM-1 also affected other endothelial adhesion molecules, such as VCAM-1 (CD106) and E-selectin (CD62E), expression of these molecules was assessed on HUVEC stimulated in the absence or presence of anakinra. In line with the *in vivo* findings, IL-1 induced ICAM-1 expression, which could specifically be inhibited by anakinra treatment. Furthermore, endothelial VCAM-1 and E-selectin also were induced in the present of IL-1 and this expression was inhibited by anakinra treatment (Figure 21). These experiments were fully done by Prof. Schön group in Göttingen , but I included them here, as we requested the collaboration partners to specifically address this question that came up during my thesis work.

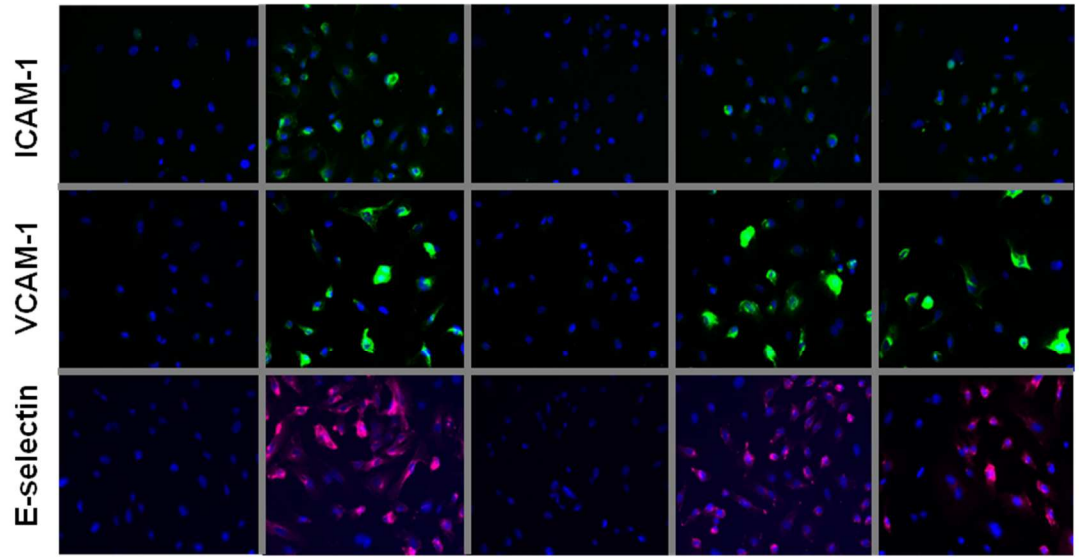

Stimulus	-	IL-1β	IL-1β	TNF-α	TNF-α
Treatment	-	-	Ana	-	Ana

Figure 21: IL-1 blockage hinderes expression of endothelial adhesion molecules in HUVEC.

Stimulation of HUCEV with either IL-1β or TNF-α leads to in increased expression of ICAM-1, VCAM-1 and E-selectin. Anakinra (Ana) selectively blocks the IL-1β, but not the TNF-α induced up-regulation of adhesion molecules. Nuclei are shown in blue, while expression of the indicated adhesion molecules is indicated in green or pink (one representative experiment out of three). These experiments were performed by Anike Lockmann, Anna-Carina Hund and Michael Schön (Dept. of Dermatology of the University of Göttingen).

4.5. Inhibition of IL-1 function is associated with a decreased dermal infiltration of granulocyte-differentiation antigen-1 (Gr-1) positive cells

Gr-1 is expressed on monocytes, neutrophils, subsets of macrophages, plasmacytoid dendritic cells, and T cells. Monocytes in the bone marrow transiently express Gr-1 during development and the expression level is strongly correlated with granulocyte differentiation and maturation. In the periphery Gr-1 is found predominantly on neutrophils. Since neutrophil depletion has been shown to protect mice from induction of skin blisters in experimental EBA [65], I next evaluated Gr-1 expression on lesional skin (blue dots in the picture). Interestingly the degree of dermal Gr-1+ infiltrates corresponded well the disease clinical phenotype (Figure 22).

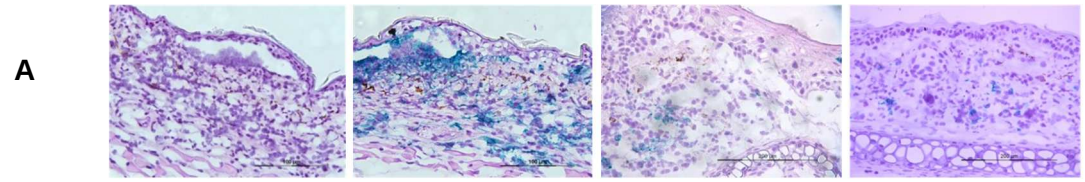

Mouse	C57Bl/6	C57Bl/6	IL-1R -/-	C57Bl/6
Treatment	-	-	-	Ana (100)
IgG	NR-igG	COL7-IgG	COL7-IgG	COL7-IgG

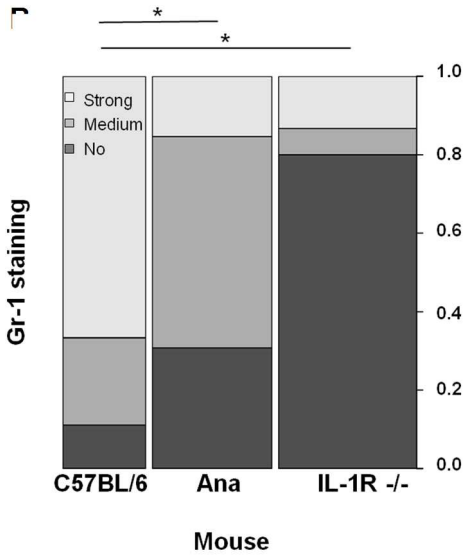

Figure 22: Decreased dermal Gr-1 staining in IL-1R deficient and anakinra treated mice after injection of anti-COL7 IgG.

A) Representative cutaneous expression of Gr-1 in the indicated treatment groups compare with negative control and IL-1R knockout group, scale bar corresponds to 100µm. B) Semiquantitative staining intensities of cutaneous Gr-1 expression on anakinra treated and IL-1 knockout group. All mice were injected with anti-COL7 IgG. Compared to C57BL/6 control mice, significant decrease on Gr-1 expression is observed in knockout mice (n=15; p=0.0020; one-way Ordered logistic regression, likelihood ratio test) and in anakinra (n=15; p=0.0095; one-way Ordered logistic regression, likelihood ratio test). Block height represents the amount of mice with the respective ranked to no, medium and strong, block width the amount of mice in the respective treatment group. Ana: anakinra 100mg/kg/day.

4.6. Effects of therapeutic application of anakinra or VX-765 in mice with already established immunization-induced EBA

To test, if inhibition of IL-1 function has also therapeutic effects, I used already established immunization-induced EBA [272] and used anakinra and VX-765 in a therapeutic setting after induction of EBA.

4.6.1. Therapeutic application of anakinra leads to improvement of already established immunization-induced EBA

EBA was induced in SJL/J mice (n=30) by immunization with vWFA2 [254]. When individual mice had 2% or more of their body surface affected by skin blistering, they were allocated to either control or anakinra. Out of 30 immunized mice, 21 were allocated to anakinra treatment and control. The remaining mice did not meet the inclusion criteria or died during the experiment. Treatments were carried out for a total of two weeks.

At the initiation treatment, clinical disease severity between mice randomly allocated to control and anakinra treatment were identical; i.e. 2.6% ± 0.2% of affected body surface area. While clinical EBA manifestations continuously progressed in PBS-injected mice (3.2% ± 0.2% on week 1 and 3.9% ± 0.1% on week 2), it declined in anakinra treated mice (2.1% ± 0.2% on week 1 and 2.0% ± 0.2% on week 2; figure 23A). In line, corresponding disease activity, expressed as AUC, monitored during the 2-week treatment period was significantly lower in the group receiving anakinra (Figure 23B).

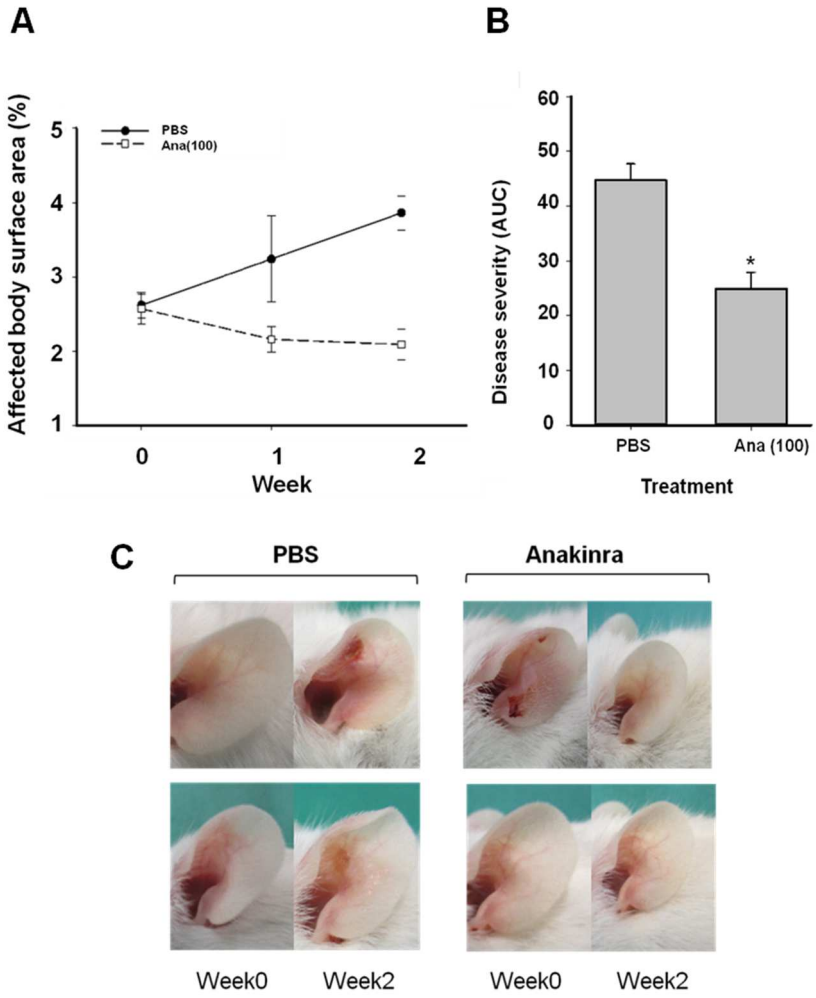

Figure 23: Treatment with anakinra reduces blisters in already established immunization-induced EBA.

SJL/J mice with already established clinical EBA manifestation after immunization with COL7 were treated with anakinra (100mg/kg, n=11) for a period of two weeks. Control mice received PBS (n=10). A) Analysis of the weekly scores shows, that clinical EBA severity increases during the observation period in PBS injected mice. In contrast, disease severity decreases in mice treated with anakinra (week 1, p=0.004; week two, p<0.001; t-test). B) Cumulative disease severity expressed as AUC during the two weeks treatment period is significantly reduced in anakinra (AUC, p<0.001; t-test). Compared to PBS injected mice, animals treated with anakinra have a significantly reduced overall disease activity. C) Representative clinical presentations of the clinical disease manifestation at the beginning of treatment (week 0) and at the end of the treatment period (week two).

4.6.2. Levels of antigen-specific antibody concentrations after immunization with vWFA2 remained unaltered during all anakinra treatment

I investigated if the decrease in disease severity in anakinra treated mice was due to changes in the level of circulating and/or tissue-bound antibodies. To address this, I tested COL7 specific antibody levels in C57BL/6 mice immunized with vWFA2 (n=10) during the two weeks period of anakinra treatment (two weeks) and in the same time points in control group without any treatment. ELISA results showed same OD score in treated groups compared to C57BL/6 (n=10) (Figure 24).

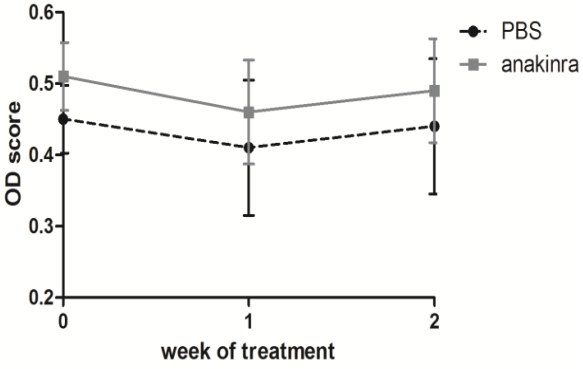

Figure 24: The mean value of anti vWFA2 remained constant during the experiment.

Blood allowed to clot and serum was separated by centrifugation at 2000 × g for 10 minutes and stored at -20 °C prior to analysis value was calculated using the OD results. Means±SEM for anakinra treated and PBS treated mice are presented.

4.6.3. VX-765 has therapeutic effects in already established immunization-induced EBA

To test for a potential therapeutic activity of VX-765 in immunization-induced EBA, a similar protocol as described for anakinra (6.6.1.) was applied. EBA was induced in SJL/J mice (n=30) by immunization with vWFA2 [254]. When individual mice had 2% or more of their body surface affected by skin blistering, they were allocated to either control or VX-765 out of the 30 immunized mice, 25 were allocated to VX-765 treatment and control. The remaining mice did not meet the inclusion criteria or died during the experiment. Treatments were carried out for a total of two weeks. Of note, these experiments were performed before the investigation of caspase-1/11 deficient mice in antibody-transfer induced EBA, where I had no indication that the effects of VX-765 may be due to other, so far uncharacterized, effects of the compound. While clinical EBA manifestations continuously progressed in PBS-injected mice (3.2% ± 0.2% on week 1 and 3.9% ± 0.1% on week 2), it declined in VX-765 treated mice (1.9% ± 0.2% on week 1 and 1.2% ± 0.1% on week 2 (Figure 25A). In line, corresponding disease activity, expressed as AUC, monitored during the two-week treatment period was significantly reduced in the group receiving VX-765 (Figure 25B).

However, as caspase-1/11 deficient mice showed no difference in antibody-transfer induced EBA (explained in 4.2.5.2.), these effects are most likely due to so far uncharacterized off-target effects of the compound *in vivo*.

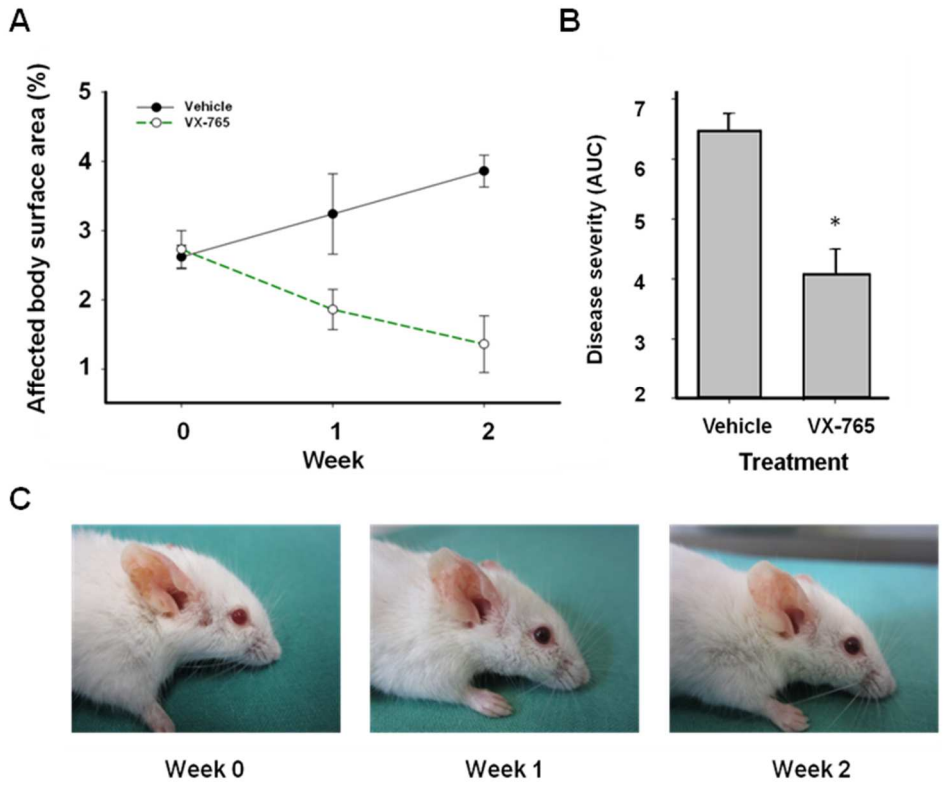

Figure 25: Treatment with VX-765 reduces induction of experimental EBA.

*SJL/J mice with already established clinical EBA manifestation after immunization with COL7 were treated with VX-765 (100mg/kg, n=15) for a period of two weeks. Control mice received PBS (n=10). A) Analysis of the weekly scores shows, that clinical EBA severity increases during the observation period in PBS injected mice. In contrast, disease severity decreases in mice treated with VX-765 (*week 1, p=0.005; week two, p<0.002, t-test); *B) Cumulative disease severity expressed as AUC during the two-week treatment period is significantly reduced in anakinra (*AUC, p<0.001, t-test*). C) The provided clinical picture documents the resolution of skin lesions during VX-765 application.*

4.6.4. Levels of antigen-specific antibody concentrations after immunization with vWFA2 stayed in the same level during the all VX-765 treatment

I investigated if the decrease in disease severity in VX-765 treated mice was not due to a decrease in the level of antibodies. To address this I tested COL7 specific antibody levels in

C57BL/6 mice immunized with vWFA2 (n=10) during the two weeks period of VX-765 treatment (two weeks) and in the same time points in control group without any treatment. ELISA results showed same OD score in treated group compared to C57BL/6 (n=10) (Figure 26).

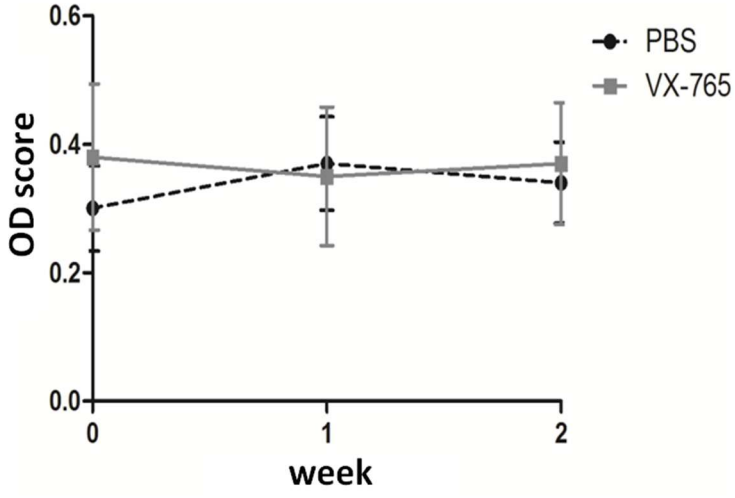

Figure 26: The mean value of anti vWFA2 stays stationary during two weeks of experiment.

Blood allowed to clot and serum was separated by centrifugation at 2000 × g for 10 minutes and stored at -20 °C prior to analysis value was calculated using the OD results. Means±SEM for VX-765 treated and PBS treated mice are presented.

4.7. No significant change in the concentration of IL-1β in IL-1R deficient mice as well as in anakinra and VX-765 treated groups

As mentioned before, induction of experimental EBA by injection of anti-COL7 IgG led to a significant increase of serum IL-1β concentrations (Figure 27). If IL-1R function is blocked either in IL-1R -/- mice or by injection of IL-1Ra, IL-1β serum levels remain almost at the same level as after EBA induction. Administration of VX-765 also did not lead to change in the serum concentration of IL-1β, compared to untreated C57BL/6 control mice with experimental EBA (Figure 27).

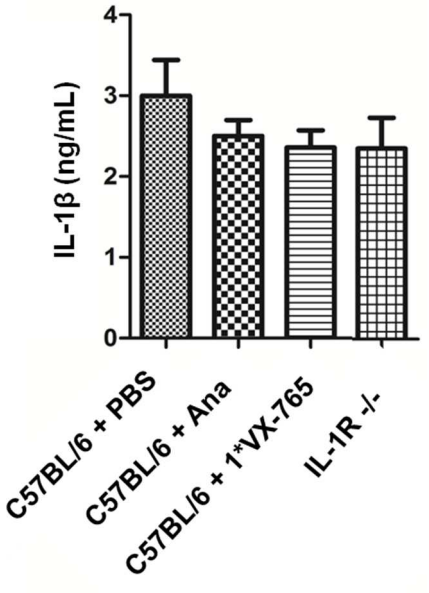

Figure 27: Serum level of IL-1β in the indicated treatment groups.

*IL-1β serum concentrations 12 days after the first injection of anti-COL7 IgG into mice. IL-1β serum concentrations shows no statistically difference in any of treatment group and IL-1R deficient mice compared to C57BL/6 control mice data is based on 5-10 mice per group Anova. Ana: anakinra, 1*VX-765: 100mg/kg/day.*

4.8. IL-1 processing in human cultured keratinocytes after stimulation with LPS and PMA

After confirming the major role of IL-1 in EBA pathogenesis and its potential therapeutic applications, I aimed to investigate the potential underlying molecular mechanisms of IL-1 production. Despite the recent progress in understanding of EBA pathogenesis, it remains unclear whether the skin can actively regulate the course of the disease. To address this, I used HaCat cells to test whether they have the capacity to release IL-1β upon appropriate stimulus. The murine monocyte-macrophage cell line P388 was used to optimize the amount of the stimulus required for IL-1β secretion and as a control in the next experiments. A dose of 150 ng/ml LPS or 50 ng/ml PMA was enough to stimulate cells for detectable IL-1β release in the supernatant of keratinocytes (Figure 28).

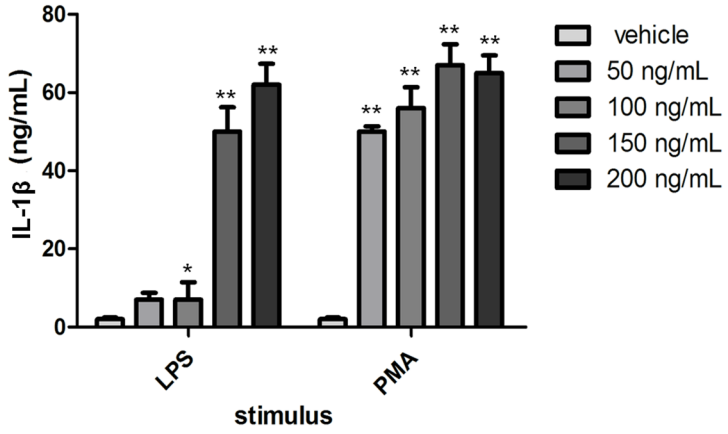

Figure 28: LPS or PMA induce the production of IL-1β from keratinocytes.

*Keratinocytes were stimulated with different concentration of stimulus (50, 100, 150, 200 ng/ml) for four hours, and the concentrations of IL-1β released into the culture supernatants were determined by ELISA and compared with vehicle. Values are compared between the stimulated and non-stimulated cells. Data from five independent measurements presented as mean±SEM. (*p<0.05, **p<0.01 one-way ANOVA followed by Tukey's multiple comparison test).*

4.9. Inhibition of IL-1 processing in human cultured keratinocytes

After establishing the optimal concentration of PMA and LPS, the capacity of VX-765 to inhibit IL-1 release from activated HaCat was studied. In brief, HaCat cells were primed with 150 ng LPS or 50 ng PMA and stimulated with 5mM ATP and were treated with VX-765 concentration ranging from 0 to 20 µg/ml and the release of IL-1β was assessed by ELISA. P388 cell line was used as control. Surprisingly, VX-765 inhibited IL-1β release from HaCat cells in a dose dependent manner, implying that keratinocytes may be a therapeutic target in EBA (Figure 29).

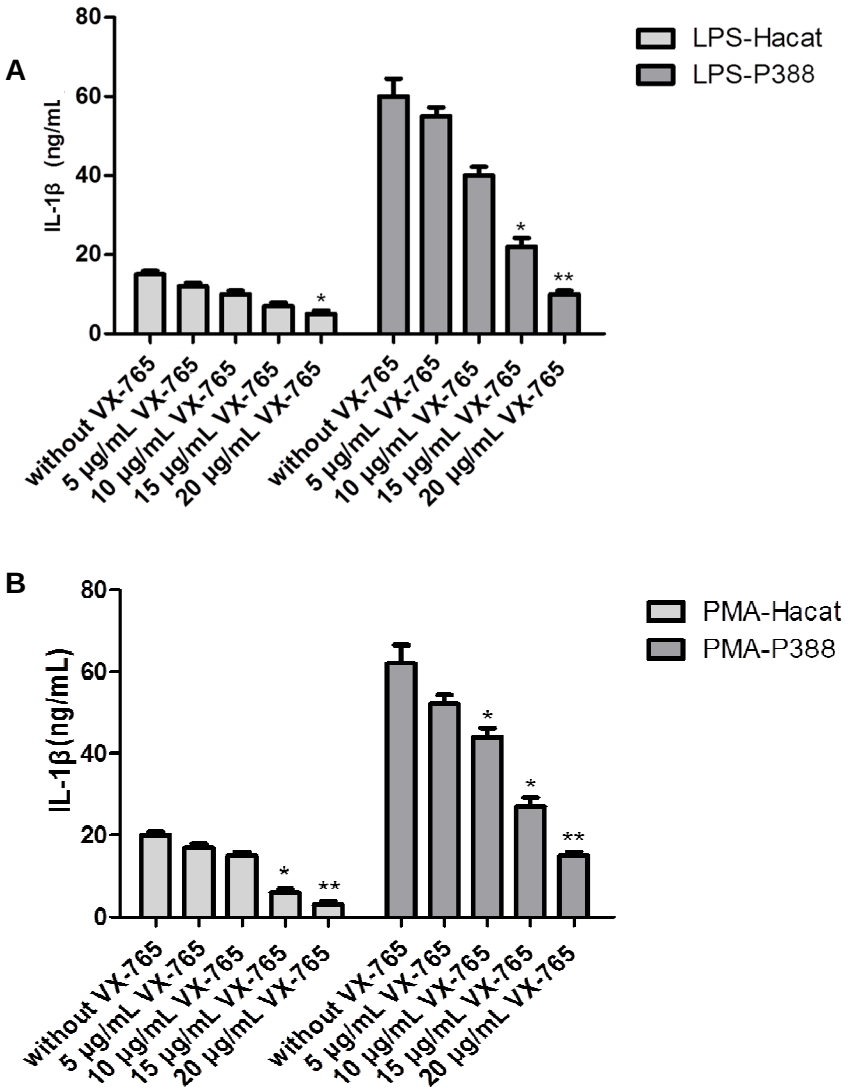

Figure 29: Inhibitory effects of VX-765 on A) LPS or B) PMA induced IL-1β production.

*Stimulated cells (Hacat or P388 cells) with A) 150 ng/ml LPS and B) 50 ng/ml PMA were treated with different concentration of VX-765 or vehicle alone without inhibitors for two hours. IL-1β released into the culture supernatants were determined by ELISA. Data from five independent measurements presented as mean±SEM. (*p<0.05, **p<0.01; ANOVA).*

After confirming the major contribution of IL-1 in EBA pathogenesis and also the lack of complete protection against EBA with IL-1 blockade, I continued with searching for additional molecules linked to IL-1 inflammatory pathways of EBA pathogenesis. To this end, I performed genetic studies; the results are presented in the next sections.

4.10. Induction of skin blistering in experimental EBA by antibody transfer is strain dependent

To identify novel EBA therapeutic targets for pharmacological modulation, a possible approach is to build-up potential pathways though the identification of genetic susceptibility loci, combined with selected molecules. To this end, I firstly wanted to identify genes controlling late disease phase, speculating that these molecules would mainly govern blister formation. This is allowed by abstracting the initial steps of EBA pathogenesis (loss of tolerance and antibody production) using antibody-transfer induced disease models. Since previous works demonstrated a strain dependency in several antibody transfer-induced animal models [239, 273] we suspected that this would also be the case for EBA, thus we aimed to identify potential disease-loci controlling blister formation.

Induction of EBA by transfer of anti-COL7 IgG induced clinical diversity among the 18 inbred mouse lines analyzed, with three different distinct responses to anti-COL7 IgG injections being observed (Table 10). In detail, 6/18 strains (NOD/ShiLtJ, FVB/NJ, A/J, SJL/J, MRL/MpJ and C3H/HeJ) were resistant to EBA induction (defined as less than 1% of affected body surface area at day 12), 4/18 (DBA/1J, NZM2410/J, PL/J, and AKR/J) showed intermediate susceptibility (defined as less than 10% of affected body surface area at day 12) and 8/18 (BALB/cJ, PWD/PhJ, CBA/J, BXD2/TyJ, C57BL/6J, B10.S-H2s/SgMcdJ, WSB/EiJ and Cast/EiJ) showed a high degree of clinical blistering (defined as more than 10% of affected body surface area at day 12). Interestingly, WSB/EiJ showed great mucous membrane involvement, and thus 50% (2/4) of the mice died before the end-point of the experiment, while scoring for Cast/EiJ refers to day eight, since all mice (5/5) died before day 12 due to severe EBA with mucous membrane involvement.

Furthermore, to exclude any contribution of pathogenic IgG levels to disease phenotype, circulating rabbit antibodies to mCOL7 were measured in 17 alive strains at day 12 by commercial ELISA for rabbit IgG. Interestingly, although circulating IgG levels were strain dependent, no significant correlation was observed between rabbit IgG concentration and disease severity (Figure 31).

Strain	Disease incidence	End-point score (Day 12)	Disease susceptibility
NOD/ShiLtJ §	0/5	N/A	Resistant to EBA
FVB/NJ §	2/5	0.1 ± 0.1	
A/J §	3/5	0.5 ± 0.3	
SJL/J §	3/6	0.8 ± 0.1	
MRL/MpJ #	6/6	1.3 ± 0.1	Intermediate susceptibility to EBA
C3H/HeJ §	5/5	1.4 ± 1.5	
DBA/1J §	6/6	2.3 ± 1.5	
NZM2410/J § #	5/5	2.4 ± 0.7	
PL/J §	5/5	6.0 ± 0,5	
AKR/J §	5/5	6.9 ± 2.5	
BALB/cJ §	6/6	10.3 ± 1.6	Severe EBA
PWD/PhJ	4/4	10.8 ± 3.8	
CBA/J §	5/5	11.5 ± 3.7	
BXD2/TyJ #	6/6	16.2 ± 5.1	
C57BL/6J §	11/11	18.4 ± 4.7	
B10.S-H2s/SgMcdJ	5/5	19.2 ± 1.6	
WSB/EiJ §	4/4	7.8 ± 0.6*	
Cast/EiJ § #	5/5	10.0 ± 3.4%$	

Table 10: Clinical characteristics of antibody-transfer induced EBA in different strains of mice.

*[§]Used for forward genetic analysis. [#]Used for intercrossing to generate AIL mice. *two mice died two days after the first IgG injection, another mouse died on day 4. [$] All died before day eight. Indicated scores correspond to scores obtained in the two surviving mice on day 12. [%]Maximum disease was reached on day 8, thereafter all mice died. Abbreviations: N/A, not applicable.*

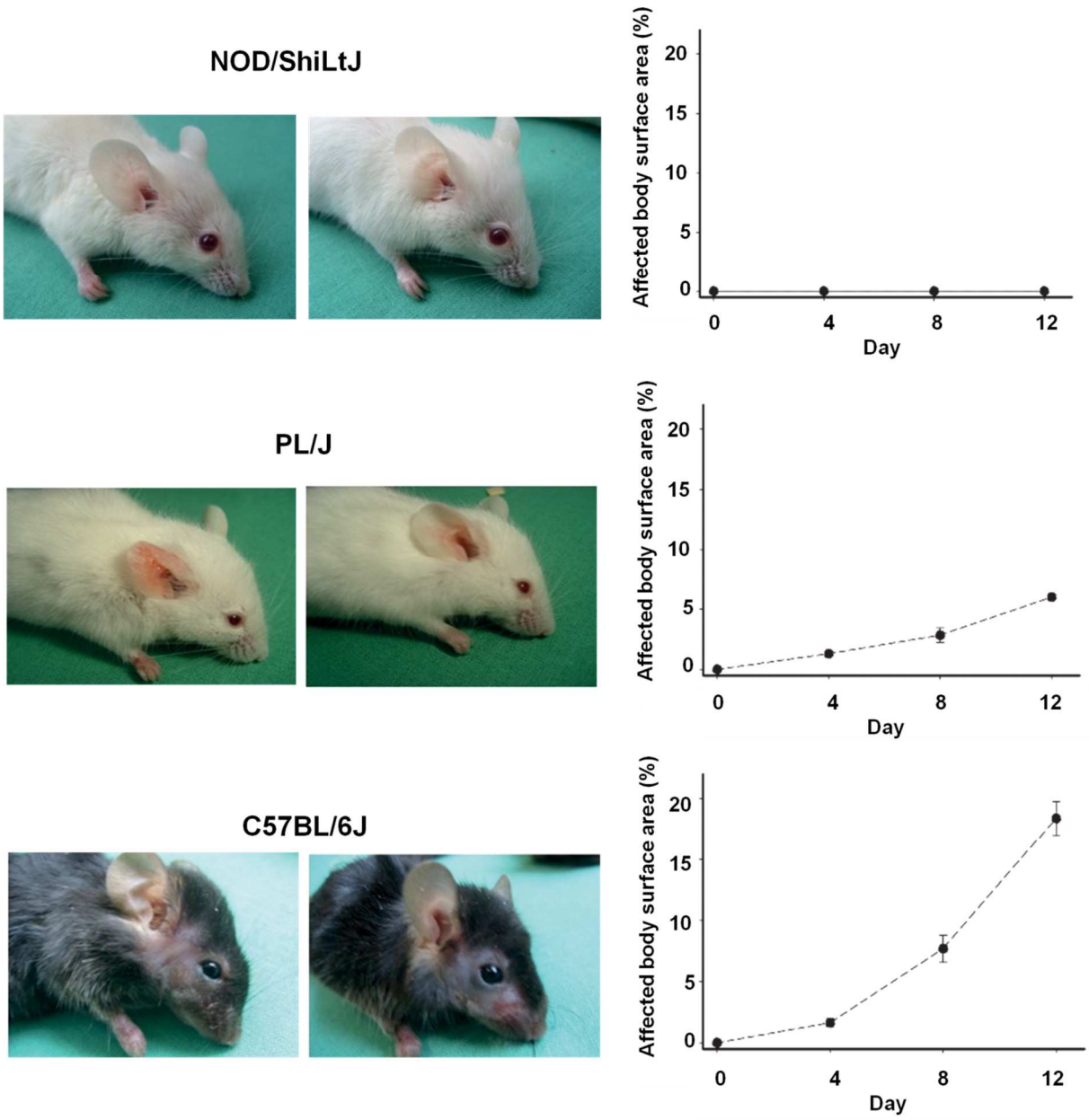

Figure 30: Induction of experimental EBA by antibody-transfer in mice is strain dependent.

Experimental EBA was induced in 18 different inbred mouse strains by transfer of anti-COL7 IgG. Three different responses to anti-COL7 IgG injections were observed, namely resistance to EBA (defined as less than 1% of affected body surface area at day 12), intermediate susceptibility (defined as less than 10% of affected body surface area at day 12) and severe EBA (defined as more than 10% of affected body surface area at day 12). Representative clinical images from day 12 after the first anti-COL7 injection (left panels) and affected body surface during the 12 days observation period (right panel) are shown for resistant NOD/ShiLtJ, intermediate susceptible PL/J, and highly susceptible C57BL/6J mice.

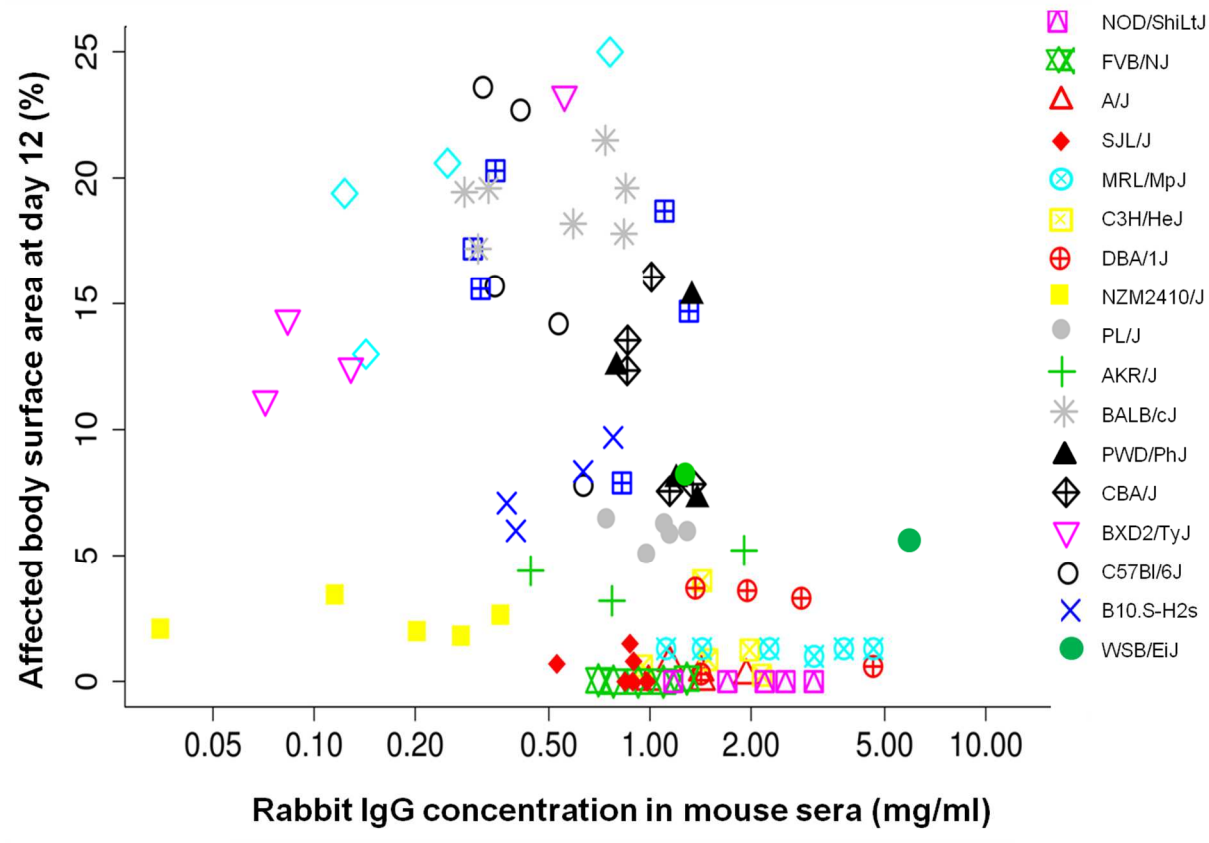

Figure 31: Rabbit IgG concentration in mouse sere tested by ELISA.

Mice were injected with rabbit anti COL7 antibodies and sera collected at the end-point of the experiment (day 12) from different 17 mice strains (out of 18, because Cast mice died before sampling day) (n=2-5/strain) were quantitatively analyzed by commercial ELISA for rabbit IgG. There is no correlation between rabbit IgG concentration in the mice sera and disease severity. Each serum was tested in duplicates, each point represent rabbit IgG concentration in X and affected body percentage at day 12 in Y axis. There was no correlation between different mouse strain and the measures serum rabbit IgG concentration.

4.11. Forward genomics identifies susceptibility loci for antibody-induced skin blistering in experimental EBA

After confirming the strain dependency in antibody-transfer induced EBA, forward genetics were used to identify a possible genetic control in these mice (statistical analysis was performed by Dr. Andreas Recke and Dr. Steffen Möller, Dept. of Dermatology, University of Lübeck). The chosen SNPs from the association study of the most susceptible versus the least susceptible strains are displayed in table 11. These best performing SNPs were taken as tags for haplotype blocks for further investigation.

Block (#: bp)[1]	**SNP ID[2]**	**Chr.[3]**	**Position (bp)[2]**	**MAF[4]**	**Alleles major (minor)**	**Estimate + SD[5]**	**unadj. p[6]**	**adj. p[7]**
A: 34019743-89135715	rs31459209	1	34019743	0.43	C (T)	0.03+0.44	0.95	0.959
B: 73683457-90622796	rs30860794	6	74799493	0.20	C (T)	0.32+0.62	0.60	0.76
C: 87192012-87908605	rs13479871	8	87590219	0.18	A (G)	0.44+0.73	0.55	0.76
D: 61628273-85033289	**rs13480247**	**9**	**65394049**	**0.09**	**C (A)**	**-2.40+1.14**	**0.036**	**0.18**
E: 62666281-110131804	rs27019283	11	110131804	0.21	A (C)	0.80+0.57	0.16	0.54
F: 92019623-94457772	rs29179064	12	92019623	0.18	C (T)	-0.16+0.54	0.76	0.85
G: 85623259-98046063	rs4212464	16	85633259	0.35	T (C)	0.51+0.49	0.30	0.60
H: 24184758-26451588	rs33217114	17	26451588	0.35	G (A)	0.48+0.44	0.27	0.60
I: 57559944-57589991	**rs29543297**	**18**	**57589991**	**0.47**	**G (A)**	**1.98+0.48**	**0.00**	**0.00**

Table 11: SNPs for antibody-induced skin blistering in experimental EBA that were identified using forward genomics.

[1]Blocks detected by forward genomics; [2]SNPs selected for individual blocks and location, NCBI build 37; [3]Chromosome; [4]minor allele frequency (MAF); [5]Coefficient of minor allele counts in a linear model for maximum disease score, including mouse gender as second covariate, SD: standard deviation; [6]Unadjusted p value of ANOVA on linear models with compared to without genomic information; [7]Adjusted p values, Benjamini-Hochberg method. SNPs confirmed for having associations with blister formation presented with bold letters.

4.12. Confirmation of rs29543297 in an autoimmune-prone advanced intercross mouse line (AIL) as a susceptibility locus for skin blistering in experimental EBA.

For the validation of the above-identified loci I induced EBA in a genetically diverse autoimmune-prone AIL [274, 275]. In detail, 315 mice of the 7th generation (G7) were injected with anti-COL7 IgG, and 310 mice were included into the analysis since five animals died before the last day of the experiment. Overall, 87% of mice developed clinical manifestations while only 13% were completely protected against EBA. More specifically mice developed no, minimal, mild, moderate or severe skin blistering corresponding to a body surface area affected by skin blistering of <1%, 1-4.9%, 5-9.9%, 10-20% or >20%, respectively (Figure 32). Other phenotypic traits, such as fur color, had no impact on clinical EBA manifestation (Figure 33). The variety of fur color in AIL mice mirrors the genetic diversity of this mouse line.

Subsequently, all of these 310 mice were genotyped using markers that distinguished the nine identified haplotype blocks. In this analysis, I confirmed associations between blister formation in antibody-transfer induced EBA and the SNPs rs13480247 and rs29543297. However, after the adjustment of the p values, only rs29543297 remained significant. Yet, taking into consideration the restricted population size, although not significant after the p value adjustment the haplotype block represented as rs13480247 was also included. All other SNPs that were used to validate the identified regions could not be confirmed in AIL mice (table 11).

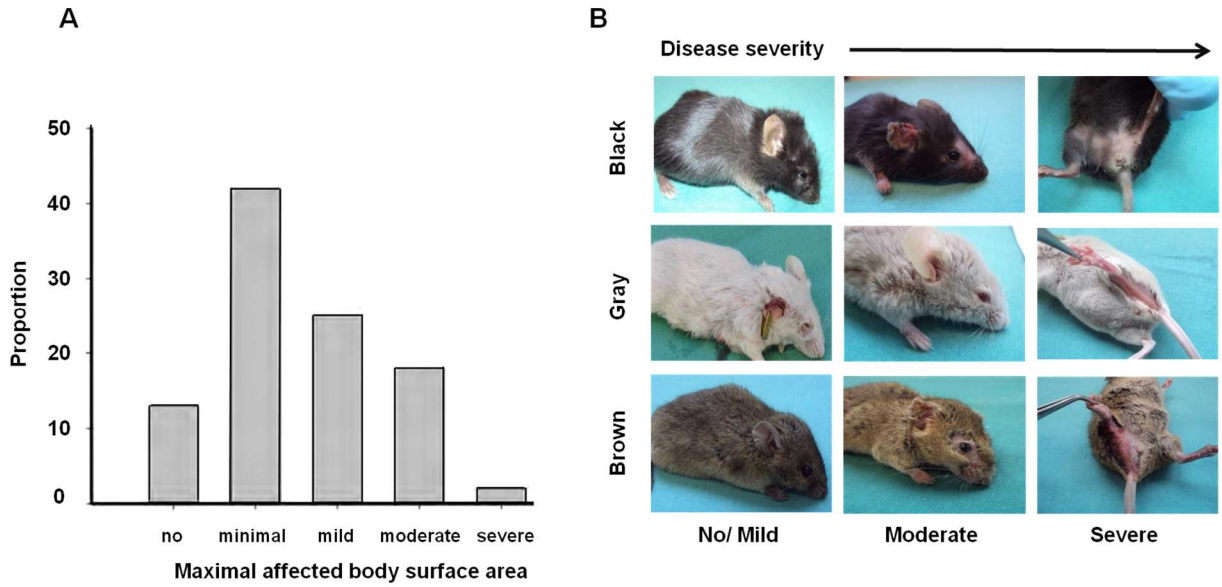

Figure 32: Mice of an autoimmune prone AIL show a high variation regarding susceptibility to antibody-transfer induced EBA.

A) Experimental EBA was induced in mice of an autoimmune prone AIL by transfer of anti-COL7 IgG. Most mice developed clinically manifest blistering. The graph shows the proportion of mice with no, minimal, mild, moderate or severe skin blistering, corresponding to a body surface area affected by skin blistering of <1%, 1-4.9%, 5-9.9%, 10-20% or >20%, respectively. B) Representative clinical photographs of AIL mice, showing no, a moderate or a severe skin blistering phenotype.

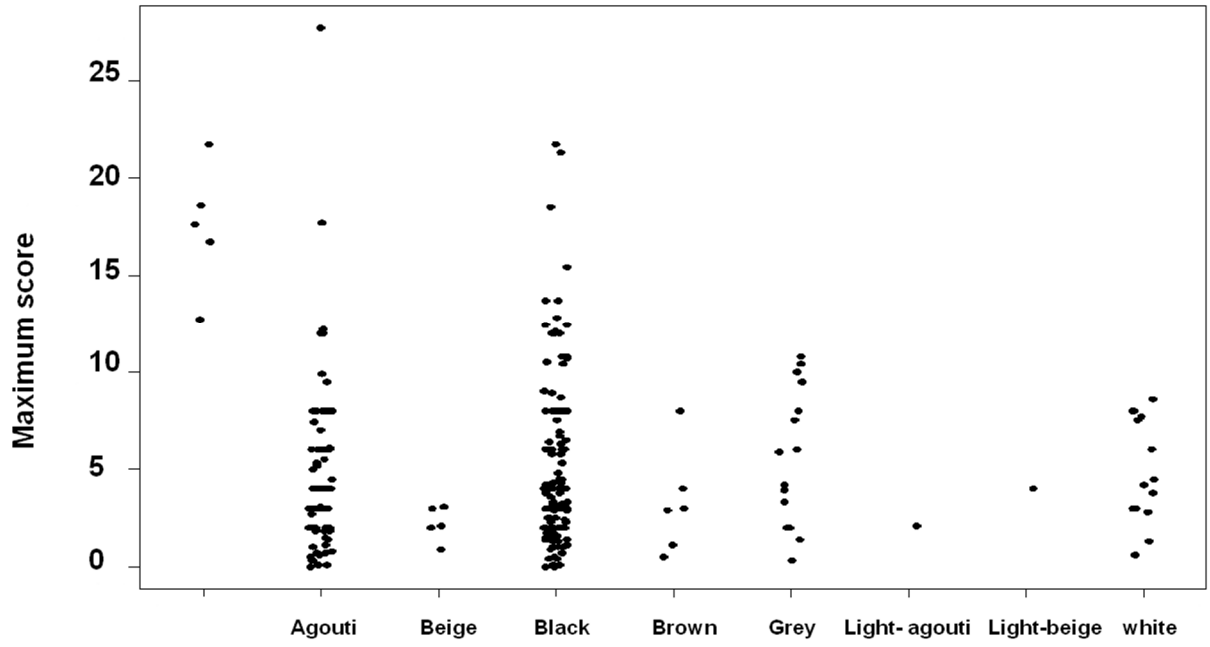

Figure 33: Fur color had no impact on clinical EBA manifestation in mice.

The genetic diversity of this so termed four-way, intercross mouse line was reflected through different morphological traits such as fur color Fur color had no impact on clinical EBA manifestation (P=0,086).

4.13. EBA susceptibility Genes

4.13.1. Expression mapping to narrow down the number of potential susceptibility genes

To identify the genetic control of antibody-induced skin blistering at the single-gene level, I examined the correlations between previous gene expression profile in the skin of antibody-transfer induced EBA [64] and genes encoded by 9:61628273-85033289 and 18:57559944-57589991 (blocks D and I from table 11). For the analysis, genes showing a greater than 2-fold change in expression in the skin of mice with EBA compared to healthy control mice were considered. To further narrow down the genomic regions associated with antibody-transfer induced EBA, only genes that had been noted to be differently expressed in antibody transfer EBA in BALB/c mice were considered [64]. This led to the identification of seven genes encoded by 9:61628273-85033289 and 18:57559944-57589991. The analysis was performed by Yask Gupta (Dept. of Dermatology, University of Lübeck) (Table 12).

CAR12	carbonic anyhydrase 12
CCNB2	cyclin D2
CLPX	caseinolytic peptidase X
RORα	retinoid-related orphan receptor α
SLTM	SAFB-like, transcription modulator
TCF12	transcription factor 12
ZFP 280	zinc finger protein 280

Table 12: Genes were identified as susceptibility genes of antibody-transfer induced EBA.

4.13.2. Identification the RORα as a risk gene for antibody-induced tissue damage in experimental EBA

To further narrow down the genes I performed STRING database analysis where I built a network using susceptible genes (table 12) and other molecules previously linked to EBA pathogenesis (table 13).

Gene	Full name	Involvement in EBA
C3	complement component 3 Gene	Complement activation Is required for blister formation in Experimental EBA [36]
IL6	interleukin 6 Gene	Recombinant IL-6 treatment protects mice from organ specific autoimmune disease by IL-6 classical signaling-dependent IL-1Ra induction [71].
Casp 1	Caspase-1 Gene	Cleaves IL-1 beta to the mature cytokine and seems to be involved in a variety of inflammatory processes in EBA (my thesis).
IL1r (I & II)	interleukin 1 receptor, Gene	Receptor for IL-1α, IL-1β, IL-1Ra. Seems to be involved in a variety of inflammatory processes in EBA (my thesis).
Fcγrt	Fc gamma receptor, IgG	FcγRIV is a key molecule in autoantibody-induced EBA [64]
Hc	hemolytic complement Gene (C5-C9)	C5-deficient mice were completely protected from induction of experimental EBA [49]
IL1rn	interleukin 1 receptor antagonist Gene	Recombinant IL-6 treatment protects mice from organ specific autoimmune disease by IL-6 classical signaling-dependent IL-1Ra induction [71].
IL1β	interleukin 1 beta Gene	IL-1 proteins are involved in the inflammatory response and seems to be involved in a variety of inflammatory processes in EBA (my thesis).

Table 13: Genes related to EBA pathogenesis.

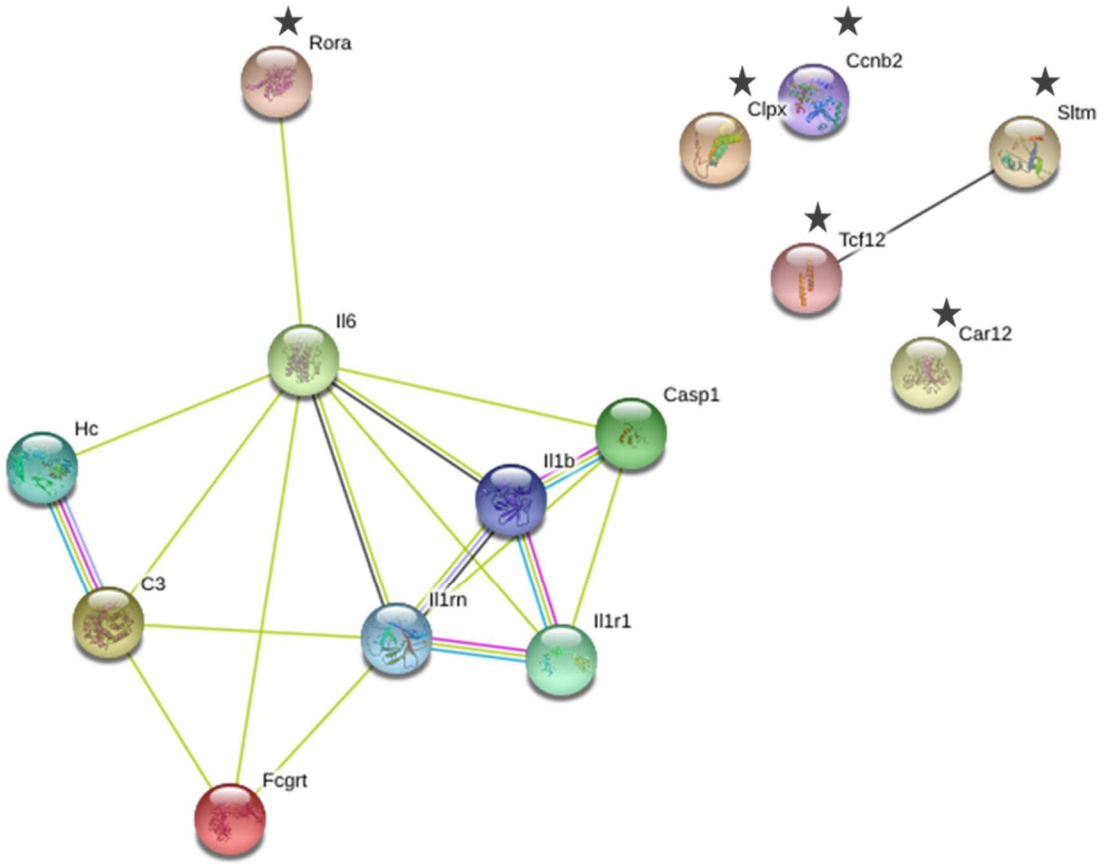

Figure 34: STRING database analysis shows that among the identified EBA susceptibility genes (marked with star), only RORα is connected to EBA network of already known genes. *Lines connecting genes represent the existence of the seven types of evidence used in predicting the associations. A green line: neighborhood evidence; a blue line: coocurrence evidence; a purple line: experimental evidence; a light blue line: database evidence; a black line: coexpression evidence.*

At low confidence, the only gene which shows association with already known genes is RORα. Therefore, RORα has been chosen for further experiments to confirm its role in blister formation in EBA.

4.13.3. Decreased skin blistering in antibody-transfer induced EBA in RORα +/- mice

Interestingly RORα protein expression has been shown in the skin [201]. For this reason, EBA was induced in the RORα +/- and in RORα -/- mice. Compared to RORα +/+ mice RORα +/- mice show less skin blistering after transfer of anti-COL7 IgG. In figure 35 the cumulative clinical disease severity expressed as AUC, calculated from the individually affected body surface area on days 4, 8 and 12, is presented.

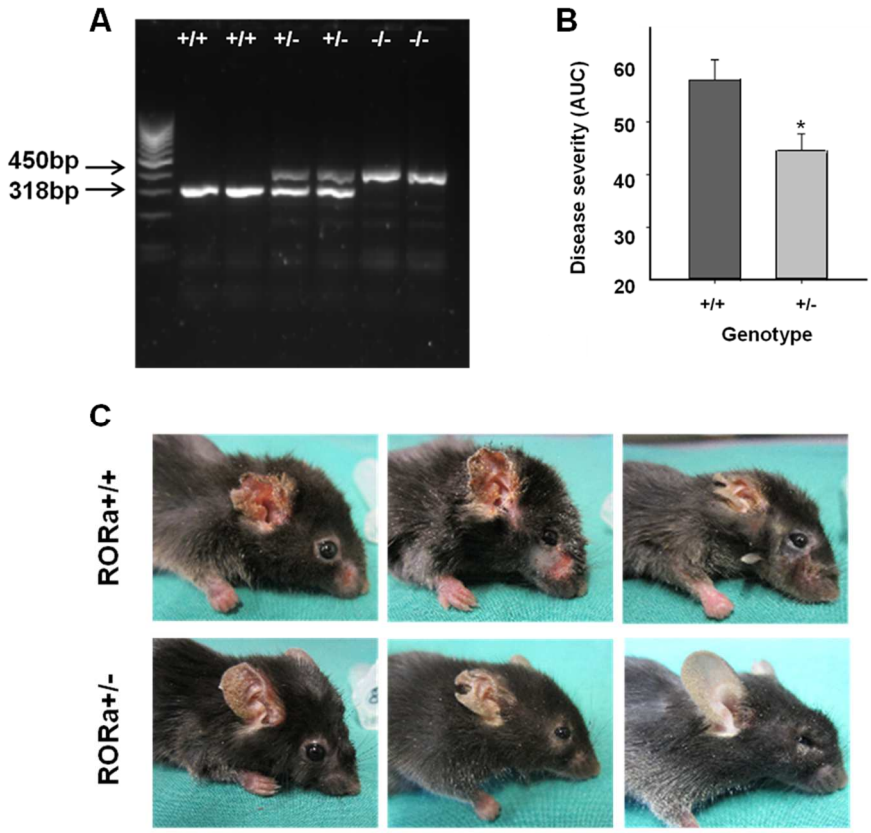

Figure 35: Reduced blister formation in RORα +/- mice.

*A) Genotype of RORα +/+, +/- or -/- mice. B) Compared to RORα +/+ mice (n=23), RORα +/- mice (n=19) showed less skin blistering after the transfer of anti-COL7 IgG. The cumulative clinical disease severity is expressed as the area under the curve (AUC), which was calculated using the individually affected body surface area on days 4, 8 and 12. *p<0.05 (two-way ANOVA, considering gender and genotype as independent variables, and the Bonferroni t-test were used for multiple comparison procedures) C) Representative clinical photographs of anti-COL7 IgG-injected RORα +/+ and +/- mice on day 12 of the* experiment.

4.13.4. Deficient RORα mice were protected against EBA

Since RORα -/- is lethal at week-five, the EBA susceptibility was tested in three weeks old mice. Disease was induce at day 0 and mice were followed up over a period of eight-days. Compared to WT littermates (n=5) that developed clinical and histological disease, RORα -/- (n=2) were completed protected against EBA since nor clinical phenotype neither histological examination pointed to EBA manifestations (Figure 36).

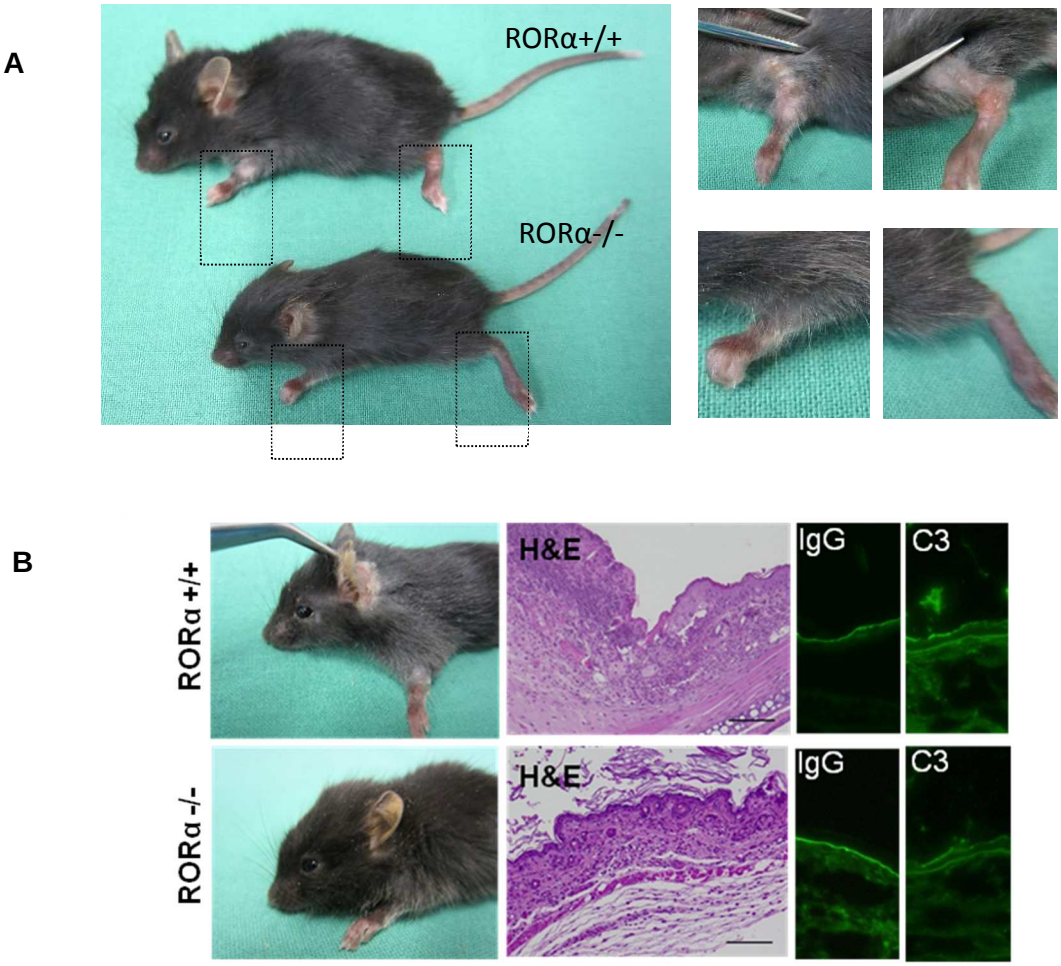

Figure 36: RORα deficient mice are protected against EBA.

Combination of forward genetics, validation in AIL mice and expression profiling identifies RORα as an EBA susceptibility gene, 2-3 weeks old mice were injected with 2 mg IgG in daily basis for ten days. Clinical photographs (and details) of skin lesions in RORα+/+ and -/- mice, demonstrating a lack of clinical evident blistering in RORα -/- mice. In line with the clinical observation, histological examination of RORα -/- skin obtained on day eight after the first anti-C7 IgG injection showed no presence of subepidermal blistering and the absence of a dermal leukocyte infiltrate (bar corresponds to 100µm). No differences regarding IgG- and C3-deposition along the DEJ were observed.

5. Discussion

The main question of my thesis was to identify if IL-1 is of functional relevance in the pathogenesis of EBA and whether IL-1 blocking could be a promising therapeutic option in EBA patients. As the effect of preventive or therapeutic IL-1 inhibition was not complete, I next used a genetic approach to identify novel therapeutic targets to modulate antibody-induced blistering in EBA.

In the first part of my thesis (contribution of IL-1 to EBA pathogenesis) I observed increased IL-1 concentrations in the serum in experimental EBA, as well as an increased cutaneous expression of IL-1. Moreover, I provided strong evidence for pro-inflammatory functions of IL-1 in experimental EBA. The findings of the current study support previous results on the role of IL-1 in other animal models of chronic inflammatory diseases such as rheumatoid arthritis [276] and in IL-1 driven diseases in human such as periodic fever syndromes. Both, genetic and pharmacological blockade of IL-1 function led to significant decrease in disease severity after injection of anti-COL7 IgG compared to control mice. Administration of recombinant IL-1Ra partially protects mice from disease. Treating mice in both active and passive EBA animal model with caspase-1 inhibitor mice improved blistering. These results are discussed in more detail below (5.1).

In the second part of my thesis, aiming to identify novel genes/pathways involved in blistering of antibody-transfer induced EBA, I identified a total of seven genes to be associated with blistering in this model. RORa was selected for further validation. In RORa -/- mice I demonstrated a complete lack of blistering after transfer of anti-COL7 IgG, supporting the notion that this gene is involved in blister formation in EBA. These results are discussed in more detail below (5.2).

5.1. Contribution of IL-1 to the pathogenesis of blistering in experimental EBA

There is ample evidence for an increased expression of several cytokines in AIBD. Despite these findings, and in contrast to other chronic inflammatory diseases [277-280] a cytokine-targeting therapy has not been established in EBA or any other AIBD with the exception of the relatively well documented beneficial effects of TNF-α inhibition in mucous membrane pemphigoid [281]. In experimental EBA, induced by transfer of anti-COL7 IgG into C57BL/6 or BALB/c mice, increased serum concentrations of several cytokines were noted [71]. This is the first experimental evidence for a direct pathogenic role of IL-1 in experimental EBA. In addition, induction of experimental EBA led to increased levels of IL-1, mainly locally in skin.

Furthermore, genetic or pharmacological blockade of IL-1 function impaired induction of experimental EBA. Interestingly, blockade of IL-1R not only impaired disease severity, but also led to a reduction of IL-1 expression in the skin. my findings are in line with observations in experimental models of arthritis [282].

5.1.1. Different pathways of IL-1β maturation are involved in EBA pathogenesis

Regarding IL-1β maturation, it is known that several blood cells are capable of synthesizing IL-1 in both cell-associated and plasma levels. Keratinocytes also produce significant amounts of the 31-kDa IL-1β precursor protein. Keratinocytes fail to convert it to the 17.5-kDa bioactive form under nonpathologic conditions, but active IL-1β was detected in keratinocytes and their supernatants treated with irritant chemicals [283].

The functional effects of IL-1β are tightly regulated on several levels, including transcription, mRNA stability, translation, maturation, secretion, receptor expression and release of soluble receptors, as well as the naturally occurring IL-1Ra. As the maturation of IL-1β into a bioactive molecule is of central importance in this regulatory cascade, it is still not entirely clear for most cell types and tissues where exactly pro-IL-1β is cleaved into the mature form and how it is secreted. There are number of findings to support that cleavage of pro-IL-1β also taking place outside the cells and this includes the observation that firstly, mature IL-1β is virtually absent inside cells and that secondly, active caspase-1 is secreted.

This scenario also underlines the importance of other proteases, involved in the cleavage and potential activation of IL-1β (table 14). These “alternative” activation mechanisms may account for a significant proportion of biologically active IL-1β, as suggested by experimental models in which deficiency of IL-1β or IL-1RI largely improved inflammatory arthritis, whereas caspase-1 inhibition leads only to partial inhibition of inflammatory changes (approximately 50%). As yet, there is only limited information on the *in vivo* significance of inflammation-associated proteases for IL-1 family activity in human disease. Of note, different proteases cleave the pro-forms of the cytokine at different sites, thereby giving rise to fragments of differential biological activity or even leading to inactivation of IL-1β.

Caspase-1 • Cysteine protease	Cleaves pro-IL-1_ (31 kDa) at to mature 17 kDa IL-1β	[284]
Neutrophil serine proteases • Proteinase-3 • Neutrophil elastase	Similar to neutrophil elastase (NE), Cleaves pro-IL-1β to mature 18.5 kDa IL-1β (16% 103activity) and to 17.5 kDa fragment (20% 103activity)	[285, 286]
Cathepsin G	Cleaves pro-IL-1β to 17.5 kDa fragment (80% 103activity)	[287, 288]
Mast cell granules • Mast cell chymase contained in secretory granules of the MCTC subtype predominant in skin and gut submucosa	Cleaves pro-IL-1β (31 kDa) to 18 kDa IL-1β (equivalent activitya)	[289]
Cytotoxic T cell granules • Granzyme A	Cleaves pro-IL-1β to 18 kDa IL-1β (30% activitya)	[290]
Trypsin	Cleaves pro-IL-1β to 25 kDa fragment (6% activity)	[115, 291]
Plasmin Poorly active, 23 kDa • Caspase-8 (not described in human cells)	Cleaves pro-IL-1_ at Asp116-Asp117 to 17 kDa IL-1β	[292]
Metalloproteases (produced/expressed by diverse cells) • MMP-9 (Gelatinase B) • MMP-3 (Stromelysin-1) • MMP-2 (Gelatinase A)	 Cleaves pro-IL-1β to 26 kDa (inactive) and 17 kDa (active) fragments Cleaves pro-IL-1_ to 28 kDa (inactive) and 14 kDa (low activity) Products Cleaves pro-IL-1_ to 16 kDa (low activity) and 10 kDa (inactive) fragments Inactivates mature IL-1β	[293, 294]
Meprin B	Cleaves pro-IL-1β to 20 kDa IL-1β (80% activity)	[295]
Pathogen associated proteases • Entamoeba histolytica cysteine proteinases	Cleaves pro-IL-1β to active 18 kDa fragment Inactivation also described	[296, 297]

Table 14. An overview of proteases which have been described to cleave pro-IL-1, adopted from [298].

It becomes apparent that in EBA IL-1 plays a major role and contributes to blister formulation. My findings suggest that not only leukocytes but also keratinocytes can be source of IL-1. However, it seems other mechanisms than caspase-1 are involved in IL-1β maturation since caspase-1/11 -/- mice were not protected against EBA. Caspase-1/11 -/- mice developed blisters to an extent similar to that in wild-type control mice. This assumption is further supported by the comparable skin concentrations of mature IL-1β in both, caspase-1/11 -/- and wild type mice. Therefore, caspase-1 independent process of IL-1β seems to mediate susceptibility in EBA. In line with these findings, in both acute and chronic streptococcal cell wall arthritis, IL-1β protein concentrations were 2–3 folds higher in caspase-1/11 -/- mice than in wild type mice [270]. Of interest, IL-1β protein concentrations declined rapidly in caspase-1/11 -/- in chronic SCW arthritis but not in acute SCW arthritis [270]. Alternative enzymes other than caspase-1 can process IL-1β *in vitro*, neutrophil-derived serine proteases, cathepsin G (CG), neutrophil elastase (NE), and proteinase 3 (PR3) as well as mast cell derived serine proteases (granzyme A and chymase) cleave the IL-1β precursor at distinct sites into a secreted biologically active form [287, 290, 292, 299-301]. These enzymes are predominantly neutrophil-derived and this can be another proof of neutrophil dependent of EBA. Interestingly, pharmacological inhibition of caspase-1 activity resulted in significantly decreased of EBA severity. Due to the aforementioned results, I argue for an off-target effect upon VX-765 treatment. Presumably, VX-765 also targets additional molecules contributing to EBA pathogenesis.

5.1.2. Signaling downstream of IL-1

Regarding the effects downstream of IL-1, here I show that induction of EBA leads to an increased endothelial ICAM-1 expression and this expression is decreased in IL-1R-deficient and anakinra-treated mice with experimental EBA. Most likely, this decrease reflects the lower clinical disease activity in these mice. IL-1β and IL-1Ra act through the IL-1RI, IL-1β or IL-1α induces the recruitment of the cytosolic adaptor protein, MyD88 or its analogs and initiates the activation of the IRAK/TRAF pathway leading to the activation of the transcription factor NF-κB and subsequently auto-induction of IL-1β synthesis. Therefore, anakinra as antagonist of the receptor prevents positive feedback induction of IL-1β and therefore decreasement of ICAM expression [269]. For the effector phase of experimental EBA, i.e. antibody-induced tissue injury, neutrophil depletion has been shown to protect mice from induction of skin blisters [65]. In line, CD18-deficient mice with impaired leukocyte extravasation into the skin are also completely resistant to blister induction [302]. In this context, IL-1 contributes to EBA-associated tissue injury by neutrophil functions and also leukocyte extravasation.

IL-1 modulated expression of endothelial cell adhesion molecules has been reported before showing expression of E-selectin and ICAM-1 on endothelial cells after induction by lipopolysaccharide-stimulated whole blood [303]. In study by Nooteboom et al., complete inhibition of E-selectin and ICAM-1 expression was observed when antibodies against TNF-alpha and IL-1 beta were added to plasma prior to the incubation to endothelial cultures [303]. The dependency of adhesion molecule expression in the pathogenesis of EBA has been demonstrated by the observed absence of skin lesions in CD18 deficient mice after injection of anti-COL7 IgG [65]. As shown here, induction of EBA leads to an increased endothelial ICAM-1 expression, which is absent if IL-1 function is blocked. *In vitro* experiments extended these findings to additional endothelial adhesion molecules such as VCAM-1 and E-selectin.

Published data suggest that interaction of leukocyte β2 integrins with endothelial adhesion molecules of the immunoglobulin superfamily is indispensable for blister formation in EBA. Similar findings have been reported in neonatal mice with experimental bullous pemphigoid: Blockade of CD11a, CD11b or CD18 protected mice from BP induction. In this model, detailed analysis of the neutrophil inflammatory response revealed, that CD11a is required for neutrophil recruitment, while CD11b mediates late neutrophil accumulation and neutrophil apoptosis [304]. In addition, neutrophil recruitment into the skin has been shown to also depend on additional adhesion molecules, including selectins [305] and junctional adhesion molecules [260]. Hence, it is tempting to speculate, that blockade of the respective adhesion molecules will also protect mice from disease development. Alternatively, as shown in my thesis, inhibition of pro-inflammatory factors (e.g. IL-1) controlling endothelial adhesion molecule expression are also potential targets to modulate the extravasation of effector leukocytes into the skin.

The process of extravasation primes the neutrophil for innate defence mechanisms such as phagocytosis, generation of reactive oxygen metabolites and release of anti-microbial and proteolytic proteins. Neutrophils can also orchestrate the inflammatory response through the production and release of cytokines and chemokines [306]. Circulating neutrophils express 500–900 IL-1RI per cell [307-309]. Interestingly, these extravasated cells are not only necessary for blister formation [65] by release of reactive oxygen species [65] and proteolytic enzymes [66], but also an increased expression of IL-1RI in extravasated neutrophils after migration has been demonstrated. This *increased* IL-1R expression was confirmed further in neutrophils by stimulation of peripheral neutrophils with IL-1 resulted in transcription of NFkB and a number of downstream chemokines and the corresponding chemokines were also induced following *in vivo* extravasationis [310]. Therefore, inhibition of IL-1 may also block this increased IL-1R expression on neutrophils, as well as the downstream neutrophil activation.

In our EBA model my results indicate a potential role for IL-1 in the activation of neutrophils at inflammatory sites. I believe that in EBA neutrophils are recruited to sites of inflammation by interaction with adhesion molecules and chemokines, which are expressed on IL-1β and TNF-α activated endothelium.

5.2. Genetic control of susceptibility to blistering in EBA

5.2.1. EBA susceptibility genes

First part of my thesis shows that blistering in EBA partially depends on IL-1. Identifying additional pathways were the focus of the second part of my thesis.

Genetic methods are valuable tools to the underlying genetic basis of skin disorders, here I used forward genomics combined with validation by genotyping and expression profiling in order to identify susceptible genes controlling blistering in EBA.

Recent advances in genomic research offer a remarkable opportunity to identify disease susceptibility genes. Incorporation of these findings into past biological knowledge and clinical experience can bring to light novel molecular networks that cause disease. The major advantages of this approach are the lower expenditures and time required to identify novel risk genes for complex diseases [54, 311].

In this study, I applied forward genomics combined with validation using genotyping, expression profiling and knock-out mice. For this purpose I checked susceptibility of 18 variant strains for developing antibody-transfer induced EBA. The results presented here provide strong evidence for strain dependency of antibody-transfer induced EBA. Interestingly other groups before also demonstrated a strain dependency of antibody-induced nephritis [239] and arthritis [273].

The result of association test on 18 mouse strains, guide us to identifying 8 quantitative trait loci (QTLs). From these QTLs, seven candidate SNPs (the most highly correlated ones) have been chosen and confirmed with a dense linkage analysis in 7th generation. I then identified seven possible genes in the chromosome nine responsible for susceptibility to passive EBA.

CAR12: Gene ID: 771, (carbonic anyhydrase 12) Carbonic anhydrases (CAs) are a large family of zinc metalloenzymes that catalyze the reversible hydration of carbon dioxide. They participate in a variety of biological processes, including respiration, calcification, acid-base balance, bone resorption, and the formation of aqueous humor, cerebrospinal fluid, saliva, and gastric acid. This gene product is a type I membrane protein that is highly expressed in normal

tissues, such as kidney, colon and pancreas, and has been found to be overexpressed in 10% of clear cell renal carcinomas. Two transcript variants encoding different isoforms have been identified for this gene (Provided by RefSeq, Jul 2008).

CCNB2: Gene ID: 12442, Cyclin-B2 is essential components of the cell cycle regulatory machinery. Cyclin B2 is a member of the cyclin family, specifically the B-type cyclins. The B-type cyclins, B1 and B2, associate with p34cdc2 and are essential components of the cell cycle regulatory machinery (Provided by RefSeq, Jul 2008).

CLPX: Gene ID: 270166, caseinolytic peptidase X is an ATP-dependent specificity component of the Clp protease. It directs the protease to specific substrates. Can perform chaperone functions in the absence of clpP. Belongs to the ClpX chaperone family

TCF12**:** Gene ID: 21406, transcription factor 12, is a member of the basic helix-loop-helix (bHLH) E-protein family that recognizes the consensus binding site (E-box) CANNTG. This encoded protein is expressed in many tissues, among them skeletal muscle, thymus, B- and T cells, and may participate in regulating lineage-specific gene expression through the formation of heterodimers with other bHLH E-proteins (Provided by RefSeq, Jul 2008).

ZFP280**:** Gene ID: 129025, zinc finger protein 280 ZNF280 is a protein-coding gene. Diseases associated with ZNF280 include doid: 4019, and articulation disorder. GO annotations related to this gene include DNA binding and zinc ion binding (Provided by RefSeq, Jul 2008).

SLTM: Gene ID: 66660 SAFB-like, transcription modulator, or also known as MET (Mesenchymal epithelial transition factor), is a proto-oncogenic receptor tyrosine kinase. The endogenous ligand for MET is hepatocyte growth factor/scatter factor (HGF), a disulfide-linked heterodimeric molecule produced predominantly by mesenchymal cells (Provided by RefSeq, Jul 2008).

RORα: Gene ID: 19883, Retinoid acid receptor-related orphan receptor α, is a member of the orphan ROR subfamily of the nuclear receptor superfamily of transcription factors which appears to have a general role in cell survival in the central nervous system (CNS). ROR-α is expressed at low to moderate levels in most physiological systems, including the central nervous system (CNS), endocrine system, gastrointestinal system, reproductive system, cardiopulmonary system and metabolic tissues. Enhanced production of IL-2 and IL-6 using CGP 52608, a specific ligand of the putative nuclear melatonin receptor RZR/ROR, raising the possibility of direct effects of melatonin on gene regulation in both TH1 cells and monocytes [312].

The possible identified risk genes (mentioned above) have been used in STRING database to find out if there are any connections with already known pathways in EBA blistering. According to STRING results, except RORa, other genes seem to have no connection to well validated pathways in EBA blistering.

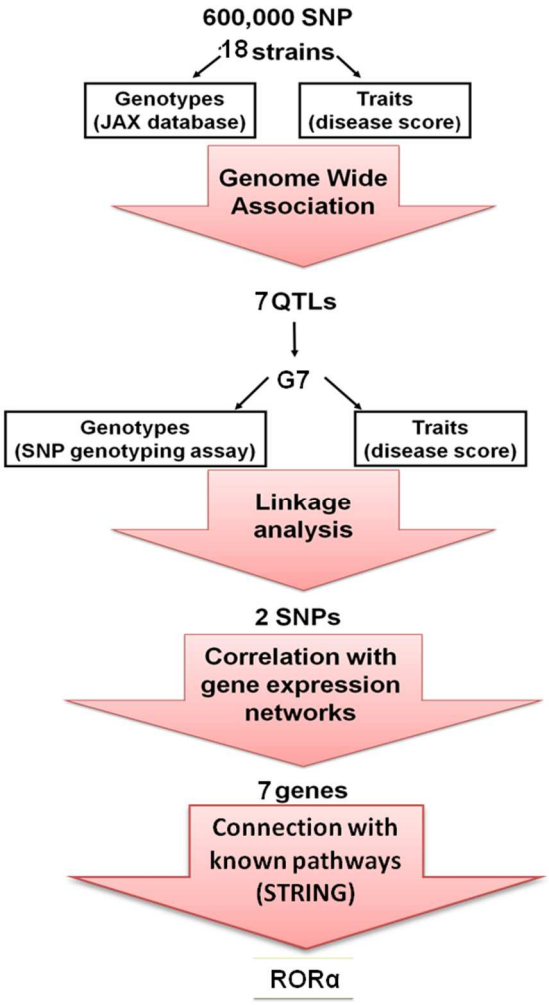

Figure 37. Combined Genome wide association study with linkage analysis used in this study resulting to identify RORa as a susceptible gene in EBA blistering. First, 18 genetically well characterized inbred strains were tested for EBA susceptibility A genome-wide association study was then performed which lead to the identification of 8 QTLs controlling autoantibody induced tissue injury in experimental EBA. For confirmation, antibody transfer EBA was induced in generation seven of mice from an advanced four-way intercross line. Two QTLs were confirmed by genotyping the respective single-nucleotide polymorphisms in the mice from the intercross line. Using haplotype-sharing analysis, we then fine mapped QTLs down to 6 Mb. Microarray data between EBA and normal mice have been used to find and differential expressed genes. Furthermore by using gene network candidate hub genes have been identified. To further narrow down the genes using STRING database analysis, a network of seven susceptible genes and other molecules previously linked to EBA pathogenesis has been built. Among these susceptibility genes only RORα shows association with already known genes.

5.2.2. RORa in EBA

RORα is a nuclear receptor involved in many pathophysiological processes such as inflammation, atherosclerosis and angiogenesis [313]. Therefore and based on STRING findings, RORa was chosen for further validation. Susceptibility of knockout RORα mice to EBA was investigated. I identified for the first time a new role for the RORα as an important

negative modulator of EBA pathogenesis. In this research, I could demonstrate that RORα deficient mice were protected against EBA.

5.2.2.1. RORa function

RORα maps to a conserved region of homology on human chromosome 15q21-q22 and mouse chromosome 9 [314]. Albeit RORα is expressed in a variety of tissues, including immune cells, it is most highly expressed in the brain. Furthermore, RORα has been shown to contribute to retinal development, bone formation, lipid metabolism and lymphocyte development [315-317], resulting in premature death of RORα deficient mice [201]. In genome-wide association studies RORα has been identified to be associated with predominant neurological disorders [318], as well as C-reactive protein levels [319], concentrations of liver enzymes in plasma [320], and asthma [321]. In the immune system RORα (together with RORγ) has been shown to modulate Th17-polarization [322]. It, however, remains unclear, if the observed defective lymphocyte development in RORα deficient mice is caused indirectly, i.e. by stress due to body imbalance of these mice, or the neurological defect in these mice resulting in abnormal activities of hormones that can affect lymphocyte development [315].

Interestingly, IL-1 regulates the expression of the transcription factors IRF4 and RORγ and RORα during Th17 cell differentiation, thus indicating a critical role of IL-1 in Th17 cell differentiation and Th17 cell-mediated autoimmunity. In fact, TH17 differentiation is initiated by TGFβ and IL-6 in mouse [323-325]. RORα is highly expressed in TH17 and induced by TGF-β and IL-6 in a STAT3-dependent manner [326]. Overexpression of RORα promotes TH17 differentiation and significantly up-regulates IL-17. Furthermore RORα deficiency results in reduced IL-17 expression *in vitro* and *in vivo*. Additionally double deficiency in RORα and RORγ entirely impair TH17 generation *in vitro* and completely inhibit experimental autoimmune encephalomyelitis (EAE) disease. In line, double deficiency in RORα and RORγ globally impair TH17 generation and completely protect mice against EAE [326].

RORα has been reported to be expressed in human primary smooth-muscle cells and that ectopic expression of RORα inhibits TNFα-induced IL-6, IL-8 and COX-2 expression [327]. Other group showed that the induction of IL-6 was greatly increased in RORα -/- mast cells and macrophages after LPS treatment in human primary smooth-muscle cells [311, 315, 328]. Mouse RORα gene is ubiquitously expressed; higher levels of expression have been observed in the Purkinje cells of the cerebellum, retina, lens, spleen, skeletal muscle, and testis [329-331].

On the other hand, RORα has been mentioned as a negative regulator of the inflammatory response [332] and in the same line RORα staggerer mice are susceptible to lipopolysaccharide-induced lung inflammation. Interestingly, RORα negatively interferes with the NF-κB signalling pathway by reducing p65 translocation. This action of RORα on NF-κB is associated with the induction of IκBα, the major inhibitory protein of the NF-κB signalling pathway, whose expression was found to be transcriptionally up-regulated by RORα [327].

5.2.2.2. RORa in the pathogenesis of EBA

In the present study, based on forward genomics combined with several validation steps, including the use of knock-out mice, I identified RORα as a requirement for development of experimental EBA. This indicates that RORα inhibition may have beneficial effects in chronic inflammatory diseases such as EBA [333], arthritis [334]. Notably, after inflammatory stimulation, the absence of RORα results in excessive IL-6 up-regulation which is principally driven by the NF-κB signalling pathway [327]. We speculate that RORα exerts an indirect repression on IL-6 probably via the inhibition of the NF-κB signalling. Although being IL-6 considered as a proinflammatory molecule, we have recently demonstrated the anti-inflammatory effects of IL-6 in experimental EBA [71].

I conclude that RORα knockout phenotype can be attributed both, to inhibition of IL-17 and induction of IL-6. Collectively, my findings pave the way for novel treatments of EBA, by pharmacological inhibition of RORα.

5.3. Summary and outlook

Taken together, I here provide novel insights into the contribution of the cytokine IL-1 to the pathogenesis of antibody-induced tissue injury in a prototypical organ-specific autoimmune disease using both patient material and experimental *in vivo* models (Figure 38). In EBA, binding of autoantibodies to COL7, located at the dermal-epidermal junction, leads to formation of a pro-inflammatory milieu including expression and up-regulation of different cytokines including IL-1. This leads to the CD18-dependent recruitment of neutrophils into the skin [36]. ICAM-1 in IL-1R deficient and anakinra treated mice decreased after EBA induction. Therefore IL-1-modulated endothelial adhesion molecule expression presumably contributes to the pathogenesis of EBA, rendering IL-1 functions a potential therapeutic target for diseases with antibody-induced tissue injury. Caspase-1 appears not to be the only way of IL-1β maturation. These findings in the mouse model may be applicable in patients with EBA, as I

also observed serum IL-1α and IL-1β concentrations of patient were increased and correlated with disease severity.

Here also I demonstrated that forward genomics combined with validation by genotyping and expression profiling is a suitable approach for identification of susceptibility genes. Based on these findings, RORα role in antibody-induced inflammation possibly is through cytokines such as IL-1 and IL-6 (Figure 38). Using this approach, RORα was identified to be essential for immune complex-mediated and should be considered as a potential therapeutic target for the treatment of EBA and possibly other antibody-induced, neutrophil-mediated diseases, such as bullous pemphigoid and rheumatoid arthritis.

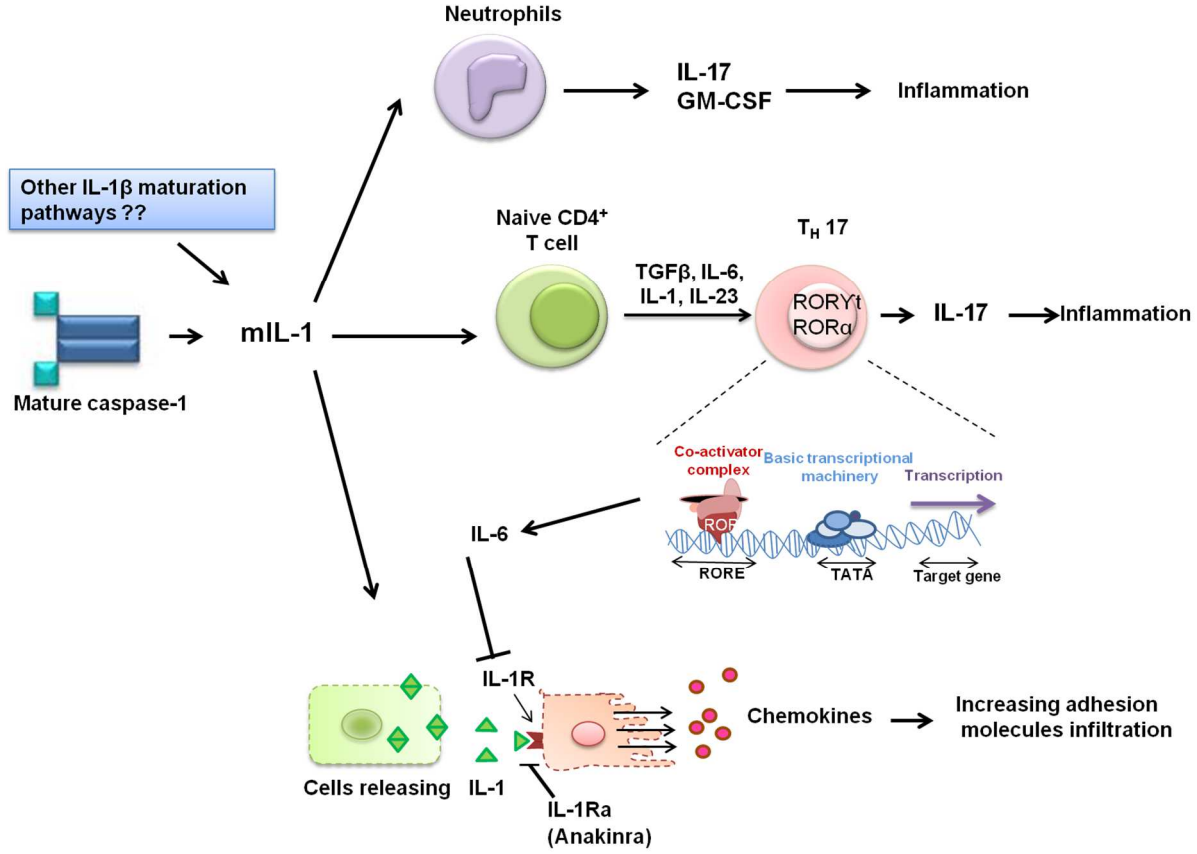

Figure 38. Schematic representation of the different sets of cellular players and molecular events linked to IL-1 network contributing to EBA pathogenesis.

6. Abstract

6.1. Abstract, English

Cytokine modulating strategies are successfully implemented in the treatment of many inflammatory conditions. However, in AIBD, despite aberrant cytokine expression, cytokine-targeting therapies have not been established, most likely due to the lack of functional data.
My study focused on the systematic analysis of IL-1 contribution to the pathogenesis of an AIBD using an animal model of EBA. In line with human case, after EBA was induced in mice by injections of anti-COL7 IgG, IL-1β concentration were increased. Genetic and pharmacologic inhibition of IL-1 signaling impaired blister formation in both antibody transfer and immunization-induced EBA. At the functional level, our findings suggested that IL-1 contributes to recruitment of adhesion molecules into the skin. Expression of ICAM-1 was decreased in IL-1R-deficient and anakinra-treated mice with experimental EBA. Furthermore, caspase-1 inhibitor (VX-765) also impaired blister formation in both EBA models. However, caspase-1/11 -/- mice could process IL-1 to the active form and these mice were not protected from antibody-transfer induced EBA, pointing towards off-target effects of VX-765. These data suggests that IL-1, independent of caspase-1, contributes to the pathogenesis of EBA through modulation of adhesion molecules.
In an effort to identify cytokine-related potential targets, an alternative method for risk-loci identification in EBA has been established. In detail, antibody-transfer induced EBA showed diverse disease severity in different inbred strains. By the use of publicly available genotyping data, haplotype blocks controlling blistering were identified, and two blocks were confirmed in outbred mice. To identify the blistering-associated genes, haplotype blocks encoding genes that are differentially expressed in EBA-affected skin were considered and seven genes were identified. To address the functional connectivity of these gene with EBA related cytokines, I interrogated the STRING database that compiles known and predicted protein-protein interactions and RORα was selected since it showed direct connection with IL-6 and indirect with IL-1. To confirm these findings, RORα deficient mice were tested for antibody-transfer induced EBA susceptibility and they were completely protected. Thus, RORα is essential for blister formation in experimental EBA. Based on these findings, RORα plays role in antibody-induced inflammation through cytokine network modulation.

In conclusion, this work paves the way for considering IL-1 targeting therapies such as Anakinra in AIBD and offers the prospect of designing novel drugs that could modulate cytokine-related molecules, like RORα.

6.2. Abstract, German

Therapeutische Strategien zur Modulation von Zytokinen werden bereits heute erfolgreich in der Behandlung vieler entzündlicher Erkrankungen angewandt. Gleichwohl sind bislang bei blasenbildenden Autoimmundermatosen (AIBD) trotz veränderter Zytokinexpression keine gezielt gegen Zytokine gerichteten Therapien etabliert. Die Ursache dafür liegt höchst wahrscheinlich an den fehlenden dafür erforderlichen funktionellen Daten.

Meine Untersuchungen im Rahmen meiner Promotion konzentrierten sich daher auf die systematische Analyse der Rolle von IL-1 zur Pathogenese einer AIBD (Epidermolysis Bullosa Acquisita, EBA).

Die Analyse wurde an einem Tiermodell (Maus) durchgeführt, bei welchem sich mit Indizierung von EBA die Konzentration von IL-1ß im Serum auf vergleichbare Werte wie bei einem Menschen erhöhen ließ.

Die genetische und pharmakologische Blockade des IL-1 verminderte die Blasenbildung sowohl in der durch Antiköpertransfer als auch in der durch Immunisierung induzierten EBA. Auf der funktionellen Ebene lassen meine Ergebnisse daher vermuten, dass IL-1 zur vermehrten Expression von Adhäsionsmolekülen in der Haut und somit zur vermehrten Rekrutierung von Effektorzellen beiträgt.

Nachfolgende funktionale Untersuchungen, die auf die Regulation des IL-1 bei EBA abzielten, zeigten des Weiteren, dass der Caspase-1-Inhibitor VX-765 auch die Blasenbildung in beiden EBA Modellen unterdrückte. Gleichwohl Caspase-1/11 defiziente Mäuse IL-1 in die aktive Form umwandeln konnten, waren diese Mäuse nicht gegen die durch Antikörpertransfer induzierter EBA geschützt. Dies weist auf unspezifische Nebeneffekte von VX-765 hin und legt nahe, dass IL-1 unabhängig von Caspase-1 zur Pathogenese von EBA durch die Modulation von Adhäsionsmolekülen beiträgt.

Da die Blockade des IL-1 die Krankheitsaktivität im Mausmodell der EBA signifikant aber nicht komplett inhibierte, wurde in einem weiteren Abschnitt meiner Arbeit nach neuen potentiellen therapeutischen Zielstrukturen gesucht. Diese Untersuchungen basierten auf der Beobachtung, dass die Induktion einer experimentellen EBA durch Antikörpertransfer ein unterschiedliches Ausmaß in verschiedenen Inzuchtstämmen aufwies. Durch die Verwendung der öffentlichen Genotypisierungsdaten dieser Mausstämme konnten mehrere Regionen des Genoms identifiziert werden, welche mit der Induktion der Blasenbildung bei experimenteller EBA assoziiert sind.

Zwei dieser Genabschnitte konnten in einem Validierungsexperiment an 315 Mäusen eines Auszuchtstamms bestätigt werden. Um die mit der Blasenbildung assoziierten Gene zu

identifizieren, wurde die differentielle mRNA Expression in EBA erkrankter Haut mit in die weitere Analyse einbezogen. Insgesamt identifizierte ich sieben Gene innerhalb dieses Genabschnittes.

Um die funktionelle Verbindung dieser Gene mit Zytokinen, assoziiert mit EBA, zu adressieren, habe ich Daten aus der STRING Datenbank abgefragt, in der bekannte und vorhersehbare Protein-Protein-Wechselwirkungen zusammengestellt sind. Ich wählte den Retinoid acid receptor-related Orphan Receptor Alpha (RORα) aus, da es eine direkte Verbindung mit IL-6 und eine indirekte mit IL-1 zeigte.

Zur Bestätigung dieser Ergebnisse, wurden RORα-defiziente Mäuse auf ihre Suszeptibilität im Antikörpertransfermodell der EBA getestet, mit dem Ergebnis, dass sie völlig geschützt waren. Somit ist RORα wichtig für die Blasenbildung in der experimentellen EBA. Basierend auf diesen Erkenntnissen kann festgehalten werden, dass RORα eine Rolle spielt in der Antikörper-induzierten Entzündung durch die Modulation des Zytokin-Netzwerks.

Zusammengefasst ebnet diese Arbeit den Weg für IL-1 gerichtete Therapien, wie Anakinra in AIBD und bietet die Aussicht auf die Entwicklung neuartiger Medikamente, die Zytokin-bezogene Moleküle wie RORα modulieren können.

7. References

1. Chan, L.S., *Human skin basement membrane in health and in autoimmune diseases.* Front Biosci, 1997. **2**: p. d343-52.

2. Harding, C.R., *The stratum corneum: structure and function in health and disease.* Dermatol Ther, 2004. **17** Suppl 1: p. 6-15.

3. McLafferty, E., C. Hendry, and F. Alistair, *The integumentary system: anatomy, physiology and function of skin.* Nurs Stand. **27**(3): p. 35-42.

4. Burgeson, R.E. and A.M. Christiano, *The dermal-epidermal junction.* Curr Opin Cell Biol, 1997. **9**(5): p. 651-8.

5. Schmidt, E. and D. Zillikens, *The diagnosis and treatment of autoimmune blistering skin diseases.* Dtsch Arztebl Int. **108**(23): p. 399-405, I-III.

6. Langan, S.M., et al., *Bullous pemphigoid and pemphigus vulgaris--incidence and mortality in the UK: population based cohort study.* BMJ, 2008. **337**: p. a180.

7. Wiens, A., et al., *Meta-analysis of the efficacy and safety of adalimumab, etanercept, and infliximab for the treatment of rheumatoid arthritis.* Pharmacotherapy. **30**(4): p. 339-53.

8. Joly, P., et al., *A comparison of oral and topical corticosteroids in patients with bullous pemphigoid.* N Engl J Med, 2002. **346**(5): p. 321-7.

9. Yancey, K.B., *The pathophysiology of autoimmune blistering diseases.* J Clin Invest, 2005. **115**(4): p. 825-8.

10. Atkins, D.H., R.A. Cox, and A.E. Eggleton, *Photochemical ozone and sulphuric acid aerosol formation in the atmosphere over Southern England.* Nature, 1972. **235**(5338): p. 372-6.

11. Vodegel, R.M., et al., *U-serrated immunodeposition pattern differentiates type VII collagen targeting bullous diseases from other subepidermal bullous autoimmune diseases.* Br J Dermatol, 2004. **151**(1): p. 112-8.

12. Schmidt, E. and D. Zillikens, *Diagnosis and treatment of patients with autoimmune bullous disorders in Germany.* Dermatol Clin. **29**(4): p. 663-71.

13. van Beek, N., et al., *Serological diagnosis of autoimmune bullous skin diseases: prospective comparison of the BIOCHIP mosaic-based indirect immunofluorescence technique with the conventional multi-step single test strategy.* Orphanet J Rare Dis. **7**: p. 49.

14. Schmidt, E. and D. Zillikens, *Pemphigoid diseases.* Lancet. **381**(9863): p. 320-32.

15. Spivey, J. and A.M. Nye, *Bullous pemphigoid: corticosteroid treatment and adverse effects in long-term care patients.* Consult Pharm. **28**(7): p. 455-62.

16. Jolles, S., *A review of high-dose intravenous immunoglobulin (hdIVIg) in the treatment of the autoimmune blistering disorders.* Clin Exp Dermatol, 2001. **26**(2): p. 127-31.

17. Mutasim, D.F., *Therapy of autoimmune bullous diseases.* Ther Clin Risk Manag, 2007. **3**(1): p. 29-40.

18. Roenigk, H.H., Jr., J.G. Ryan, and W.F. Bergfeld, *Epidermolysis bullosa acquisita. Report of three cases and review of all published cases.* Arch Dermatol, 1971. **103**(1): p. 1-10.

19. Ishii, N., et al., *Epidermolysis bullosa acquisita: what's new?* J Dermatol. **37**(3): p. 220-30.

20. Remington, J., et al., *Injection of recombinant human type VII collagen corrects the disease phenotype in a murine model of dystrophic epidermolysis bullosa.* Mol Ther, 2009. **17**(1): p. 26-33.

21. Callot-Mellot, C., et al., *Epidermolysis bullosa acquisita in childhood.* Arch Dermatol, 1997. **133**(9): p. 1122-6.

22. Sitaru, C., *Experimental models of epidermolysis bullosa acquisita.* Exp Dermatol, 2007. **16**(6): p. 520-31.

23. Fine, J.D., et al., *Revised clinical and laboratory criteria for subtypes of inherited epidermolysis bullosa. A consensus report by the Subcommittee on Diagnosis and Classification of the National Epidermolysis Bullosa Registry.* J Am Acad Dermatol, 1991. **24**(1): p. 119-35.

24. Pearson, R.W., *Studies on the pathogenesis of epidermolysis bullosa.* J Invest Dermatol, 1962. **39**: p. 551-75.

25. Sasidharan, C.K., M. Vijayakumar, and M.S. Vinodkumor, *Effect of phenytoin sodium in reducing blistering of epidermolysis bullosa report of four cases.* Indian J Dermatol Venereol Leprol, 2002. **68**(4): p. 217-9.

26. Nieboer, C., et al., *Epidermolysis bullosa acquisita. Immunofluorescence, electron microscopic and immunoelectron microscopic studies in four patients.* Br J Dermatol, 1980. **102**(4): p. 383-92.

27. Caux, F., *[Epidermolysis bullosa acquisita].* Presse Med. **39**(10): p. 1081-8.

28. De Jong, M.C., et al., *Bullous pemphigoid and epidermolysis bullosa acquisita. Differentiation by fluorescence overlay antigen mapping.* Arch Dermatol, 1996. **132**(2): p. 151-7.

29. Kazama, T., et al., *Application of confocal laser scanning microscopy to differential diagnosis of bullous pemphigoid and epidermolysis bullosa acquisita.* Br J Dermatol, 1998. **138**(4): p. 593-601.

30. Chen, M., et al., *Development of an ELISA for rapid detection of anti-type VII collagen autoantibodies in epidermolysis bullosa acquisita.* J Invest Dermatol, 1997. **108**(1): p. 68-72.

31. Komorowski, L., et al., *Sensitive and specific assays for routine serological diagnosis of epidermolysis bullosa acquisita.* J Am Acad Dermatol. **68**(3): p. e89-95.

32. Gammon, W.R., et al., *Autoantibodies to type VII collagen recognize epitopes in a fibronectin-like region of the noncollagenous (NC1) domain.* J Invest Dermatol, 1993. **100**(5): p. 618-22.

33. Buijsrogge, J.J., et al., *The many faces of epidermolysis bullosa acquisita after serration pattern analysis by direct immunofluorescence microscopy.* Br J Dermatol. **165**(1): p. 92-8.

34. Ishiko, A., et al., *Epidermolysis bullosa acquisita: report of a case with comparison of immunogold electron microscopy using pre- and postembedding labelling.* Br J Dermatol, 1996. **134**(1): p. 147-51.

35. Terra, J.B., et al., *Low sensitivity of type VII collagen enzyme-linked immunosorbent assay in epidermolysis bullosa acquisita: serration pattern analysis on skin biopsy is required for diagnosis.* Br J Dermatol. **169**(1): p. 164-7.

36. Ludwig, R.J., *Clinical presentation, pathogenesis, diagnosis, and treatment of epidermolysis bullosa acquisita.* ISRN Dermatol. **2013**: p. 812029.

37. Woodley, D.T., et al., *Identification of the skin basement-membrane autoantigen in epidermolysis bullosa acquisita.* N Engl J Med, 1984. **310**(16): p. 1007-13.

38. Yoshiike, T., D.T. Woodley, and R.A. Briggaman, *Epidermolysis bullosa acquisita antigen: relationship between the collagenase-sensitive and -insensitive domains.* J Invest Dermatol, 1988. **90**(2): p. 127-33.

39. Leineweber, S., S. Schonig, and K. Seeger, *Insight into interactions of the von-Willebrand-factor-A-like domain 2 with the FNIII-like domain 9 of collagen VII by NMR and SPR.* FEBS Lett. **585**(12): p. 1748-52.

40. Christiano, A.M., et al., *The large non-collagenous domain (NC-1) of type VII collagen is amino-terminal and chimeric. Homology to cartilage matrix protein, the type III domains of fibronectin and the A domains of von Willebrand factor.* Hum Mol Genet, 1992. **1**(7): p. 475-81.

41. Uitto, J., L.C. Chung-Honet, and A.M. Christiano, *Molecular biology and pathology of type VII collagen.* Exp Dermatol, 1992. **1**(1): p. 2-11.

42. Jones, D.A., et al., *Immunodominant autoepitopes of type VII collagen are short, paired peptide sequences within the fibronectin type III homology region of the noncollagenous (NC1) domain.* J Invest Dermatol, 1995. **104**(2): p. 231-5.

43. Tanaka, T., F. Furukawa, and S. Imamura, *Epitope mapping for epidermolysis bullosa acquisita autoantibody by molecularly cloned cDNA for type VII collagen.* J Invest Dermatol, 1994. **102**(5): p. 706-9.

44. Chen, M., et al., *The cartilage matrix protein subdomain of type VII collagen is pathogenic for epidermolysis bullosa acquisita.* Am J Pathol, 2007. **170**(6): p. 2009-18.

45. Gandhi, K., et al., *Autoantibodies to type VII collagen have heterogeneous subclass and light chain compositions and their complement-activating capacities do not correlate with the inflammatory clinical phenotype.* J Clin Immunol, 2000. **20**(6): p. 416-23.

46. Lapiere, J.C., et al., *Epitope mapping of type VII collagen. Identification of discrete peptide sequences recognized by sera from patients with acquired epidermolysis bullosa.* J Clin Invest, 1993. **92**(4): p. 1831-9.

47. Gupta, R., D.T. Woodley, and M. Chen, *Epidermolysis bullosa acquisita.* Clin Dermatol. **30**(1): p. 60-9.

48. Sitaru, C., et al., *Induction of complement-fixing autoantibodies against type VII collagen results in subepidermal blistering in mice.* J Immunol, 2006. **177**(5): p. 3461-8.

49. Sitaru, C., et al., *Induction of dermal-epidermal separation in mice by passive transfer of antibodies specific to type VII collagen.* J Clin Invest, 2005. **115**(4): p. 870-8.

50. Iwata, H., et al., *B cells, dendritic cells, and macrophages are required to induce an autoreactive CD4 helper T cell response in experimental epidermolysis bullosa acquisita.* J Immunol. **191**(6): p. 2978-88.

51. Gammon, W.R., et al., *Increased frequency of HLA-DR2 in patients with autoantibodies to epidermolysis bullosa acquisita antigen: evidence that the expression of autoimmunity to type VII collagen is HLA class II allele associated.* J Invest Dermatol, 1988. **91**(3): p. 228-32.

52. Lee, C.W., S.C. Kim, and H. Han, *Distribution of HLA class II alleles in Korean patients with epidermolysis bullosa acquisita.* Dermatology, 1996. **193**(4): p. 328-9.

53. Zumelzu, C., et al., *Black patients of African descent and HLA-DRB1*15:03 frequency overrepresented in epidermolysis bullosa acquisita.* J Invest Dermatol. **131**(12): p. 2386-93.

54. Ludwig, R.J., et al., *Identification of quantitative trait loci in experimental epidermolysis bullosa acquisita.* J Invest Dermatol. **132**(5): p. 1409-15.

55. Sitaru, A.G., et al., *T cells are required for the production of blister-inducing autoantibodies in experimental epidermolysis bullosa acquisita.* J Immunol. **184**(3): p. 1596-603.

56. Kuo, T.T., et al., *Neonatal Fc receptor: from immunity to therapeutics.* J Clin Immunol. **30**(6): p. 777-89.

57. Li, N., et al., *Complete FcRn dependence for intravenous Ig therapy in autoimmune skin blistering diseases.* J Clin Invest, 2005. **115**(12): p. 3440-50.

58. Sesarman, A., et al., *Neonatal Fc receptor deficiency protects from tissue injury in experimental epidermolysis bullosa acquisita.* J Mol Med (Berl), 2008. **86**(8): p. 951-9.

59. Sitaru, C., et al., *Autoantibodies to type VII collagen mediate Fcgamma-dependent neutrophil activation and induce dermal-epidermal separation in cryosections of human skin.* Am J Pathol, 2002. **161**(1): p. 301-11.

60. Sitaru, C. and D. Zillikens, *Mechanisms of blister induction by autoantibodies.* Exp Dermatol, 2005. **14**(12): p. 861-75.

61. Woodley, D.T., et al., *Evidence that anti-type VII collagen antibodies are pathogenic and responsible for the clinical, histological, and immunological features of epidermolysis bullosa acquisita.* J Invest Dermatol, 2005. **124**(5): p. 958-64.

62. Woodley, D.T., et al., *Induction of epidermolysis bullosa acquisita in mice by passive transfer of autoantibodies from patients.* J Invest Dermatol, 2006. **126**(6): p. 1323-30.

63. Sitaru, C., M. Goebeler, and D. Zillikens, *[Bullous autoimmune dermatoses (I): Pathogenesis and diagnosis].* J Dtsch Dermatol Ges, 2004. **2**(2): p. 123-8; quiz 139-40.

64. Kasperkiewicz, M., et al., *Genetic identification and functional validation of FcgammaRIV as key molecule in autoantibody-induced tissue injury.* J Pathol. **228**(1): p. 8-19.

65. Chiriac, M.T., et al., *NADPH oxidase is required for neutrophil-dependent autoantibody-induced tissue damage.* J Pathol, 2007. **212**(1): p. 56-65.

66. Shimanovich, I., et al., *Granulocyte-derived elastase and gelatinase B are required for dermal-epidermal separation induced by autoantibodies from patients with epidermolysis bullosa acquisita and bullous pemphigoid.* J Pathol, 2004. **204**(5): p. 519-27.

67. Engineer, L. and A.R. Ahmed, *Emerging treatment for epidermolysis bullosa acquisita.* J Am Acad Dermatol, 2001. **44**(5): p. 818-28.

68. Balkwill, F.R. and F. Burke, *The cytokine network.* Immunol Today, 1989. **10**(9): p. 299-304.

69. Ludwig, R.J. and E. Schmidt, *Cytokines in autoimmune bullous skin diseases. Epiphenomena or contribution to pathogenesis?* G Ital Dermatol Venereol, 2009. **144**(4): p. 339-49.

70. Feliciani, C., et al., *In vitro and in vivo expression of interleukin-1alpha and tumor necrosis factor-alpha mRNA in pemphigus vulgaris: interleukin-1alpha and tumor necrosis factor-alpha are involved in acantholysis.* J Invest Dermatol, 2000. **114**(1): p. 71-7.

71. Samavedam, U.K., et al., *Recombinant IL-6 treatment protects mice from organ specific autoimmune disease by IL-6 classical signalling-dependent IL-1ra induction.* J Autoimmun. **40**: p. 74-85.

72. Grando, S.A., et al., *Mediators of inflammation in blister fluids from patients with pemphigus vulgaris and bullous pemphigoid.* Arch Dermatol, 1989. **125**(7): p. 925-30.

73. Ameglio, F., et al., *Cytokine pattern in blister fluid and serum of patients with bullous pemphigoid: relationships with disease intensity.* Br J Dermatol, 1998. **138**(4): p. 611-4.

74. Schmidt, E., et al., *Detection of IL-1 alpha, IL-1 beta and IL-1 receptor antagonist in blister fluid of bullous pemphigoid.* J Dermatol Sci, 1996. **11**(2): p. 142-7.

75. Kumari, S., et al., *Interleukin 1 components in cicatricial pemphigoid. Role in intravenous immunoglobulin therapy.* Cytokine, 2001. **14**(4): p. 218-24.

76. D'Auria, L., P. Cordiali Fei, and F. Ameglio, *Cytokines and bullous pemphigoid.* Eur Cytokine Netw, 1999. **10**(2): p. 123-34.

77. Smith, K.A., *Interleukin-2: inception, impact, and implications.* Science, 1988. **240**(4856): p. 1169-76.

78. Schaller, J., et al., *Interleukin-2 receptor expression and interleukin-2 production in bullous pemphigoid.* Arch Dermatol Res, 1990. **282**(4): p. 223-6.

79. Wagemaker, G., et al., *Interleukin-3.* Biotherapy, 1990. **2**(4): p. 337-45.

80. D'Auria, L., et al., *Relationship between theoretical molecular weight and blister fluid/serum ratio of cytokines and five other molecules evaluated in patients with bullous pemphigoid.* J Biol Regul Homeost Agents, 1998. **12**(3): p. 76-80.

81. Ariizumi, K., et al., *IFN-gamma-dependent IL-7 gene regulation in keratinocytes.* J Immunol, 1995. **154**(11): p. 6031-9.

82. Giacalone, B., et al., *Decreased interleukin-7 and transforming growth factor-beta1 levels in blister fluids as compared to the respective serum levels in patients with bullous pemphigoid. Opposite behavior of TNF-alpha, interleukin-4 and interleukin-10.* Exp Dermatol, 1998. **7**(4): p. 157-61.

83. Cassatella, M.A. and P.P. McDonald, *Interleukin-15 and its impact on neutrophil function.* Curr Opin Hematol, 2000. **7**(3): p. 174-7.

84. Castillo, E.F. and K.S. Schluns, *Regulating the immune system via IL-15 transpresentation.* Cytokine. **59**(3): p. 479-90.

85. Musikacharoen, T., et al., *Interleukin-15 induces IL-12 receptor beta1 gene expression through PU.1 and IRF 3 by targeting chromatin remodeling.* Blood, 2005. **105**(2): p. 711-20.

86. D'Auria, L., et al., *Increased serum interleukin-15 levels in bullous skin diseases: correlation with disease intensity.* Arch Dermatol Res, 1999. **291**(6): p. 354-6.

87. Hibbs, M.L., et al., *Mice lacking three myeloid colony-stimulating factors (G-CSF, GM-CSF, and M-CSF) still produce macrophages and granulocytes and mount an inflammatory response in a sterile model of peritonitis.* J Immunol, 2007. **178**(10): p. 6435-43.

88. Hamilton, J.A. and G.P. Anderson, *GM-CSF Biology.* Growth Factors, 2004. **22**(4): p. 225-31.

89. Schmidt, E., et al., *Detection of elevated levels of IL-4, IL-6, and IL-10 in blister fluid of bullous pemphigoid.* Arch Dermatol Res, 1996. **288**(7): p. 353-7.

90. Candi, E., R. Schmidt, and G. Melino, *The cornified envelope: a model of cell death in the skin.* Nat Rev Mol Cell Biol, 2005. **6**(4): p. 328-40.

91. Su, H., et al., *Modulation of bullous pemphigoid antigens by gamma interferon in cultured human keratinocytes.* J Dermatol, 1990. **17**(1): p. 16-23.

92. Sugita, Y., et al., *Modulation of bullous pemphigoid antigen gene expression by gamma-interferon in cultured keratinocytes.* Br J Dermatol, 1992. **126**(5): p. 468-73.

93. Kaneko, T., et al., *Interferon-gamma down-regulates expression of the 230-kDa bullous pemphigoid antigen gene (BPAG1) in epidermal keratinocytes via novel chimeric sequences of ISRE and GAS.* Exp Dermatol, 2006. **15**(4): p. 308-14.

94. Odanagi, M., et al., *Transcriptional regulation of the 230-kDa bullous pemphigoid antigen gene expression by interferon regulatory factor 1 and interferon regulatory factor 2 in normal human epidermal keratinocytes.* Exp Dermatol, 2004. **13**(12): p. 773-9.

95. Tamai, K., et al., *Interferon-gamma-mediated inactivation of transcription of the 230-kDa bullous pemphigoid antigen gene (BPAG1) provides novel insight into keratinocyte differentiation.* J Biol Chem, 1995. **270**(1): p. 392-6.

96. Kotnik, V., *Complement in skin diseases.* Acta Dermatovenerol Alp Panonica Adriat. **20**(1): p. 3-11.

97. Lessey, E., et al., *Complement and cutaneous autoimmune blistering diseases.* Immunol Res, 2008. **41**(3): p. 223-32.

98. Lomova, R.I., *[Chronic gastritis].* Med Sestra, 1975. **34**(3): p. 26-30.

99. Tanaka, M. and A. Miyajima, *Oncostatin M, a multifunctional cytokine.* Rev Physiol Biochem Pharmacol, 2003. **149**: p. 39-52.

100. Maghazachi, A.A., A. Al-Aoukaty, and T.J. Schall, *CC chemokines induce the generation of killer cells from CD56+ cells.* Eur J Immunol, 1996. **26**(2): p. 315-9.

101. Khalil, N., *TGF-beta: from latent to active.* Microbes Infect, 1999. **1**(15): p. 1255-63.

102. Giomi, B., et al., *Th1, Th2 and Th3 cytokines in the pathogenesis of bullous pemphigoid.* J Dermatol Sci, 2002. **30**(2): p. 116-28.

103. Samarakoon, R., J.M. Overstreet, and P.J. Higgins, *TGF-beta signaling in tissue fibrosis: redox controls, target genes and therapeutic opportunities.* Cell Signal. **25**(1): p. 264-8.

104. Clark, I.A., *How TNF was recognized as a key mechanism of disease.* Cytokine Growth Factor Rev, 2007. **18**(3-4): p. 335-43.

105. Mantovani, A., et al., *Neutrophils in the activation and regulation of innate and adaptive immunity.* Nat Rev Immunol. **11**(8): p. 519-31.

106. Nozaki, S., C. Feliciani, and D.N. Sauder, *Keratinocyte cytokines.* Adv Dermatol, 1992. **7**: p. 83-100; discussion 101.

107. Sauder, D.N., *Interleukin 1.* Arch Dermatol, 1989. **125**(5): p. 679-82.

108. Feldmeyer, L., et al., *The inflammasome mediates UVB-induced activation and secretion of interleukin-1beta by keratinocytes.* Curr Biol, 2007. **17**(13): p. 1140-5.

109. Watanabe, H., et al., *Activation of the IL-1beta-processing inflammasome is involved in contact hypersensitivity.* J Invest Dermatol, 2007. **127**(8): p. 1956-63.

110. Atkins, E. and P. Bodel, *Fever.* N Engl J Med, 1972. **286**(1): p. 27-34.

111. Dinarello, C.A., N.P. Goldin, and S.M. Wolff, *Demonstration and characterization of two distinct human leukocytic pyrogens.* J Exp Med, 1974. **139**(6): p. 1369-81.

112. Dinarello, C.A., *Biologic basis for interleukin-1 in disease.* Blood, 1996. **87**(6): p. 2095-147.

113. Broz, P., et al., *Differential requirement for Caspase-1 autoproteolysis in pathogen-induced cell death and cytokine processing.* Cell Host Microbe. **8**(6): p. 471-83.

114. Kobayashi, Y., et al., *Identification of calcium-activated neutral protease as a processing enzyme of human interleukin 1 alpha.* Proc Natl Acad Sci U S A, 1990. **87**(14): p. 5548-52.

115. Black, R.A., et al., *Generation of biologically active interleukin-1 beta by proteolytic cleavage of the inactive precursor.* J Biol Chem, 1988. **263**(19): p. 9437-42.

116. Mosley, B., et al., *The interleukin-1 receptor binds the human interleukin-1 alpha precursor but not the interleukin-1 beta precursor.* J Biol Chem, 1987. **262**(7): p. 2941-4.

117. Mizutani, H., R. Black, and T.S. Kupper, *Human keratinocytes produce but do not process pro-interleukin-1 (IL-1) beta. Different strategies of IL-1 production and processing in monocytes and keratinocytes.* J Clin Invest, 1991. **87**(3): p. 1066-71.

118. Mizutani, H., et al., *Rapid and specific conversion of precursor interleukin 1 beta (IL-1 beta) to an active IL-1 species by human mast cell chymase.* J Exp Med, 1991. **174**(4): p. 821-5.

119. Eder, C., *Mechanisms of interleukin-1beta release.* Immunobiology, 2009. **214**(7): p. 543-53.

120. Dinarello, C.A., *Interleukin-1 and interleukin-1 antagonism.* Blood, 1991. **77**(8): p. 1627-52.

121. Dinarello, C.A., *Blocking interleukin-1 in disease.* Blood Purif, 1993. **11**(2): p. 118-27.

122. Mantovani, A., et al., *Regulation of inhibitory pathways of the interleukin-1 system.* Ann N Y Acad Sci, 1998. **840**: p. 338-51.

123. Orlando, S., et al., *Role of metalloproteases in the release of the IL-1 type II decoy receptor.* J Biol Chem, 1997. **272**(50): p. 31764-9.

124. Symons, J.A., P.R. Young, and G.W. Duff, *Soluble type II interleukin 1 (IL-1) receptor binds and blocks processing of IL-1 beta precursor and loses affinity for IL-1 receptor antagonist.* Proc Natl Acad Sci U S A, 1995. **92**(5): p. 1714-8.

125. Ferrari, D., et al., *The P2X7 receptor: a key player in IL-1 processing and release.* J Immunol, 2006. **176**(7): p. 3877-83.

126. Gross, O., et al., *The inflammasome: an integrated view.* Immunol Rev. **243**(1): p. 136-51.

127. Petrilli, V., et al., *Activation of the NALP3 inflammasome is triggered by low intracellular potassium concentration.* Cell Death Differ, 2007. **14**(9): p. 1583-9.

128. Solle, M., et al., *Altered cytokine production in mice lacking P2X(7) receptors.* J Biol Chem, 2001. **276**(1): p. 125-32.

129. Zhou, R., et al., *A role for mitochondria in NLRP3 inflammasome activation.* Nature. **469**(7329): p. 221-5.

130. Jones, J.W., P. Broz, and D.M. Monack, *Innate immune recognition of francisella tularensis: activation of type-I interferons and the inflammasome.* Front Microbiol. **2**: p. 16.

131. BeSaw, L., *MDs & DOs. Allopaths and osteopaths have learned to coexist.* Tex Med, 1997. **93**(4): p. 34-9.

132. Bauernfeind, F., et al., *Cutting edge: reactive oxygen species inhibitors block priming, but not activation, of the NLRP3 inflammasome.* J Immunol. **187**(2): p. 613-7.

133. Martinon, F., *Signaling by ROS drives inflammasome activation.* Eur J Immunol. **40**(3): p. 616-9.

134. Zhou, R., et al., *Thioredoxin-interacting protein links oxidative stress to inflammasome activation.* Nat Immunol. **11**(2): p. 136-40.

135. Nakahira, K., et al., *Autophagy proteins regulate innate immune responses by inhibiting the release of mitochondrial DNA mediated by the NALP3 inflammasome.* Nat Immunol. **12**(3): p. 222-30.

136. Meissner, F., K. Molawi, and A. Zychlinsky, *Superoxide dismutase 1 regulates caspase-1 and endotoxic shock.* Nat Immunol, 2008. **9**(8): p. 866-72.

137. Meissner, F., et al., *Inflammasome activation in NADPH oxidase defective mononuclear phagocytes from patients with chronic granulomatous disease.* Blood. **116**(9): p. 1570-3.

138. Bergsbaken, T., S.L. Fink, and B.T. Cookson, *Pyroptosis: host cell death and inflammation.* Nat Rev Microbiol, 2009. **7**(2): p. 99-109.

139. Adcock, I.M., *Transcription factors as activators of gene transcription: AP-1 and NF-kappa B.* Monaldi Arch Chest Dis, 1997. **52**(2): p. 178-86.

140. Palanki, M.S., *Inhibitors of AP-1 and NF-kappa B mediated transcriptional activation: therapeutic potential in autoimmune diseases and structural diversity.* Curr Med Chem, 2002. **9**(2): p. 219-27.

141. Dyson, H.J. and E.A. Komives, *Role of disorder in IkappaB-NFkappaB interaction.* IUBMB Life. **64**(6): p. 499-505.

142. O'Donnell, M.A. and A.T. Ting, *NFkappaB and ubiquitination: partners in disarming RIPK1-mediated cell death.* Immunol Res. **54**(1-3): p. 214-26.

143. Burns, K., et al., *MyD88, an adapter protein involved in interleukin-1 signaling.* J Biol Chem, 1998. **273**(20): p. 12203-9.

144. Kanamori, M., et al., *NF-kappaB activator Act1 associates with IL-1/Toll pathway adaptor molecule TRAF6.* FEBS Lett, 2002. **532**(1-2): p. 241-6.

145. Swantek, J.L., et al., *IL-1 receptor-associated kinase modulates host responsiveness to endotoxin.* J Immunol, 2000. **164**(8): p. 4301-6.

146. Deng, L., et al., *Activation of the IkappaB kinase complex by TRAF6 requires a dimeric ubiquitin-conjugating enzyme complex and a unique polyubiquitin chain.* Cell, 2000. **103**(2): p. 351-61.

147. Silverman, N. and T. Maniatis, *NF-kappaB signaling pathways in mammalian and insect innate immunity.* Genes Dev, 2001. **15**(18): p. 2321-42.

148. Jiang, Z., et al., *Pellino 1 is required for interleukin-1 (IL-1)-mediated signaling through its interaction with the IL-1 receptor-associated kinase 4 (IRAK4)-IRAK-tumor necrosis factor receptor-associated factor 6 (TRAF6) complex.* J Biol Chem, 2003. **278**(13): p. 10952-6.

149. Landstrom, M., *The TAK1-TRAF6 signalling pathway.* Int J Biochem Cell Biol. **42**(5): p. 585-9.

150. Mercurio, F., et al., *IKK-1 and IKK-2: cytokine-activated IkappaB kinases essential for NF-kappaB activation.* Science, 1997. **278**(5339): p. 860-6.

151. Yamazaki, K., et al., *Two mechanistically and temporally distinct NF-kappaB activation pathways in IL-1 signaling.* Sci Signal, 2009. **2**(93): p. ra66.

152. Murphy, J.E., C. Robert, and T.S. Kupper, *Interleukin-1 and cutaneous inflammation: a crucial link between innate and acquired immunity.* J Invest Dermatol, 2000. **114**(3): p. 602-8.

153. Kupper, T.S. and R.W. Groves, *The interleukin-1 axis and cutaneous inflammation.* J Invest Dermatol, 1995. **105**(1 Suppl): p. 62S-66S.

154. Dustin, M.L., et al., *Induction by IL 1 and interferon-gamma: tissue distribution, biochemistry, and function of a natural adherence molecule (ICAM-1). J. Immunol. 1986. 137: 245-254.* J Immunol. **186**(9): p. 5024-33.

155. Roebuck, K.A. and A. Finnegan, *Regulation of intercellular adhesion molecule-1 (CD54) gene expression.* J Leukoc Biol, 1999. **66**(6): p. 876-88.

156. Wertheimer, S.J., et al., *Intercellular adhesion molecule-1 gene expression in human endothelial cells. Differential regulation by tumor necrosis factor-alpha and phorbol myristate acetate.* J Biol Chem, 1992. **267**(17): p. 12030-5.

157. Baeuerle, P.A., *Pro-inflammatory signaling: last pieces in the NF-kappaB puzzle?* Curr Biol, 1998. **8**(1): p. R19-22.

158. Malinin, N.L., et al., *MAP3K-related kinase involved in NF-kappaB induction by TNF, CD95 and IL-1.* Nature, 1997. **385**(6616): p. 540-4.

159. Lee, S.J., et al., *Transcriptional regulation of the intercellular adhesion molecule-1 gene by proinflammatory cytokines in human astrocytes.* Glia, 1999. **25**(1): p. 21-32.

160. Myers, C.L., et al., *Induction of ICAM-1 by TNF-alpha, IL-1 beta, and LPS in human endothelial cells after downregulation of PKC.* Am J Physiol, 1992. **263**(4 Pt 1): p. C767-72.

161. Lin, F.S., et al., *Involvement of p42/p44 MAPK, JNK, and NF-kappaB in IL-1beta-induced ICAM-1 expression in human pulmonary epithelial cells.* J Cell Physiol, 2005. **202**(2): p. 464-73.

162. Lawson, C. and S. Wolf, *ICAM-1 signaling in endothelial cells.* Pharmacol Rep, 2009. **61**(1): p. 22-32.

163. Bullard, D.C., et al., *P-selectin/ICAM-1 double mutant mice: acute emigration of neutrophils into the peritoneum is completely absent but is normal into pulmonary alveoli.* J Clin Invest, 1995. **95**(4): p. 1782-8.

164. Sligh, J.E., Jr., et al., *Inflammatory and immune responses are impaired in mice deficient in intercellular adhesion molecule 1.* Proc Natl Acad Sci U S A, 1993. **90**(18): p. 8529-33.

165. Carlos, T.M. and J.M. Harlan, *Leukocyte-endothelial adhesion molecules.* Blood, 1994. **84**(7): p. 2068-101.

166. Luscinskas, F.W., et al., *Cytokine-activated human endothelial monolayers support enhanced neutrophil transmigration via a mechanism involving both endothelial-leukocyte adhesion molecule-1 and intercellular adhesion molecule-1.* J Immunol, 1991. **146**(5): p. 1617-25.

167. Smith, C.W., et al., *Recognition of an endothelial determinant for CD 18-dependent human neutrophil adherence and transendothelial migration.* J Clin Invest, 1988. **82**(5): p. 1746-56.

168. Furie, M.B., M.C. Tancinco, and C.W. Smith, *Monoclonal antibodies to leukocyte integrins CD11a/CD18 and CD11b/CD18 or intercellular adhesion molecule-1 inhibit chemoattractant-stimulated neutrophil transendothelial migration in vitro.* Blood, 1991. **78**(8): p. 2089-97.

169. Kadono, T., *[The role of adhesion molecules in cutaneous inflammation].* Nihon Rinsho Meneki Gakkai Kaishi. **33**(5): p. 242-8.

170. Raab, M., et al., *Variation of adhesion molecule expression on human umbilical vein endothelial cells upon multiple cytokine application.* Clin Chim Acta, 2002. **321**(1-2): p. 11-6.

171. Isaev, P.I., et al., *[Metabolism of articular cartilage in the presence of interleukin-I alpha, its inhibitor and blood serum].* Biull Eksp Biol Med, 1992. **114**(9): p. 269-71.

172. Niki, Y., et al., *Membrane-associated IL-1 contributes to chronic synovitis and cartilage destruction in human IL-1 alpha transgenic mice.* J Immunol, 2004. **172**(1): p. 577-84.

173. Smeets, R.L., et al., *Effectiveness of the soluble form of the interleukin-1 receptor accessory protein as an inhibitor of interleukin-1 in collagen-induced arthritis.* Arthritis Rheum, 2003. **48**(10): p. 2949-58.

174. Buchan, G., et al., *Interleukin-1 and tumour necrosis factor mRNA expression in rheumatoid arthritis: prolonged production of IL-1 alpha.* Clin Exp Immunol, 1988. **73**(3): p. 449-55.

175. Graudal, N.A., et al., *Variant mannose-binding lectin genotypes and outcome in early versus late rheumatoid arthritis: comment on the article by Ip et al.* Arthritis Rheum, 2002. **46**(2): p. 555-6.

176. Lee, Y.M., et al., *IL-1 plays an important role in the bone metabolism under physiological conditions.* Int Immunol. **22**(10): p. 805-16.

177. Prens, E.P., et al., *Interleukin-1 and interleukin-6 in psoriasis.* J Invest Dermatol, 1990. **95**(6 Suppl): p. 121S-124S.

178. Gilson, M., et al., *Treatment of Schnitzler's syndrome with anakinra.* Clin Exp Rheumatol, 2007. **25**(6): p. 931.

179. Goldbach-Mansky, R., *Blocking interleukin-1 in rheumatic diseases.* Ann N Y Acad Sci, 2009. **1182**: p. 111-23.

180. Samavedam, U.K., et al., *GM-CSF modulates autoantibody production and skin blistering in experimental epidermolysis bullosa acquisita.* J Immunol. **192**(2): p. 559-71.

181. Staats, J., *Standardized nomenclature for inbred strains of mice: fifth listing.* Cancer Res, 1972. **32**(8): p. 1609-46.

182. Staats, J., *Standardized nomenclature for inbred strains of mice: sixth listing.* Cancer Res, 1976. **36**(12): p. 4333-77.

183. Staats, J., *Standardized nomenclature for inbred strains of mice: seventh listing for the International Committee on Standardized Genetic Nomenclature for Mice.* Cancer Res, 1980. **40**(7): p. 2083-128.

184. Staats, J., *Standardized Nomenclature for Inbred Strains of Mice: eighth listing.* Cancer Res, 1985. **45**(3): p. 945-77.

185. Bryant, C.D., *The blessings and curses of C57BL/6 substrains in mouse genetic studies.* Ann N Y Acad Sci. **1245**: p. 31-3.

186. Zurita, E., et al., *Genetic polymorphisms among C57BL/6 mouse inbred strains.* Transgenic Res. **20**(3): p. 481-9.

187. Melo, J.A., et al., *Identification of sex-specific quantitative trait loci controlling alcohol preference in C57BL/ 6 mice.* Nat Genet, 1996. **13**(2): p. 147-53.

188. Peirce, J.L., et al., *A major influence of sex-specific loci on alcohol preference in C57Bl/6 and DBA/2 inbred mice.* Mamm Genome, 1998. **9**(12): p. 942-8.

189. Lin, S., et al., *Development of high fat diet-induced obesity and leptin resistance in C57Bl/6J mice.* Int J Obes Relat Metab Disord, 2000. **24**(5): p. 639-46.

190. Mills, E., et al., *Hypertension in CB57BL/6J mouse model of non-insulin-dependent diabetes mellitus.* Am J Physiol, 1993. **264**(1 Pt 2): p. R73-8.

191. Nishina, P.M., et al., *Atherosclerosis and plasma and liver lipids in nine inbred strains of mice.* Lipids, 1993. **28**(7): p. 599-605.

192. Keetch, D.W., P. Humphrey, and T.L. Ratliff, *Development of a mouse model for nonbacterial prostatitis.* J Urol, 1994. **152**(1): p. 247-50.

193. Fantuzzi, G., et al., *Response to local inflammation of IL-1 beta-converting enzyme- deficient mice.* J Immunol, 1997. **158**(4): p. 1818-24.

194. Kuida, K., et al., *Altered cytokine export and apoptosis in mice deficient in interleukin-1 beta converting enzyme.* Science, 1995. **267**(5206): p. 2000-3.

195. Miao, E.A., J.V. Rajan, and A. Aderem, *Caspase-1-induced pyroptotic cell death.* Immunol Rev. **243**(1): p. 206-14.

196. Green, D.R., *Immunology: A heavyweight knocked out.* Nature. **479**(7371): p. 48-50.

197. Bordon, Y., *Innate immunity: a new path uncovers a wrongful conviction.* Nat Rev Immunol. **11**(12): p. 801.

198. Kayagaki, N., et al., *Non-canonical inflammasome activation targets caspase-11.* Nature. **479**(7371): p. 117-21.

199. Glaccum, M.B., et al., *Phenotypic and functional characterization of mice that lack the type I receptor for IL-1.* J Immunol, 1997. **159**(7): p. 3364-71.

200. Hultgren, O.H., L. Svensson, and A. Tarkowski, *Critical role of signaling through IL-1 receptor for development of arthritis and sepsis during Staphylococcus aureus infection.* J Immunol, 2002. **168**(10): p. 5207-12.

201. Sidman, R.L., P.W. Lane, and M.M. Dickie, *Staggerer, a new mutation in the mouse affecting the cerebellum.* Science, 1962. **137**(3530): p. 610-2.

202. Hamilton, B.A., et al., *Disruption of the nuclear hormone receptor RORalpha in staggerer mice.* Nature, 1996. **379**(6567): p. 736-9.

203. Steinmayr, M., et al., *staggerer phenotype in retinoid-related orphan receptor alpha-deficient mice.* Proc Natl Acad Sci U S A, 1998. **95**(7): p. 3960-5.

204. Castonguay, A., P. Pepin, and G.D. Stoner, *Lung tumorigenicity of NNK given orally to A/J mice: its application to chemopreventive efficacy studies.* Exp Lung Res, 1991. **17**(2): p. 485-99.

205. Shimkin, M.B., et al., *Lung tumor response in strain A mice as a quantitative bioassay of carcinogenic activity of some carbamates and aziridines.* Cancer Res, 1969. **29**(12): p. 2184-90.

206. Gallou-Kabani, C., et al., *C57BL/6J and A/J mice fed a high-fat diet delineate components of metabolic syndrome.* Obesity (Silver Spring), 2007. **15**(8): p. 1996-2005.

207. Coutinho, M., et al., *C5 deficiency in A/J mice is not associated with resistance to the development of secondary amyloidosis.* Eur J Immunogenet, 1992. **19**(6): p. 419-23.

208. Nilsson, U.R. and H.J. Muller-Eberhard, *Deficiency of the fifth component of complement in mice with an inherited complement defect.* J Exp Med, 1967. **125**(1): p. 1-16.

209. O'Malley, J., et al., *Comparison of acute endotoxin-induced lesions in A/J and C57BL/6J mice.* J Hered, 1998. **89**(6): p. 525-30.

210. Shimkin, M.B. and M.J. Polissar, *Growth of pulmonary tumors in mice of strains A and C3H.* J Natl Cancer Inst, 1958. **21**(3): p. 595-610.

211. Festing, M.F. and D.K. Blackmore, *Life span of specified-pathogen-free (MRC category 4) mice and rats.* Lab Anim, 1971. **5**(2): p. 179-92.

212. Karpova, G.V., et al., *Hemopoietic and lymphoid organs in AKR/JY mice with thymic lymphoma.* Bull Exp Biol Med, 2002. **134**(1): p. 69-72.

213. Rowe, W.P. and T. Pincus, *Quantitative studies of naturally occurring murine leukemia virus infection of AKR mice.* J Exp Med, 1972. **135**(2): p. 429-36.

214. Hiai, H., *Genetic predisposition to lymphomas in mice.* Pathol Int, 1996. **46**(10): p. 707-18.

215. Morse, H.C., 3rd, et al., *Bethesda proposals for classification of lymphoid neoplasms in mice.* Blood, 2002. **100**(1): p. 246-58.

216. Morse, H.C., 3rd, et al., *Combined histologic and molecular features reveal previously unappreciated subsets of lymphoma in AKXD recombinant inbred mice.* Leuk Res, 2001. **25**(8): p. 719-33.

217. Byrd, L.G., et al., *Specific pathogen-free BALB/cAn mice are refractory to plasmacytoma induction by pristane.* J Immunol, 1991. **147**(10): p. 3632-7.

218. Potter, M. and R.C. Maccardle, *Histology of Developing Plasma Cell Neoplasia Induced by Mineral Oil in Balb/C Mice.* J Natl Cancer Inst, 1964. **33**: p. 497-515.

219. Potter, M., J.S. Wax, and E. Blankenhorn, *BALB/c subline differences in susceptibility to plasmacytoma induction.* Curr Top Microbiol Immunol, 1985. **122**: p. 234-41.

220. Sass, B., R.L. Peters, and G.J. Kelloff, *Differences in tumor incidence in two substrains of Claude BALB/c (BALB/cfCd) mice, emphasizing renal, mammary, pancreatic, and synovial tumors.* Lab Anim Sci, 1976. **26**(5): p. 736-41.

221. Jungmann, P., et al., *Murine acariasis: I. Pathological and clinical evidence suggesting cutaneous allergy and wasting syndrome in BALB/c mouse.* Res Immunol, 1996. **147**(1): p. 27-38.

222. Crabbe, J.C., *Provisional mapping of quantitative trait loci for chronic ethanol withdrawal severity in BXD recombinant inbred mice.* J Pharmacol Exp Ther, 1998. **286**(1): p. 263-71.

223. Mountz, J.D., et al., *Genetic segregation of spontaneous erosive arthritis and generalized autoimmune disease in the BXD2 recombinant inbred strain of mice.* Scand J Immunol, 2005. **61**(2): p. 128-38.

224. Bihl, F., M. Brahic, and J.F. Bureau, *Two loci, Tmevp2 and Tmevp3, located on the telomeric region of chromosome 10, control the persistence of Theiler's virus in the central nervous system of mice.* Genetics, 1999. **152**(1): p. 385-92.

225. Klein, J., F. Figueroa, and D. Klein, *H-2 haplotypes, genes, and antigens: second listing. I. Non-H-2 loci on chromosome 17.* Immunogenetics, 1982. **16**(4): p. 285-317.

226. Encinas, J.A., et al., *Genetic analysis of susceptibility to experimental autoimmune encephalomyelitis in a cross between SJL/J and B10.S mice.* J Immunol, 1996. **157**(5): p. 2186-92.

227. Soutiere, S.E. and W. Mitzner, *On defining total lung capacity in the mouse.* J Appl Physiol (1985), 2004. **96**(5): p. 1658-64.

228. Tankersley, C.G., R. Rabold, and W. Mitzner, *Differential lung mechanics are genetically determined in inbred murine strains.* J Appl Physiol (1985), 1999. **86**(6): p. 1764-9.

229. Drinkwater, N.R. and J.J. Ginsler, *Genetic control of hepatocarcinogenesis in C57BL/6J and C3H/HeJ inbred mice.* Carcinogenesis, 1986. **7**(10): p. 1701-7.

230. Kamath, A.B., et al., *Toll-like receptor 4-defective C3H/HeJ mice are not more susceptible than other C3H substrains to infection with Mycobacterium tuberculosis.* Infect Immun, 2003. **71**(7): p. 4112-8.

231. McDonald, T.P. and C.W. Jackson, *Mode of inheritance of the higher degree of megakaryocyte polyploidization in C3H mice. I. Evidence for a role of genomic imprinting in megakaryocyte polyploidy determination.* Blood, 1994. **83**(6): p. 1493-8.

232. Sundberg, J.P., et al., *C3H/HeJ mouse model for alopecia areata.* J Invest Dermatol, 1995. **104**(5 Suppl): p. 16S-17S.

233. Chapman, V.M. and F.H. Ruddle, *Glutamate oxaloacetate transaminase (got) genetics in the mouse: polymorphism of got-1.* Genetics, 1972. **70**(2): p. 299-305.

234. Ishikawa, A., *Wild mice as bountiful resources of novel genetic variants for quantitative traits.* Curr Genomics. **14**(4): p. 225-9.

235. Drager, U.C. and D.H. Hubel, *Studies of visual function and its decay in mice with hereditary retinal degeneration.* J Comp Neurol, 1978. **180**(1): p. 85-114.

236. Sidman, R.L. and M.C. Green, *Retinal Degeneration in the Mouse: Location of the Rd Locus in Linkage Group Xvii.* J Hered, 1965. **56**: p. 23-9.

237. Nicoletti, F., et al., *Protection from experimental autoimmune thyroiditis in CBA mice with the novel immunosuppressant deoxyspergualin.* Scand J Immunol, 1994. **39**(3): p. 333-6.

238. Taylor, P.C., et al., *Transfer of type II collagen-induced arthritis from DBA/1 to severe combined immunodeficiency mice can be prevented by blockade of Mac-1.* Immunology, 1996. **88**(2): p. 315-21.

239. Terato, K., et al., *Physicochemical and immunological studies of the renatured alpha 1(II) chains and isolated cyanogen bromide peptides of type II collagen.* Coll Relat Res, 1985. **5**(6): p. 469-80.

240. Kanazawa, S., et al., *Aberrant MHC class II expression in mouse joints leads to arthritis with extraarticular manifestations similar to rheumatoid arthritis.* Proc Natl Acad Sci U S A, 2006. **103**(39): p. 14465-70.

241. Xie, C., et al., *Strain distribution pattern of susceptibility to immune-mediated nephritis.* J Immunol, 2004. **172**(8): p. 5047-55.

242. Taketo, M., et al., *FVB/N: an inbred mouse strain preferable for transgenic analyses.* Proc Natl Acad Sci U S A, 1991. **88**(6): p. 2065-9.

243. Kawikova, I., et al., *Airway hyper-reactivity mediated by B-1 cell immunoglobulin M antibody generating complement C5a at 1 day post-immunization in a murine hapten model of non-atopic asthma.* Immunology, 2004. **113**(2): p. 234-45.

244. Mori, L. and G. de Libero, *Genetic control of susceptibility to collagen-induced arthritis in T cell receptor beta-chain transgenic mice.* Arthritis Rheum, 1998. **41**(2): p. 256-62.

245. Mastellos, D., et al., *A novel role of complement: mice deficient in the fifth component of complement (C5) exhibit impaired liver regeneration.* J Immunol, 2001. **166**(4): p. 2479-86.

246. Kanno, H., et al., *Spontaneous development of pancreatitis in the MRL/Mp strain of mice in autoimmune mechanism.* Clin Exp Immunol, 1992. **89**(1): p. 68-73.

247. Festing, M.F., et al., *Revised nomenclature for strain 129 mice.* Mamm Genome, 1999. **10**(8): p. 836.

248. DiLorenzo, T.P., et al., *During the early prediabetic period in NOD mice, the pathogenic CD8(+) T-cell population comprises multiple antigenic specificities.* Clin Immunol, 2002. **105**(3): p. 332-41.

249. Rudofsky, U.H., et al., *Differences in expression of lupus nephritis in New Zealand mixed H-2z homozygous inbred strains of mice derived from New Zealand black and New Zealand white mice. Origins and initial characterization.* Lab Invest, 1993. **68**(4): p. 419-26.

250. Heber-Katz, E. and H. Acha-Orbea, *The V-region disease hypothesis: evidence from autoimmune encephalomyelitis.* Immunol Today, 1989. **10**(5): p. 164-9.

251. Singh, K., et al., *Reduced CD18 levels drive regulatory T cell conversion into Th17 cells in the CD18hypo PL/J mouse model of psoriasis.* J Immunol. **190**(6): p. 2544-53.

252. Crispens, C.G., *Some characteristics of strain SJL-JDg mice.* Lab Anim Sci, 1973. **23**(3): p. 408-13.

253. Johnson, D.A., L.D. Shultz, and H.G. Bedigian, *Immunodeficiency and reticulum cell sarcoma in mice segregating for HRS/J and SJL/J genes.* Leuk Res, 1982. **6**(5): p. 711-20.

254. Krementsov, D.N., et al., *Studies in experimental autoimmune encephalomyelitis do not support developmental bisphenol a exposure as an environmental factor in increasing multiple sclerosis risk.* Toxicol Sci. **135**(1): p. 91-102.

255. Ludwig, R.J., et al., *Generation of antibodies of distinct subclasses and specificity is linked to H2s in an active mouse model of epidermolysis bullosa acquisita.* J Invest Dermatol. **131**(1): p. 167-76.

256. Wegener, H., S. Leineweber, and K. Seeger, *The vWFA2 domain of type VII collagen is responsible for collagen binding.* Biochem Biophys Res Commun. **430**(2): p. 449-53.

257. Ludwig, R.J., *Model systems duplicating epidermolysis bullosa acquisita: a methodological review.* Autoimmunity. **45**(1): p. 102-10.

258. Kasperkiewicz, M., et al., *Heat-shock protein 90 inhibition in autoimmunity to type VII collagen: evidence that nonmalignant plasma cells are not therapeutic targets.* Blood. **117**(23): p. 6135-42.

259. Fischer, A.H., et al., *Hematoxylin and eosin staining of tissue and cell sections.* CSH Protoc, 2008. **2008**: p. pdb prot4986.

260. Ramos-Vara, J.A., *Principles and methods of immunohistochemistry.* Methods Mol Biol. **691**: p. 83-96.

261. Ramos-Vara, J.A., *Technical aspects of immunohistochemistry.* Vet Pathol, 2005. **42**(4): p. 405-26.

262. Ludwig, R.J., et al., *Junctional adhesion molecules (JAM)-B and -C contribute to leukocyte extravasation to the skin and mediate cutaneous inflammation.* J Invest Dermatol, 2005. **125**(5): p. 969-76.

263. Chen, M., et al., *Interactions of the amino-terminal noncollagenous (NC1) domain of type VII collagen with extracellular matrix components. A potential role in epidermal-dermal adherence in human skin.* J Biol Chem, 1997. **272**(23): p. 14516-22.

264. Pendaries, V., et al., *Immune reactivity to type VII collagen: implications for gene therapy of recessive dystrophic epidermolysis bullosa.* Gene Ther. **17**(7): p. 930-7.

265. Saleh, M.A., et al., *Development of NC1 and NC2 domains of type VII collagen ELISA for the diagnosis and analysis of the time course of epidermolysis bullosa acquisita patients.* J Dermatol Sci. **62**(3): p. 169-75.

266. Barrett, J.C., et al., *Haploview: analysis and visualization of LD and haplotype maps.* Bioinformatics, 2005. **21**(2): p. 263-5.

267. Franceschini, A., et al., *STRING v9.1: protein-protein interaction networks, with increased coverage and integration.* Nucleic Acids Res. **41**(Database issue): p. D808-15.

268. Ludwig, R.J., et al., *Platelet, not endothelial, P-selectin expression contributes to generation of immunity in cutaneous contact hypersensitivity.* Am J Pathol. **176**(3): p. 1339-45.

269. Ludwig, R.J., et al., *Junctional adhesion molecule (JAM)-B supports lymphocyte rolling and adhesion through interaction with alpha4beta1 integrin.* Immunology, 2009. **128**(2): p. 196-205.

270. Wannamaker, W., et al., *(S)-1-((S)-2-{[1-(4-amino-3-chloro-phenyl)-methanoyl]-amino}-3,3-dimethyl-butanoy l)-pyrrolidine-2-carboxylic acid ((2R,3S)-2-ethoxy-5-oxo-tetrahydro-furan-3-yl)-amide (VX-765), an orally available selective interleukin (IL)-converting enzyme/caspase-1 inhibitor, exhibits potent anti-inflammatory activities by inhibiting the release of IL-1beta and IL-18.* J Pharmacol Exp Ther, 2007. **321**(2): p. 509-16.

271. Dupaul-Chicoine, J. and M. Saleh, *A new path to IL-1beta production controlled by caspase-8.* Nat Immunol. **13**(3): p. 211-2.

272. Joosten, L.A., et al., *Inflammatory arthritis in caspase 1 gene-deficient mice: contribution of proteinase 3 to caspase 1-independent production of bioactive interleukin-1beta.* Arthritis Rheum, 2009. **60**(12): p. 3651-62.

273. Schon, M.P. and R.J. Ludwig, *Lymphocyte trafficking to inflamed skin--molecular mechanisms and implications for therapeutic target molecules.* Expert Opin Ther Targets, 2005. **9**(2): p. 225-43.

274. Kasperkiewicz, M., et al., *Clearance rates of circulating and tissue-bound autoantibodies to type VII collagen in experimental epidermolysis bullosa acquisita.* Br J Dermatol. **162**(5): p. 1064-70.

275. Ji, H., et al., *Genetic influences on the end-stage effector phase of arthritis.* J Exp Med, 2001. **194**(3): p. 321-30.

276. Asghari, F., et al., *Identification of quantitative trait loci for murine autoimmune pancreatitis.* J Med Genet. **48**(8): p. 557-62.

277. Srinivas, G., et al., *Genome-wide mapping of gene-microbiota interactions in susceptibility to autoimmune skin blistering.* Nat Commun. **4**: p. 2462.

278. Kay, J. and L. Calabrese, *The role of interleukin-1 in the pathogenesis of rheumatoid arthritis.* Rheumatology (Oxford), 2004. **43 Suppl 3**: p. iii2-iii9.

279. Elliott, M.J., et al., *Randomised double-blind comparison of chimeric monoclonal antibody to tumour necrosis factor alpha (cA2) versus placebo in rheumatoid arthritis.* Lancet, 1994. **344**(8930): p. 1105-10.

280. Lovell, D.J., et al., *Adalimumab with or without methotrexate in juvenile rheumatoid arthritis.* N Engl J Med, 2008. **359**(8): p. 810-20.

281. Mease, P.J., et al., *Etanercept in the treatment of psoriatic arthritis and psoriasis: a randomised trial.* Lancet, 2000. **356**(9227): p. 385-90.

282. Sandborn, W.J., et al., *Adalimumab induction therapy for Crohn disease previously treated with infliximab: a randomized trial.* Ann Intern Med, 2007. **146**(12): p. 829-38.

283. John, H., A. Whallett, and M. Quinlan, *Successful biologic treatment of ocular mucous membrane pemphigoid with anti-TNF-alpha.* Eye (Lond), 2007. **21**(11): p. 1434-5.

284. Dinarello, C.A. and J.W. van der Meer, *Treating inflammation by blocking interleukin-1 in humans.* Semin Immunol. **25**(6): p. 469-84.

285. Zepter, K., et al., *Induction of biologically active IL-1 beta-converting enzyme and mature IL-1 beta in human keratinocytes by inflammatory and immunologic stimuli.* J Immunol, 1997. **159**(12): p. 6203-8.

286. Black, R.A., et al., *A pre-aspartate-specific protease from human leukocytes that cleaves pro-interleukin-1 beta.* J Biol Chem, 1989. **264**(10): p. 5323-6.

287. Coeshott, C., et al., *Converting enzyme-independent release of tumor necrosis factor alpha and IL-1beta from a stimulated human monocytic cell line in the presence of activated neutrophils or purified proteinase 3.* Proc Natl Acad Sci U S A, 1999. **96**(11): p. 6261-6.

288. Sugawara, S., *Immune functions of proteinase 3.* Crit Rev Immunol, 2005. **25**(5): p. 343-60.

289. Hazuda, D.J., et al., *Processing of precursor interleukin 1 beta and inflammatory disease.* J Biol Chem, 1990. **265**(11): p. 6318-22.

290. Robertson, S.E., et al., *Expression and alternative processing of IL-18 in human neutrophils.* Eur J Immunol, 2006. **36**(3): p. 722-31.

291. Irmler, M., et al., *Granzyme A is an interleukin 1 beta-converting enzyme.* J Exp Med, 1995. **181**(5): p. 1917-22.

292. Matsushima, K., et al., *Intracellular localization of human monocyte associated interleukin 1 (IL 1) activity and release of biologically active IL 1 from monocytes by trypsin and plasmin.* J Immunol, 1986. **136**(8): p. 2883-91.

293. Maelfait, J., et al., *Stimulation of Toll-like receptor 3 and 4 induces interleukin-1beta maturation by caspase-8.* J Exp Med, 2008. **205**(9): p. 1967-73.

294. Ito, A., et al., *Degradation of interleukin 1beta by matrix metalloproteinases.* J Biol Chem, 1996. **271**(25): p. 14657-60.

295. Schonbeck, U., F. Mach, and P. Libby, *Generation of biologically active IL-1 beta by matrix metalloproteinases: a novel caspase-1-independent pathway of IL-1 beta processing.* J Immunol, 1998. **161**(7): p. 3340-6.

296. Herzog, C., G.P. Kaushal, and R.S. Haun, *Generation of biologically active interleukin-1beta by meprin B.* Cytokine, 2005. **31**(5): p. 394-403.

297. Que, X., et al., *A surface amebic cysteine proteinase inactivates interleukin-18.* Infect Immun, 2003. **71**(3): p. 1274-80.

298. Zhang, Z., et al., *Entamoeba histolytica cysteine proteinases with interleukin-1 beta converting enzyme (ICE) activity cause intestinal inflammation and tissue damage in amoebiasis.* Mol Microbiol, 2000. **37**(3): p. 542-8.

299. Wittmann, M., S.R. Kingsbury, and M.F. McDermott, *Is caspase 1 central to activation of interleukin-1?* Joint Bone Spine. **78**(4): p. 327-30.

300. Black, R., et al., *The proteolytic activation of interleukin-1 beta.* Agents Actions Suppl, 1991. **35**: p. 85-9.

301. Dinarello, C.A., et al., *Multiple biological activities of human recombinant interleukin 1.* J Clin Invest, 1986. **77**(6): p. 1734-9.

302. Radeke, H.H., R.J. Ludwig, and W.H. Boehncke, *Experimental approaches to lymphocyte migration in dermatology in vitro and in vivo.* Exp Dermatol, 2005. **14**(9): p. 641-66.

303. Nooteboom, A., C.J. van der Linden, and T. Hendriks, *Modulation of adhesion molecule expression on endothelial cells after induction by lipopolysaccharide-stimulated whole blood.* Scand J Immunol, 2004. **59**(5): p. 440-8.

304. Liu, Z., et al., *Differential roles for beta2 integrins in experimental autoimmune bullous pemphigoid.* Blood, 2006. **107**(3): p. 1063-9.

305. Munro, J.M., J.S. Pober, and R.S. Cotran, *Recruitment of neutrophils in the local endotoxin response: association with de novo endothelial expression of endothelial leukocyte adhesion molecule-1.* Lab Invest, 1991. **64**(2): p. 295-9.

306. Theilgaard-Monch, K., B.T. Porse, and N. Borregaard, *Systems biology of neutrophil differentiation and immune response.* Curr Opin Immunol, 2006. **18**(1): p. 54-60.

307. Borish, L., et al., *Recombinant interleukin-1 beta interacts with high-affinity receptors to activate neutrophil leukotriene B4 synthesis.* Inflammation, 1990. **14**(2): p. 151-62.

308. Parker, K.P., et al., *Presence of IL-1 receptors on human and murine neutrophils. Relevance to IL-1-mediated effects in inflammation.* J Immunol, 1989. **142**(2): p. 537-42.

309. Rhyne, J.A., et al., *Characterization of the human interleukin 1 receptor on human polymorphonuclear leukocytes.* Clin Immunol Immunopathol, 1988. **48**(3): p. 354-61.

310. Paulsson, J.M., et al., *In-vivo extravasation induces the expression of interleukin 1 receptor type 1 in human neutrophils.* Clin Exp Immunol. **168**(1): p. 105-12.

311. Yin, X., et al., *Five regulatory genes detected by matching signatures of eQTL and GWAS in psoriasis.* J Dermatol Sci.

312. Garcia-Maurino, S., et al., *Melatonin enhances IL-2, IL-6, and IFN-gamma production by human circulating CD4+ cells: a possible nuclear receptor-mediated mechanism involving T helper type 1 lymphocytes and monocytes.* J Immunol, 1997. **159**(2): p. 574-81.

313. Chauvet, C., et al., *The gene encoding human retinoic acid-receptor-related orphan receptor alpha is a target for hypoxia-inducible factor 1.* Biochem J, 2004. **384**(Pt 1): p. 79-85.

314. Giguere, V., et al., *The orphan nuclear receptor ROR alpha (RORA) maps to a conserved region of homology on human chromosome 15q21-q22 and mouse chromosome 9.* Genomics, 1995. **28**(3): p. 596-8.

315. Dzhagalov, I., V. Giguere, and Y.W. He, *Lymphocyte development and function in the absence of retinoic acid-related orphan receptor alpha.* J Immunol, 2004. **173**(5): p. 2952-9.

316. Jetten, A.M., *Retinoid-related orphan receptors (RORs): critical roles in development, immunity, circadian rhythm, and cellular metabolism.* Nucl Recept Signal, 2009. **7**: p. e003.

317. Pozo, D., et al., *mRNA expression of nuclear receptor RZR/RORalpha, melatonin membrane receptor MT, and hydroxindole-O-methyltransferase in different populations of human immune cells.* J Pineal Res, 2004. **37**(1): p. 48-54.

318. Soria, V., et al., *Differential association of circadian genes with mood disorders: CRY1 and NPAS2 are associated with unipolar major depression and CLOCK and VIP with bipolar disorder.* Neuropsychopharmacology. **35**(6): p. 1279-89.

319. Dehghan, A., et al., *Meta-analysis of genome-wide association studies in >80 000 subjects identifies multiple loci for C-reactive protein levels.* Circulation. **123**(7): p. 731-8.

320. Chambers, J.C., et al., *Genome-wide association study identifies loci influencing concentrations of liver enzymes in plasma.* Nat Genet. **43**(11): p. 1131-8.

321. Moffatt, M.F., et al., *A large-scale, consortium-based genomewide association study of asthma.* N Engl J Med. **363**(13): p. 1211-21.

322. Solt, L.A., et al., *Suppression of TH17 differentiation and autoimmunity by a synthetic ROR ligand.* Nature. **472**(7344): p. 491-4.

323. Bettelli, E., et al., *Reciprocal developmental pathways for the generation of pathogenic effector TH17 and regulatory T cells.* Nature, 2006. **441**(7090): p. 235-8.

324. Mangan, J.K., et al., *Granulocyte colony-stimulating factor-induced upregulation of Jak3 transcription during granulocytic differentiation is mediated by the cooperative action of Sp1 and Stat3.* Oncogene, 2006. **25**(17): p. 2489-99.

325. Veldhoen, M., et al., *TGFbeta in the context of an inflammatory cytokine milieu supports de novo differentiation of IL-17-producing T cells.* Immunity, 2006. **24**(2): p. 179-89.

326. Yang, X.O., et al., *T helper 17 lineage differentiation is programmed by orphan nuclear receptors ROR alpha and ROR gamma.* Immunity, 2008. **28**(1): p. 29-39.

327. Delerive, P., et al., *The orphan nuclear receptor ROR alpha is a negative regulator of the inflammatory response.* EMBO Rep, 2001. **2**(1): p. 42-8.

328. Kopmels, B., et al., *Evidence for a hyperexcitability state of staggerer mutant mice macrophages.* J Neurochem, 1992. **58**(1): p. 192-9.

329. Koibuchi, N. and W.W. Chin, *ROR alpha gene expression in the perinatal rat cerebellum: ontogeny and thyroid hormone regulation.* Endocrinology, 1998. **139**(5): p. 2335-41.

330. Matsui, T., et al., *An orphan nuclear receptor, mROR alpha, and its spatial expression in adult mouse brain.* Brain Res Mol Brain Res, 1995. **33**(2): p. 217-26.

331. Sashihara, S., et al., *Orphan nuclear receptor ROR alpha gene: isoform-specific spatiotemporal expression during postnatal development of brain.* Brain Res Mol Brain Res, 1996. **42**(1): p. 109-17.

332. Stapleton, C.M., et al., *Enhanced susceptibility of staggerer (RORalphasg/sg) mice to lipopolysaccharide-induced lung inflammation.* Am J Physiol Lung Cell Mol Physiol, 2005. **289**(1): p. L144-52.

333. Ludwig, R.J., et al., *Emerging treatments for pemphigoid diseases.* Trends Mol Med. **19**(8): p. 501-12.

334. Wipke, B.T. and P.M. Allen, *Essential role of neutrophils in the initiation and progression of a murine model of rheumatoid arthritis.* J Immunol, 2001. 167(3): p. 1601-8.

335. REMICADE, Retrieved July 6, 2014, from: *http://www.accessdata.fda.gov/drugsatfda_docs/label/2009/103772s5234lbl.pdf*

336. REMICADE, Retrieved July 6, 2014, from: *http://www.accessdata.fda.gov/drugsatfda_docs/label/2008/103795s5359lbl.pdf*

337. REMICADE, Retrieved July 6, 2014, from: *http://www.accessdata.fda.gov/drugsatfda_docs/label/2011/125057s0276lbl.pdf*

338. REMICADE, Retrieved July 6, 2014, from: *http://www.accessdata.fda.gov/drugsatfda_docs/label/2009/125261lbl.pdf*

339. Center Watch, Retrieved July 6, 2014, from: *https://www.centerwatch.com/drug-information/fda-approved-drugs/drug/1246/kineret-anakinra*

340. U.S. food and drug administration, Retrieved July 30, 2014, from: *http://www.fda.gov/Drugs/DevelopmentApprovalProcess/HowDrugsareDevelopedandApproved/ApprovalApplications/TherapeuticBiologicApplications/ucm080650.htm*

341. The R Project for Statistical Computing, Retrieved June 30, 2012, from: *http://www.r-project.org*

342. Mouse phenome database at the jackson laboratory, Retrieved June 30, 2012, from: *http://phenome.jax.org*

343. ImageJ,Retrieved April 2, 2011, from: h*ttp://rsbweb.nih.gov/ij/*

344. Mouse phenome database at the jackson laboratory, Retrieved June 30, 2012, from: *http://phenome.jax.org/db/q?rtn=snp/home*

8. Appendix

8.1. List of abbreviations

AIBD	autoimmune bullous dermatoses
AIL	advanced intercross mouse line
AIM2	absent in melanoma 2
AP-1	activator protein 1
ASC	apoptosis-associated speck-like protein containing a CARD
ATP	adenosin tree phosphate
AUC	area under the curve
BCA	based on bicinchoninic acid
BDL	bellow detection limit
BMZ	basement membrane zone
BP	bullous pemphigoid
BSA	bovine serum albumin
C domain	collagenous domain
C/EBP	CCAAT-enhancer-binding proteins
Ca^{2+}	calcium
CD	cluster of differentiation
cDNA	complementary DNA
CMP	cartilage matrix protein
COL4	type IV collagen
COL7	type VII collagen
CP	cicatricial pemphigoid
DEJ	dermal-epidermal junction
dsDNA	doppelstrand-DNA

Dsg	desmoglein
EAE	experimental autoimmune encephalomyelitis
EBA	epidermolysis bullosa acquisita
ECM	extracellular matrix
EGF	epidermal growth factor
ELISA	enzyme-linked immunosorbent assay
Fab	fragment antigen-binding (of immunoglobulin)
Fc	fragment crystallizable (of immunoglobulin)
FcgR	Fc gamma receptor
FcRn	Fc receptor
FDA	Food and Drug Administration (US)
FITC	fluorescein isothiocyanate
FNIII	fibronectin like domain III
G4	4th offspring generation
GM-CSF	granulocyte macrophage colony-stimulating factor
Gr-1	granulocyte-differentiation antigen-1
GST	glutathione S transferase
H&E	hematoxylin and eosin
HaCaT	human keratinocyte line
HIN	hemopoietic IFN-inducible nuclear proteins
HLA	human leukocyte antigen
HRP	horse radish peroxidase
HUVEC	human umbilical vein endothelial cells
ICAM	Intercellular adhesion molecule
ICE	interleukin-1β converting enzyme

IF	immunofluorescence
IFN	interferon
IgA	immunoglobulin A
IgE	immunoglobulin E
IgG	immunoglobulin G
IL	interleukin
IL-12Rβ1	interleukin-12 receptor, beta 1
IL-1R	interleukin-1 receptor
IL-1RAcP	interleukin-1 receptor accessory protein
IL-1Ra	interleukin-1 receptor antagonist
IL-1Ra^{int}	interleukin-1 receptor antagonist (intracellular)
IL-1Ra^{sol}	interleukin-1 receptor antagonist (soluble)
IL-1RI	interleukin-1 receptor type I
IL-1RII	interleukin-1 receptor type II
iNOS	Inducible nitric oxide synthase
IRAK-1	interleukin-1 receptor-associated kinase 1
IRAK-2	interleukin-1 receptor-associated kinase 2
IRAK-4	interleukin-1 receptor-associated kinase 4
IVIG	intravenous Immunoglobulin
kDa	Kilodalton
KO	knock out
LABD	linear IgA bullous dermatosis
LAD-1	linear IgA dermatosis antigen-1
LD	linkage disequilibrium
LFA-1	leukocyte function-associated antigen-1

LPS	lipopolysaccharide
LRR	leucine rich repeats
m.m.m.	mus musculus musculus
MAC-1	macrophage-1 Ag
MAF	minor allele frequency
MAP	mitogen-activated protein
MAPK	mitogen-activated protein kinase
mCOL7	murine type VII collagen
MCP-1	monocyte chemotactic protein-1
MEKK3	mitogen-activated protein kinase kinase kinase 3
Mg	milligram
MGSA	melanoma growth stimulatory activity
MHC	major histocompatibility complex
MIP	macrophage inflammatory protein
Ml	milliliter
MLN51	metastatic lymph node 51
MMP	mucous membrane pemphigoid
mRNA	messenger ribonucleic acid
MyD88	myeloid differentiation primary response gene 88
NADPH	nicotinamidadenindinukleotidphosphat
NC domain	non collagenous domain
ND	not done
NEMO	NF-kappa-B essential modulator
NF-κB	nuclear factor kappa-light-chain-enhancer of activated B cells

Ng	nano gram
NGF	nerve growth factor
NHS	normal human serum
NIK	NF-κB inducing kinase
NLR	nucleotide-binding oligomerization domain (*NOD*) like receptor
NLRC	NLR family CARD domain-containing protein
NLRP	*NOD*-like receptor family, pyrin domain containing
NOD	non obese diabetic
NR	normal rabbit
NSBF	normal suction blister fluid
OD	optical density
p200	200 kDa protein
p200	200-kDa protein
PBS	phosphate buffered saline
PBST 20	phosphate buffered saline tween 20
PCR	polymerase chain reaction
PDGF	platelet-derived growth factor
PF	pemphigus foliaceus
PMA	phorbol myristate acetate
PR3	proteinase 3
PV	pemphigus vulgaris
QPCR	quantitative polymerase chain reaction
QTL	quantitative trait locus
ROR	retinoid-related orphan receptor

ROS	reactive oxygen species
rt	room temperature
RT	reverse Transcription
SEM	standard error of the mean
SNP	single-nucleotide polymorphism
T3SS	type III secretion systems
TBS-T	tris buffered saline with tween
TGF	transforming growth factor
TLR	toll like receptor
TNF	tumor necrosis factors
TRAF	TNF receptor associated factor
TRX	thioredoxin
tSNP	tagging SNP
TXNIP	thioredoxin interacting protein
VCAM	vascular cell adhesion molecule
VEGF	vascular endothelial growth factor
vWFA	von-Willebrand-factor-A
WB	western blot
WT	wild type

8.2. List of tables

8.3. List of figures

8.4. List of mice used in this study

A/J	inbred mouse strain
AKR/J	inbred mouse strain
B10.S-H2s/SgMcdJ	inbred mouse strain
BALB	inbred mouse strain
BALB/cJ	inbred mouse strain
BXD2/TyJ	inbred mouse strain
C3H/HeJ	inbred mouse strain
C57BL/10SnSg	inbred mouse strain
C57BL/6J	inbred mouse strain
Cast/EiJL	inbred mouse strain
CBA/J	inbred mouse strain
DBA1/J	inbred mouse strain
FVB/NJ	inbred mouse strain
MRL/MpJ	inbred mouse strain
NOD/ShiLtJ	inbred mouse strain
NZB/WF1	inbred mouse strain
NZM2410/J	inbred mouse strain
PL/J	inbred mouse strain
PWD/PhJ	inbred mouse strain
SJL/J	inbred mouse strain
WSP/EiJ	inbred mouse strain

8.5. Acknowledgments

One of the joys of completion is to look over the journey past and remember all the friends and family who have helped and supported me along this long but fulfilling road. It would not have been possible to write my doctoral thesis without the help and support of all kind people around me, to only some of whom it is possible to give particular mention here.

First and foremost I want to thank my supervisor, Prof. Ralf Ludwig, who has supported me throughout my thesis with his patience and knowledge, I appreciate all his contributions of time, ideas, and funding to make my Ph.D. experience productive and stimulating. I had a great freedom to plan and execute my ideas in research. One simply could not wish for a better or friendlier supervisor.

I would like to express my gratitude to Prof. Dr. Detlef Zillikens, Director of the Department of Dermatology, Allergology and Venereology, University of Lübeck for providing me this opportunity to start my scientific career and for his priceless guidance. It has been such a pleasure to know and work with a pioneer in the field.

I would like also to express my special appreciation and thanks to Prof. Saleh Ibrahim, his advice and suggestions on both research as well as on my career have been priceless.

Most of the results described in this thesis would not have been obtained without a close collaboration with few laboratories. I owe a great deal of appreciation and gratitude to this project has also been shaped by a number of out helps: I greatly acknowledge the supportive collaborators of Prof. Michael P. Schön, (University of Göttingen), I thank Prof. Jean Mariani (Laboratoire Développement et Vieillissement du Système Nerveux, Institute des Neurosciences, Université P. and M. Curie, Paris, France) and Prof. Arturo Zychlinsky (Max-Planck-Institut für Infektionsbiologie Berlin). who greatly supported me with knockout mice strains. I also greatly appriciate the collaboration of Dr. Kathrin Kalies (Institute for Anatomy Universität zu Lübeck).

My gratitude is also extended to Dr. Andreas Recke, he was one of the first friendly faces to greet me when I began this doctoral program and has always been a tremendous help. I thank Dr. Steffen Möller and Yask Gupta for helping me in statistic analysis. I appreciate Claudia Kauderer, Miriam Freitag, and Vanessa Krull, for all their help these years with bringing our needed chemicals and supplies and their help in general, I thank Rebecca Cames who kindly prepared my histology samples.

My time in Lübeck was made enjoyable in large part due to the many friends and colleagues that became a part of my life, of whom Elena Pipi stands out notoriously as an amazing friend with warm and kind heart, thank you for all your genuine caring and concern, for all nice memories and useful discussions. I thank Franziska Schulze for being always so helpful, kind and hospitable. And thanks to all the other friends and members of Dermatology Department for all the nice and precious memories along the way. I am also very grateful to Dr. Stefan Grewe, who incented me to strive towards my goal, thank you for your faithful support during the final stages of this Ph.D.

Of course no acknowledgments would be complete without giving thanks to my family. To mom, especially, she is a great role model of resilience, strength and character thank you for calling me almost every day and making me feel your care and love. Thanks to my father to be there always for me and to my brother Ali, who has been my best friend all my life and made me laugh countless times from distance, I love you dearly and thank you for all your advice and support.

8.6. Declaration / Copyright statement

No part of the work referred to in this dissertation has been submitted in support of an application for any degree or qualification of The University of Lübeck or any other University or Institute of learning.